Sulphatising roasting of a Greenlandic uranium ore, reactivity of minerals and recovery

Forskningscenter Risø, Roskilde

Publication date:
1977

Document Version
Publisher's PDF, also known as Version of record

Risø Report No. 355

Risø Report No. 355

Risø National Laboratory

Sulphatising Roasting of a Greenlandic Uranium Ore, Reactivity of Minerals and Recovery

by J. K. Gamborg Hansen

March 1977

Sales distributors: Jul. Gjellerup, Sølvgade 87, DK-1307 Copenhagen K, Denmark

Available on exchange from: Risø Library, Risø National Laboratory, DK-4000 Roskilde, Denmark

INIS descriptors

CHEMICAL REACTION KINETICS
ELECTRON MICROPROBE ANALYSIS
GREENLAND
MOESSBAUER SPECTROMETERS
ORE PROCESSING
REFRACTORIES
ROASTING
SULFATES
SULFUR OXIDES
THERMAL GRAVIMETRIC ANALYSIS
URANIUM ORES
X-RAY DIFFRACTION

UDC 669.822.3:622.782

March 1977 Risø Report No. 355

Sulphatising Roasting of a Greenlandic Uranium ore, Reactivity of Minerals and Recovery

by

J. K. Gamborg Hansen

Risø National Laboratory
Chemistry Department

Abstract

Uranium in the lujavrite ore from Kvanefjeld, South Greenland, can be solubilised by sulphatising roasting at 700°C. The reactivity of various lujavrite minerals in the roasting process and the mechanism of the reaction were investigated by X-ray diffraction, optical microscopy, electron microprobe, thermal analysis, Mössbauer and infrared spectroscopy. Soluble sulphates are formed on the surface of the grains; an outer zone of the grains is transformed; usually a core remains unchanged.

Variations in uranium recovery can be explained by variations in the contents of the uranium-bearing minerals, steenstrupine and uranium-containing pigmentary material (altered Zr containing silicate minerals), and in the degree of alteration of steenstrupine. Characterization of these minerals required many qualitative and a few quantitative electron microprobe analyses.

CONTENTS

Page

Page

1. INTRODUCTION

Since 1955 the uranium deposit near Narssaq in South Greenland has been investigated with a view to the recovery of the uranium[1,2,3,4,5].

The ore is rather poor. The average uranium content is approximately 300 ppm in the investigated area. Geologically, the ore is different from all other uranium ores.

It is not possible to use traditional methods to recover the uranium. The only method that can be used is the so-called sulphatising roasting in which the ore is treated with SO_2 and air at 700°C. The ore itself catalyzes the formation of SO_3, which among other things attacks the uranium minerals. A layer of sulphates is formed on the surface of the mineral grains. The main component of this phase is Na_2SO_4, but most of the other metalions are also found in it. The sulphates may be extracted with a slightly acid solution and the uranium is then recovered by solvent extraction.

This report deals with an investigation of the mechanism of the sulphatising roasting of some minerals in the ore and of the recovery of uranium compared to the uranium mineralisation.

The mechanism investigation mainly concentrated on the minerals arfvedsonite and steenstrupine. The first is the most widespread and is the single mineral that contributes most to the sulphates. The second is the main uranium mineral. A few other minerals including analcime, natrolite and sodalite were briefly investigated.

The recovery of uranium by this method depends on the type of mineralisation and the SO_3 take-up. Recovery can differ from 20 to 80% using the same treatment of different ore samples. These differences relate to uranium mineralisation. Microprobe investigations were performed to characterise the uranium minerals.

For some types of ore recovery may be improved by treating the ore with diluted sulphuric acid before roasting.

2. LITERATURE SURVEY

In the following chapter a survey is given of the literature on the geology and mineralogy of the uranium minerals and of sulphatising roasting, especially of this ore.

2.1. Geology and Mineralogy of the Ore

The uranium/thorium deposit at Kvanefjeld is located in the north-

western part of the Ilimaussaq alkaline intrusion. The intrusion has been very thoroughly investigated on account of its special geology and the many rare minerals it contains. Most of the literature has been listed by H. Sørensen et al.[6]. A general geological description of the Kvanefjeld area was given by H. Sørensen, J. Hansen and G. Bonnesen[7].

In Kvanefjeld, 43 drilling cores were made to demarcate the uranium mineralisation and to determine the tonnage. A geological description of the drilling cores and a calculation of the tonnage has been given by H. Sørensen et al.[6], and by H. Sørensen, J. Rose-Hansen and B. Leth Nielsen[8]. The estimated reserves are almost 16 000 metric tons of uranium of an ore grade of approximately 300 ppm. Besides U, there is about 2.6 times as much Th. A new drilling programme is planned and it is hoped that the reserves will be found to be considerably increased.

The uranium is found in type of ore called lujavrite, in which the most widespread minerals are,

Arfvedsonite : $Na_3Fe^{2+}{}_4Fe^{3+}((Si_8O_{22})(OH)_2)$

Analcime : $Na(AlSi_2O_6)H_2O$

Microcline : $K(AlSi_3O_8)$

Albite : $Na(AlSi_3O_8)$.

The following minerals are locally widespread,

Nepheline : $KNa_3(AlSiO_4)_4$

Sodalite : $Na_8(Cl_2(AlSiO_4)_6)$

Natrolite : $Na_2(Al_2Si_3O_{10}).2H_2O$

Acmite/Aegirine : $NaFeSi_2O_6$

Naujakasite : $(Na,K)_6(Fe,Mn,Ca)(Al,Fe)_4Si_8O_{26},H_2O$[9].

The designation "white minerals" is commonly used for the minerals analcime, microcline, albite, nepheline, natrolite, and sodalite. The ore is enriched in the elements Be, Li, Zn, F, rare earths, U, and Th. Many of these elements are concentrated in rare minerals. The uranium-containing ones are among these, as given below:

Steenstrupine : $Na_2Ce(Mn,Fe,...)H_2((Si,P)O_4)_3$[10]

Monazite : $CePO_4$

Thorite : $(Th,U)SiO_4$

Less well defined pigmentary material: Composition poorly known.

Steenstrupine is the most important, and pigmentary material is of some importance, while monazite and thorite are of less importance.

The type of ore called lujavrite is not homogeneous and the composition can change very much within small areas. Four types of lujavrite are recognised through their mineralogical composition.

1. Arfvedsonite lujavrite
2. Medium- to coarse-grained arfvedsonite lujavrite
3. Naujakasite lujavrite
4. Aegirine lujavrite.

Naujakasite is a very rare mineral only found in the Ilimaussaq intrusion. The uranium minerals will be described in more detail in the following.

2.1.1. Steenstrupine

The mode of occurrence of steenstrupine has been thoroughly investigated by H. Sørensen[11]. It is a very rare mineral that is only found at Lovozero on the Kola peninsula in USSR in addition to Ilimaussaq.

In table 2.1 two analyses are given of the mineral. The first analysis is of steenstrupine from Ilimaussaq, while the second is from Lovozero. The samples analysed from Ilimaussaq are from a coarse-grained vein and not from the lujavrites at Kvanefjeld.

There are some remarkable differences between steenstrupine from Lovozero and from Ilimaussaq. The first is rich in Th, Mn, and Si, while the other is rich in Na and P. Apparently, the Ilimaussaq steenstrupine is rich in Nb, but this was not confirmed by the present investigation (cf. chapter 8). Vlaslov[12] explains the differences in composition by substitutions such as $Na^{+} + Ce^{3+} \simeq 2(Ca^{2+}, Mn^{2+})$, $Na^{+} + P^{5+} \simeq (Ca^{2+}, Mn^{2+}) + Si^{4+}$, and $Th^{4+} + Si^{4+} \simeq Ce^{3+} + P^{5+}$.

There are some remarkable differences between steenstrupines in different lujavrite samples. The mineral is usually metamict and therefore isotropic because of irradiation damage of the structure, but U-Th deficient types may be anisotropic. The colour may vary from colourless to yellow, brown or red as a result of the metamictisation. The uranium and thorium contents of steenstrupines from Ilimaussaq have been determined by chemical analysis[10], autoradiography[14], and fission track analysis[15]. The uranium content may vary from 0.2 to 1.4% and the thorium from 0.2 to 7.4%. The contents also vary between grains in a thin section[15]. Steenstrupine may also vary from a homogeneous to a strongly altered mineral.

Table 2.1

Analysis of steenstrupine from Ilimaussaq (1), and from Lovozero (2)

	1	2
SiO_2	26.72	32.36
TiO_2	-	0.68
ThO_2	2.13	10.09
$(Nb,Ta)_2O_5$	4.37	0.14
$(Ce,La)_2O_3$	29.60	23.34
Y_2O_3	0.36	-
Fe_2O_3	2.67	3.68
MnO	6.60	9.97
MgO	0.31	-
CaO	2.33	3.33
Na_2O	11.23	6.51
K_2O	-	0.83
H_2O	3.53	3.56
F_2	1.24	-
P_2O_5	8.19	5.32
total	99.20	99.81
Reference	10	12

2.1.2. Monazite

This mineral is widespread in the Ilimaussaq intrusion. Usually it occurs as aggregates of small crystals (c.f. M. Danø, and H. Sørensen[13]). According to autoradiographic analysis[14], the monazite of Ilimaussaq is only weakly radioactive. Monazite samples from Kvanefjeld have been reported to contain 1.28%[1], and 0.5[15] per cent U, but in both samples an essential part of the uranium is supposed to be contained in thorite[6]. In the present investigation this has been proved for the first-mentioned monazite. Most of the uranium is contained in uranumthorite and there is at most a few parts per thousand in the monazite grains (cf. section 7.5).

2.1.3. Thorite

This mineral occurs as small yellow grains that are isotropic in thin sections[11]. It is usually associated with monazite or steenstrupine. Fission-track analysis[15] gave 2-3 per cent U and 28-53 per cent Th.

2.1.4. Pigmentary Material

Pigmentary material has only been sporadically investigated. Hansen[16] investigated one kind occurring in some radioactive veins from outside the Kvanefjeld area. It was not possible to determine any crystal structure, but hematite was detected on X-ray diffractograms of the material. This kind of pigmentary material is not necessarily the same as that found in the lujavrites. The pigmentary material in the lujavrites may be associated with altered steenstrupine and it also occurs as crusts on arfvedsonite.

By fission-track analysis Wollenberg[15] found a U-content of less than 2.5 per cent and no Th in the pigmentary material from the lujavrites.

2.2. Recovery of Uranium, Choice of Method

Because of the low ore grade, the possibilities of a physical concentration of the ore were investigated by E. Sørensen and T. Lundgaard[2]. It was possible to make a concentration by magnetic separation and by flotation, but the loss in tailings was too large. The whole ore must therefore be processed.

The standard method for recovery of uranium is leaching with diluted sulphuric acid. Some steenstrupines are very easily dissolved in the acid solution but others are almost insoluble. Pigmentary material is insoluble in cold acid but partly soluble in warm acid under oxidising conditions[72]. This might indicate U in the +4 state. There is too little recovery of uranium by this method. Another condition making the use of this method impossible is the solubility of the felsic minerals, such as analcime, natrolite, nepheline, and sodalite, in the acid solution. The amount of colloidal silica in the leach liquor becomes too large for the further processing of the solution.

Recovery by carbonate leaching, which is the other common method of uranium recovery, proved unsuitable because the recovery was even lower than when using sulfuric acid leaching.

Sulphatising roasting has been the only technically applicable method for extracting uranium from this ore as described by E. Sørensen[4].

2.3. Sulphatising Roasting

Sulphatising roasting is a process in which a solid is treated with SO_2 or SO_3 at an elevated temperature. As a result of the reaction, a layer of sulphates is formed on the surface of the grains.

Literature on sulphatising roasting is very limited. The method seems to have been of theoretical interest, but there is no industrial utilisation.

Most of the literature is listed by Asmund[1], but a short survey will be given here. The method has been proposed for the recovery of, for example, Mn[17, 18, 19, 20, 21, 22, 23, 44], Cu[24, 25, 42], Ni[26, 27, 28, 29, 30, 31, 32, 43], Zn[33, 34, 35, 45], Al[36]. Pb[37] and Co[38] from oxide, sulphide or carbonate ores.

Only in a few cases has the method been proposed for silicate minerals. Recovery of Be from montmorrilonite ($Na_{<1}(H_2O)_nAl_{<2}(OH)_2Si_4O_{10}$) and helvite ($Mn(BeSiO_4)_3S$) has been patented[37], and so has the recovery of Li from polylithionite ($KLi_{1\frac{1}{2}}Al_{1\frac{1}{2}}((F,OH)_2AlSi_3O_{10})$)[39]. The recovery of Al from kaolinite ($Al_2(OH)_4Si_2O_5$) and halloysite ($Al_2(OH)_4Si_2O_5 \cdot H_2O$) has also been investigated[36].

Sulphatising roasting was patented for the recovery of uranium from Swedish alunshales[40]. Nevertheless, the method was given up in favour of the traditional leaching with diluted sulphuric acid.

Asmund[1] investigated the sulphatising roasting of arfvedsonite, aegirine, monazite and steenstrupine from Ilimaussaq. His results will be referred to in section 2.4.

Montmorrilonite, polylithionite, kaolinite and halloysite are all layer silicates of which the structure is seriously altered by heating to the reaction temperature of 500-700°C. A rapid diffusion along the layers may be expected if the crystal structure is not completely altered by heating. This may explain why these minerals are easily roasted.

The structure of helvite is similar to that of sodalite. Be substitutes for Al and Cl for S. Sodalite has shown to be one of the fastest reacting minerals from Ilimaussaq (cf. chapter 4), so there might be a structural explanation of the reactivity. In the case of helvite it might also be explained by the content of S^{2-}. The sulphide ion may be oxidised and hence the crystal structure decomposed.

In Denmark, sulphatising roasting has been used to recover manganese as $MnSO_4$ from pog iron ore[75]. The ore was mixed with 20% used gas purifying material. Roasting was carried out in a tunnel oven in which the material, placed in 5-cm-thick layers on trays, was moved through the oven in counter-stream with atmospheric air. The reaction temperature was approximately 500°C and the yield was 70-80%.

2.4. Sulphatising Roasting of Minerals from Ilimaussaq

Asmund[1] investigated the rate of reaction of some of the minerals from Ilimaussaq. His results are shown in fig. 2.1, where weight increase

during roasting is shown versus time. The roasting gas was 5% SO_2 in air. An SO_3 catalyst was not used in these experiments[41].

Asmund concentrated his investigations on the minerals arfvedsonite, steenstrupine, aegirine and monazite. The essential conclusions from his experiments are reported below.

2.4.1. Arfvedsonite

When arfvedsonite is roasted an incoherent layer of sulphates is formed on the surface of the grains. It is immediately soluble in water. The form and size of the grains are not changed, but the colour alters from bluish-green to red as a result of the reaction. The X-ray diffractograms are also unchanged. Asmund proposed a mechanism where the metalions are moved through an unaltered lattice to the surface where they react to form sulphates. Electroneutrallity in the lattice is partly maintained by an Fe^{2+} oxidation and partly by an oxygen ion transport to the surface. The two reactions are described by,

1. a) in the lattice : $2Fe^{2+} \rightleftharpoons 2F^{3+} + 2e^-$,

   b) transport : $2Me^+ + 2e^-$ to the surface,

   c) surface reaction : $2Me^+ + 2e^- + SO_2 + O_2 \rightleftharpoons Me_2SO_4$

2. a) transport : $2Me^+ + O^{2-}$ to the surface,

   b) surface reaction : $2Me^+ + O^{2-} + SO_2 + \frac{1}{2}O_2 \rightleftharpoons Me_2SO_4$.

Hematite is formed by the oxidation of Fe^{2+} and it is identified by the Mössbauer spectra. The composition of the sulphates is not changed during the roasting. Na is the main component of the sulphates, but smaller amounts of other metalions are also represented. Arfvedsonite is an excellent catalyst for SO_3 formation.

Some additional investigations are presented and the mechanism of the roasting discussed in chapter 5.

2.4.2. Aegirine

The shape of the grains, the X-ray diffractograms, and the Mössbauer spectra are unchanged by the roasting.

Asmund proposed a mechanism in which the metalions are moved through an unchanged lattice to the surface where they react with the gas to form sulphates. The reaction may be described by the second reaction in the arfvedsonite results above. The rate of reaction is considerably slower than that of arfvedsonite.

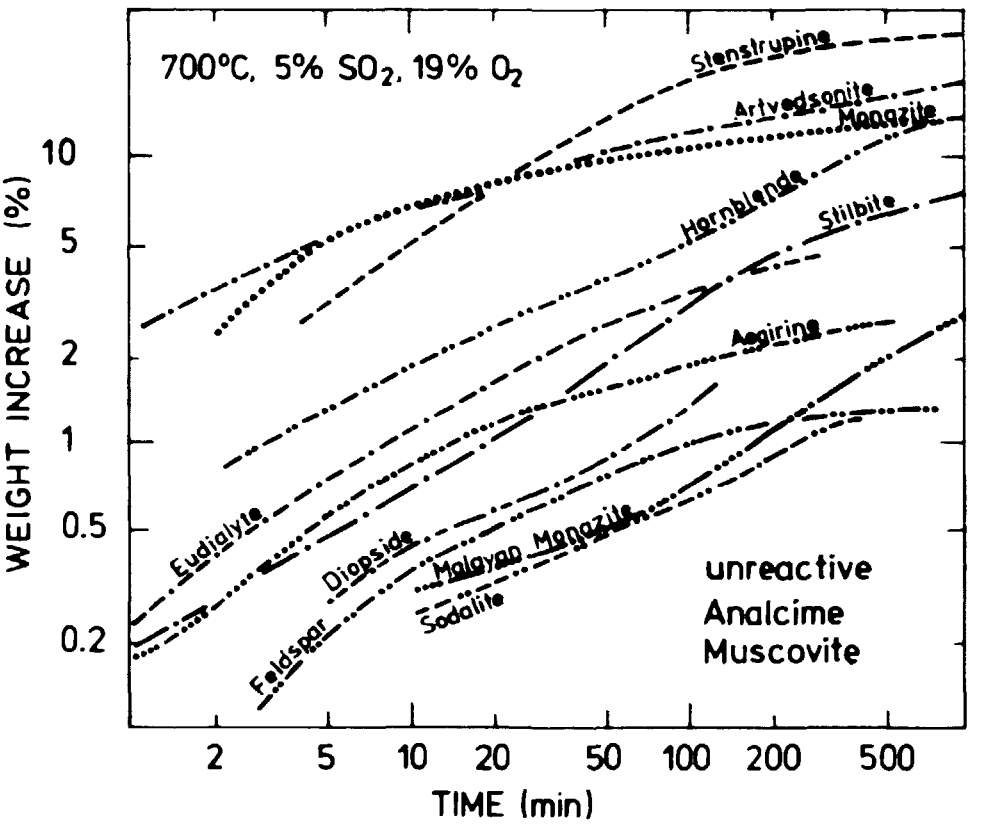

Fig. 2.1. Sulphatising roasting of different minerals, the weight increase is depicted versus time.

The rate is increased and the X-ray diffractograms are changed if roasting continues for many hours.

Aegirine is the only mineral in which Asmund found pyrosulphate in the sulphates. The composition of the sulphates is not changed during the roasting.

A few further investigations are presented in section 7.4, where the proposed mechanism is also discussed.

2.4.3. Steenstrupine

The shape of small grains is unchanged by roasting while larger grains may crack. The X-ray diffractograms of roasted and heat-treated samples are altered, but Asmund was unable to resolve them.

Asmund proposed a mechanism by which metalions are moved to the surface, where they react with the gas to form sulphates. The ions are supposed to be transported through a variable number of pores. A number of these are blocked as the reaction proceeds and the reaction rate is slowed

down. The pores are regarded as a transport possibility; the size, number, and nature of the pores are unknown.

The reaction rate is increased by the addition of water vapour to the roasting gas. The role of the vapour is unknown.

The composition of the sulphates changes considerably during roasting. The recovery of the ions versus the weight increase as found by Asmund is shown in fig. 2.2.

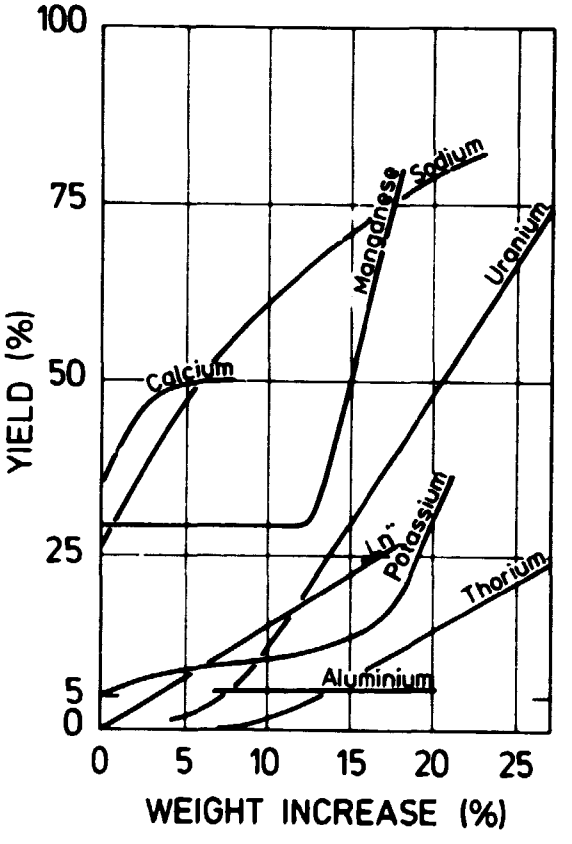

Fig. 2.2. Sulphatising roasting of steenstrupine by 5% SO_2 in atmospheric air.

Na and Ca move fastest into the sulphates. Below a 10-15% weight increase, there are only minor amounts of the other cations in the sulphates. The recovery of the rare earths is very poor.

In chapter 6 some new investigations are presented and the proposed mechanism is discussed.

2.4.4. Monazite

The shape of the grains and the X-ray diffractograms are unchanged during roasting. Asmund suggests a mechanism of the same kind as that

of steenstrupine. The recoveries of Na, Ca and U are high, while those of Th and the rare earths are low.

The roasting of monazite will be briefly discussed in section 7.5.

2.4.5. Roasting of a Medium- to Coarse-grained Lujavrite Sample

Asmund investigated the sulphatising roasting of a medium- to coarse grained arfvedsonite lujavrite sample from the mine material. (During 1962, 200 tons of the ore were mined from a small experimental mine. This material is termed "mine material" in the following). The present investigations showed that this material is not representative of the ore (cf. section 9.3). The content of uranium containing pigmentary material is too high and the content of steenstrupine is too low.

The mineralogical composition of the sample was calculated on the basis of a chemical analysis as given in table 2.2.

Table 2.2

The mineralogical composition of the mine sample

Mineral	weight per cent
arfvedsonite	31
analcime + natrolite	38
sodalite	0.5
steenstrupine + monazite	1.9-3.2
microline + albite + nepheline	28

The recovery of metalions versus weight increase is shown in fig. 2.3.

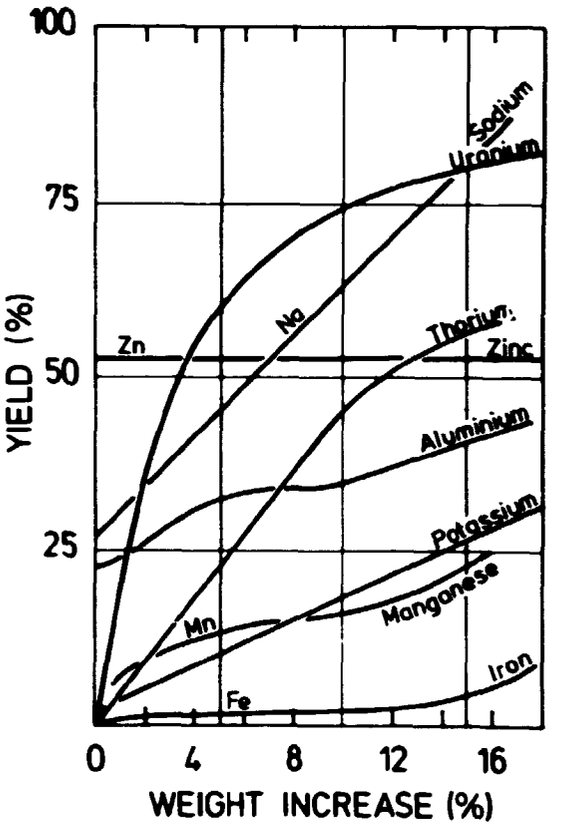

Fig. 2.3. Sulphatising roasting of lujavrite, 5% SO_2 in atmospheric air.

3. METHODS USED IN THE PRESENT INVESTIGATION

In the following chapter a survey is given of the methods used in these investigations, how they were used and what information they provided.

A major part of the investigations was concentrated on the structural changes that occur as a result of the heating to and the roasting at 700°C. Another part was concentrated on a characterisation of the uranium-containing minerals in the Kvanefjeld ore.

The following methods were used:

1. Thermal analysis, including differential thermal analysis and thermal gravimetric analysis (in the following abbreviated as DTA and TG).
2. Optical microscopy.
3. X-ray diffraction.

4. Electron microprobe.

5. Mössbauer spectroscopy.

6. Infrared spectroscopy.

The equipment used for these investigations is located at the Institute of Ceramics (I.C.) and the Department of Metallurgy (D. M.) at the Technical University of Denmark and at the Chemistry Department (C. D.), Research Establishment, Risø.

3.1. Thermal Analysis

Thermal gravimetric analysis and differential thermal analysis were carried out on all the minerals investigated. Equipment manufactured by Mettler was used at I. C.

All the sulphatising roasting experiments were carried out using other TG equipment, manufactured by Linseis at C. D. Using this equipment it was possible to follow the change in weight during sulphatising roasting as a function of, for instance, temperature, grain size and gas composition. In the experiments 100-1000 mg, of the sample were placed on the balance arm of the equipment and heated to the roasting temperature, 650-750°C. The heating rate was usually 20°C/min and heating was carried out in atmospheric air. The gas composition was then rapidly changed to the roasting gas, usually 5 or 10 volume per cent SO_2 in atmospheric air. The flow through the apparatus was roughly 400 cm^3/min.

A platinum catalyst was placed in the heating zone just in front of the sample when samples without arfvedsonite were roasted. Arfvedsonite and its roasting products (hematite dispersed in a prodominant Na_2SO_4 phase) are excellent catalysts for SO_3 formation, so a catalyst is unnecessary in these cases.

3.2. Optical Microscopy

Reflection and transmission microscopical investigations were performed with a Leitz orthoplan microscope at the I. C.

Reflection microscopical investigations were made on untreated, heat-treated and roasted samples of the investigated minerals in plane polished samples.

Some lujavrite samples were investigated in polished thin sections. Uranium mineralisation and the main minerals were determined.

Some of the samples investigated were also used for electron microprobe investigations.

3.3. X-ray Diffraction

A camera of Guinier type at I.C. was used for these investigations.

Each mineral has a characteristic diffraction pattern, because the interplanar distances and the intensities of the diffractions differ. By means of the ASTM standard file, it is possible to identify almost all known minerals. In the present investigation X-ray diffraction was widely used in the identification of the minerals.

It is possible to make high-temperature, X-ray diffractograms using the Guinier camera in question. The sample is heated in a furnace and the diffractogram is recorded simultaneously on the film, which is moved at a constant speed. Thus phase transformations, and the temperatures at which they occur, may be recorded on the film.

3.4. Electron Microprobe

These investigations were mostly carried out by an ARL microprobe at D.M. This microprobe makes it possible to perform qualitative and quantitative analysis for sodium and heavier elements. The resolution is about 3 microns.

The present investigations were mainly qualitative. The distribution of the elements within areas of a few hundred microns may be investigated by scanning of the electron beam. The elements in interesting grains of steenstrupine and pigmentary material grains was determined and the distribution of the elements was then investigated. This was carried out both by distribution pictures of back-scattered electrons abbreviated (below as B-S-E) and by pictures showing the distribution of the single elements. It is possible to distinguish between areas of different average atomic weight on the B-S-E pictures because the electrons are better reflected by the heavier elements. The element distribution pictures show where the element is concentrated within the investigated area. It is therefore possible to make an element distribution map of a grain. Of course, a sample is first investigated in the microscope and the interesting areas marked before the sample is investigated in the microprobe.

The distribution of the elements was also investigated by concentration profiles, or more correctly by measured X-ray intensity profiles. The X-ray intensity for some elements is measured in intervals of, for instance, 3 microns, and the intensity is depicted versus distance. These curves are only qualitative, as matrix corrections were not performed.

Quantitative investigations were made in a few cases. Silicate or oxide

minerals of known composition were used as standards. U and Th standards were made for these investigations. To a glass containing a composition having the lowest melting point in the $CaO-Al_2O_3-SiO_2$ system was added 15% UO_2 and ThO_2, respectively. The glasses were homogeneised at 1500°C.

The composition of the samples was calculated by a computer program prepared by J. Rønsbo of the Institute of Geology, University of Copenhagen.

3.5. Mössbauer Spectroscopy

For some isotopes, of which ^{57}Fe is the most important, there is the possibility of recoil-free emission and absorption of gamma quanta, permitting resonance absorption or Mössbauer spectroscopy. The theory of Mössbauer spectroscopy has been presented by Wertheim[46].

Mössbauer absorption spectra were recorded with a source of ^{57}Co diffused into palladium on a conventional spectrometer of the constant acceleration type operating in multiscaler mode. A description of the arrangement has been given by Andersen[47].

When ^{57}Co decay to ^{57}Fe the process may occur through the first excited state of ^{57}Fe and by the decay to the ground state a 14.4 keV gamma quantum is emitted. This transition constitutes the basis of Mössbauer spectroscopy of ^{57}Fe.

There are small but distinctive differences in the absorption energy in different samples because of the different surroundings of the Fe atom.

The Mössbauer spectrum is recorded by moving the source and the absorber relative to each other. Hereby a Doppler displacement of energy occurs, and the absorptions may be detected in a small energy interval around 14.4 keV. The Mössbauer spectrum is a delineation of the gamma ray intensity versus a velocity (which is proportional to an energy).

The resolution of the Mössbauer spectrum in sums of Lorentzian lines is carried out by computer[48].

The following parameters are usually derived from the Mössbauer spectrum.

1. The isomer shift. This is the displacement of the absorption relative to a chosen standard.
2. The quadrupole coupling. If the charge density around the nucleus is not uniform, the absorption will split up into two symmetrical absorptions. The quadrupole coupling is the distance in a velocity unit between the two absorptions. In some cases a further splitting

of the absorption occurs, but this is of no interest in the present investigation.

3. The absorption area. This is proportional to the ^{57}Fe content in the lattice position. A correction has to be made by quantitative determinations of the Fe content in different lattice positions.

The application of the Mössbauer effect mineralogy has been treated by Maddock[49].

This technique was used in the investigation of arfvedsonite. It was used for the following purposes:

1. Determination of the Fe^{2+}/Fe^{3+} ratio (cf. E. B. Andersen[47], and E. B. Andersen, J. Fenger, and J. Rose Hansen[50]).
2. Determination of the Fe^{2+} or Fe^{3+} contents in different lattice positions. A ^{57}Fe atom in different lattice positions should in principle give different absorptions. In practice, the differences in parameters may be too small to get a good resolution of the two absorptions.
3. Investigation of structural transformations. The Mössbauer spectrum may be regarded as a kind of "finger-print" of the mineral so a change in structure, for example, in the oxidation state, electron configuration, coordination number or symmetry, will cause changes in the Mössbauer spectrum.

3.6. Infrared Spectroscopy

This technique was only used in the investigations of arfvedsonite.

The OH absorption band of the amphibole structure is characteristic for the mineral. Dehydrogenation or dehydroxylation may be investigated by this technique. The silicate structure also gives a characteristic absorption band and so, for instance, a structural break-down may also change the spectrum.

Perkin Elmer 221 apparatus at C.D. was used in these investigations. 1-2 mg of very fine powdered arfvedsonite were pelletized with 200 mg of KBr.

4. COMPARISON OF ROASTING RATES FOR DIFFERENT MINERALS

During the sulphatising roasting of different lujavrite samples it was discovered that the reaction rate depends very much on the mineralogical composition of the sample (cf. chapter 9). This discovery led to the following investigations, where the rate of roasting for a grain size fraction is compared for many of the minerals in the ore. There is some disagreement with the results of Asmund (cf. section 2.4) because some of the minerals that Asmund found to be unreactive or slow reacting were here found to be fast reacting.

4.1. The Reactivity of Minerals During Roasting

As already mentioned in section 2.1, the most important minerals in the ore are arfvedsonite, analcime, microcline, albite, nepheline, acmite, aegirine, natrolite, sodalite and naujakasite. A very rough estimate of the amounts of the minerals gives 30-40% arfvedsonite and a falling content through the series. There are only small amounts of the three last-named minerals.

The reactivity of pure samples of the above minerals was investigated, except for nepheline and naujakasite. Besides these minerals, pyrochlore, steenstrupine, monazite and olivine were also investigated. Except for monazite and olivine, the samples originated from the Ilimaussaq intrusion. Most of the samples were taken from coarse-grained pegmatites, facilitating the isolation of the pure minerals. One of the arfvedsonite samples investigated was taken from an arfvedsonite lujavrite from drilling core 16 (71-73 m depth). A 90% pure fraction was made by magnetic separation. The microline sample was chosen under the microscope from a coarse-grained arfvedsonite lujavrite. The olivine sample originates from Greenland and the monazite sample from Malaya.

The purity of the samples was controlled by microscopic investigations and by X-ray diffractograms. Most of the samples were very pure, although the felspar samples both had impurities of the other felspar. The pyrochlore sample was rather special. The X-ray diffractogram was that of pyrochlore, but microprobe investigations showed that it was composed of more Nb/Si-containing minerals.

A fraction of 40-100 microns was used in the investigation of the reaction rate of sulphatising roasting. The samples were heated to 700°C with a heating rate of 20°C/min. A platinum catalyst was placed in front of the sample in the heating zone. The roasting gas was 5 volume per cent SO_2 in atmospheric air.

No catalyst was used in Asmund's experiments[41]. However, in all experiments including samples without arfvedsonite a catalyst is required and it was therefore used in these experiments. Both arfvedsonite and the sulphates it forms when roasted (hematite dispersed in a melt mainly containing Na_2SO_4) catalyze SO_3 formation (cf. section 5.11.3). The SO_2-SO_3 equilibrium is thereby adjusted.

The weight increase in sulphatising roasting is used as a measure for the reactivity of the mineral. It is supposed that most metal ions released by the crystal structure are bound as sulphate. Oxides, alkaline sulphates and pyrosulphates might, of course, also be formed. The equivalents of SO_3 take-up might therefore not be proportional to the equivalents of metal ions released from the crystal structure. We do not know much about the equilibrium conditions in the sulphate phase, but the rate of weight increase is supposed to be a usable measure for the reactivity.

Figure 4.1 shows the weight increase versus time for the sulphatising roasting of the investigated minerals. Analcine is rather special because the weight increase depends upon the rate of heating to the reaction temperature. This phenomenon will be discussed in section 7.1.

The minerals nepheline and naujakasite were not investigated in pure samples, but in fractions enriched in these minerals. The roasting rate of these fractions clearly indicates that these minerals are among the faster reacting ones.

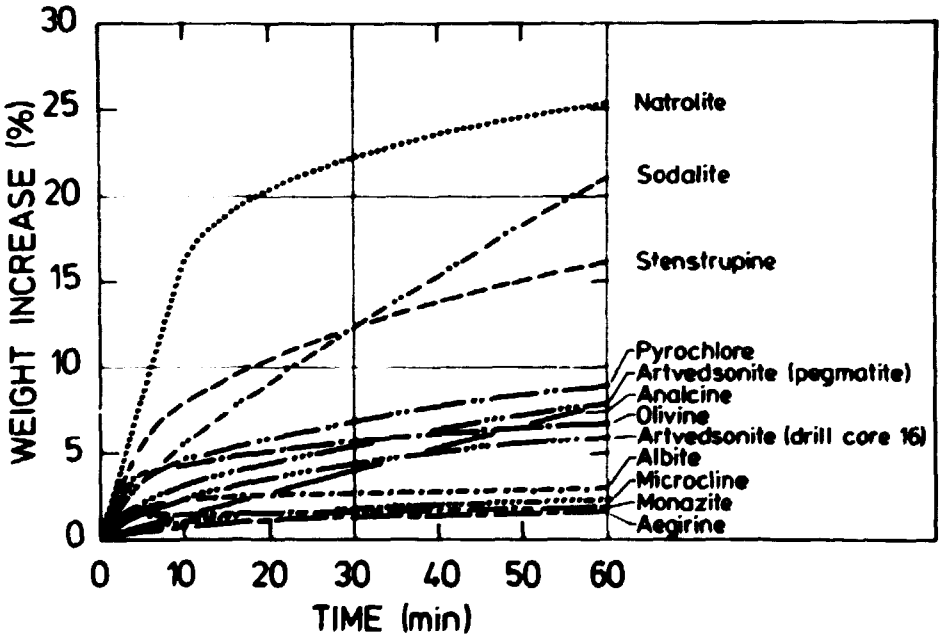

Fig. 4.1. Sulphatising roasting of some minerals at 700°C, grain size 40 - 100 microns, roasting gas 5% SO_2 in atmospheric air.

From these experiments it is concluded, contrary to Asmund's conclusions, that an essential part of the sulphates formed by roasting of a lujavrite sample must originate from the white minerals, especially sodalite, natrolite, and analcime. An additional experiment was made to get a rough estimate of the proportion between sulphate formed from arfvedsonite and from the white minerals in an ore. Some average samples of the ore were prepared by E. Sørensen and T. Lundgaard from several drill cores (cf. chapter 9). From the first sample a fraction greater than 75 microns was magnetically separated into a predominantly arfvedsonite and a predominantly white mineral fraction. Figure 3.2 shows the weight increase versus time for the sulphatising roasting of these samples. The reaction rate is higher for the white mineral fraction than for the arfvedsonite fraction. The ore is supposed to consists of approximately one third arfvedsonite. Thus, for instance, by roasting for 15 minutes at least 60% of the sulphates must originate from the white minerals. The SO_3 take-up for arfvedsonite in a lujavrite sample may be greater than the take-up of a pure sample, because the content of Na_2SO_4 in the sulphates is increased on account of the white minerals, and the stability of ferric sulphate is thereby increased (cf. Wickert[65]).

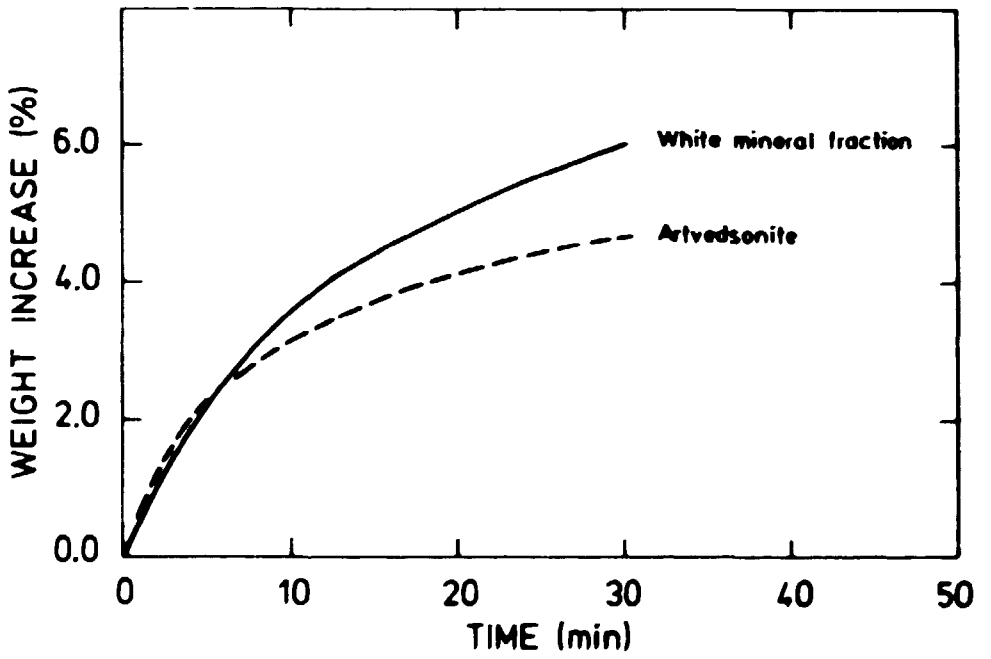

Fig. 4.2. Sulphatising roasting of magnetically separated fractions from an average sample at 700°C by 5% in atmospheric air.

4.2. Discussion

Minerals such as natrolite, sodalite, steenstrupine, and probably also nepheline and naujakasite, are fast-reacting minerals in roasting, while arfvedsonite and analcime are slower, and the felspars and monazite react very slowly.

The fast-reacting minerals make up a smaller part of the ore, but their contribution to the sulphates is essential. Arfvedsonite is the mineral that contributes most to the sulphates, as about 40% originate from this mineral. Analcime is rather special because the weight increase is proportional to time; thus if an analcime-containing sample is roasted for a long time, a greater part of the sulphates will originate from this mineral.

The two arfvedsonite samples investigated had almost the same reaction rate, in spite of different compositions (cf. section 5.4).

The roasting rates found here for the pure fractions were found to be at least qualitatively correct for the lujavrite samples (cf. section 9.4).

5. STRUCTURAL STUDIES OF ARFVEDSONITE

5.1. Introduction

Although arfvedsonite is not a uranium-containing mineral, it is one of the most important minerals in relation to sulphatising roasting of the lujavrites. It is the most widespread mineral and, as shown in chapter four, approximately 40% of the sulphates originate from this mineral. In addition, arfvedsonite and the sulphate phase formed by its roasting (hematite dispersed in a predominantly Na_2SO_4 phase) catalyze the formation of SO_3.

The present investigations were concentrated on a comparative structural study of heat-treated and roasted arfvedsonite.

5.2. Raw Material

Arfvedsonite is widespread in the lujavrites and in many places it is found in large crystals. A coarse-grained pegmatite arfvedsonite, originating from the position marked 1 on the map in fig. 9.1, was used in most of these investigations. It was ground and magnetically separated, and yielded an at least 99% pure fraction.

A microprobe investigation of arfvedsonite from six drilling core samples showed that this arfvedsonite had an unusual composition for the lujavrites, because the SiO_2 content was rather low. Hence a few microprobe investigations were carried out on an arfvedsonite of more common composition. A fraction was made from a sample from drilling core 16 (71-73 m depth) by magnetic separation. An at least 90% pure fraction was obtained.

5.3. Crystal Structure

Arfvedsonite is an amphibole, so the structure consists of double chains of Si-O tetrahedrons. It is depicted in fig. 5.1.

The chains are separated and bound with layers of cations. The cations occupy the positions M_1 (nearly octahedral symmetry, usually contains Fe^{2+} and Mg^{2+}), M_2 (distorted from octahedral symmetry, usually contains Fe^{3+} and Al^{3}), M_3 (nearly octahedral symmetry, usually contains Fe^{2+} and Mg^{2+}) and M_4 (highly distorted from octahedral symmetry, usually contains Na^{+}, Li^{+}, K^{+}, and Ca^{2+}). The A-cation position is usually coordinated with 10-12 anions and is occupied by Na^{+}. Si occupies the tetrahedral positions Si_1 and Si_2. Al may substitute for Si to a lesser extent.

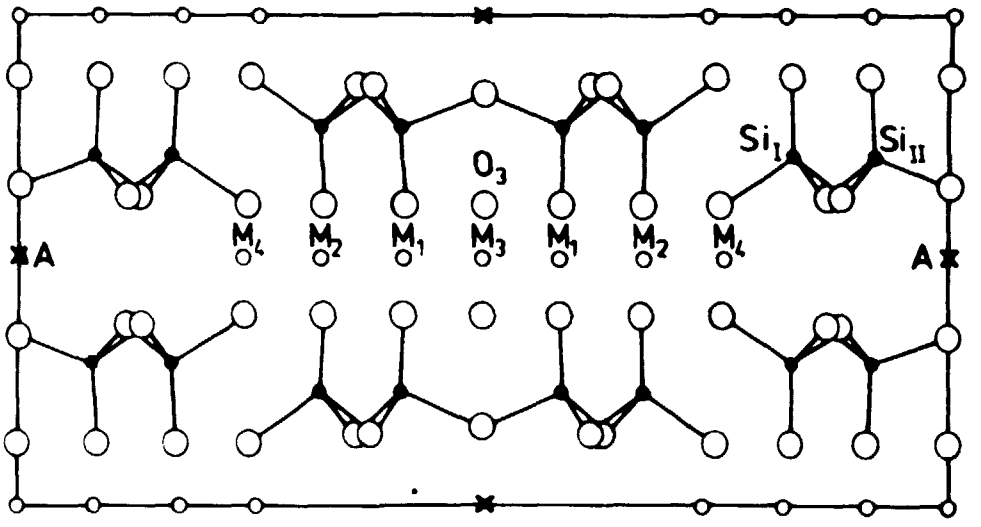

Fig. 5.1. Crystal structure of arfvedsonite, projection on the (110) plane, after Ghose[51].

There are seven different anion positions, of which six are occupied by O^{2-}, and the seventh, O_3, is occupied by a monovalent anion such as OH^- or F^-. The theoretical formula of arfvedsonite is given by Ernst[52]: $Na_3Fe^{2+}_4Fe^{3+}(Si_8O_{22})(OH, F)_2$.

5.4. Chemical Analysis

The composition of the pegmatite arfvedsonite was determined by a wet chemical and by a microprobe analysis. The material was homogeneous, so the microprobe analysis was made on one grain. The arfvedsonite sample from drilling core 16 was also analysed by microprobe. The compositions are given in table 5.1.

A formula was calculated from the two microprobe analyses. This is based on 23 oxygen and one H_2O atoms per formula unit. The pegmatite arfvedsonite:

$$(Na_{2.54}K_{0.33}Ca_{0.07})(Fe^{2+}_{3.18}Fe^{3+}_{1.41}Ca_{0.24}Mn_{0.08}Ti_{0.07}Mg_{0.02})$$
$$(Si_{7.52}Al_{0.47})O_{23}, (H_2O).$$

The Fe^{2+}/Fe^{3+} ratio is not known for the lujavrite arfvedsonite, but the same ratio is assumed.

The lujavrite arfvedsonite:

$$(Na_{2.44}K_{0.60})(Fe^{2+}_{2.57}Fe^{3+}_{1.10}Mn_{0.22}Al_{0.16}Ti_{0.10}Ca_{0.06}Mg_{0.02})$$
$$Si_{8.25}O_{23}, (H_2O).$$

The formula of the pegmatite arfvedsonite is in excellent agreement with the theoretical one (cf. section 5.3). Al occupies tetrahedral positions. The M_1 and M_3 positions must be almost completely filled by Fe^{2+}, while the M_2 position contains some other cations besides Fe^{3+}.

The lujavrite arfvedsonite has a higher Si content. The SiO_2 content is too high and the sum of the cations occupying the M_1, M_2, and M_3 positions is low.

5.5. Heat-treatment, Sulphatising Roasting, and Reduction Experiments

Heat treatment experiments were carried out in the interval 300-800°C, mainly in an oxidising atmosphere, but a few experiments were carried out in an argon atmosphere. The roasting experiments were carried out in the interval 650-750°C. The roasting gas was 5 or 10 volume % SO_2 in atmospheric air. No catalyst was used.

Two grain fractions 56-400 and ⟨20 microns were used in most of the experiments.

Table 5.1

Analysis of arfvedsonite

	Pegmatite arfvedsonite		Lujavrite arfvedsonite
	Wet chemical analysis	Microprobe analysis	Microprobe analysis
SiO_2	49.8 [1]	47.1	50.4
Al_2O_3	2.73 [2]	2.5	0.9
MnO	0.62 [2]	0.6	1.6
CaO	0.52 [2]	1.6	0.3
MgO	-	0.1	0.1
TiO_2	-	0.6	0.8
Na_2O	9.30 [2]	8.2	7.7
K_2O	2.09 [2]	1.6	2.9
FeO	21.9 [3]	23.7 [4]	29.9 as Fe_2O_3
Fe_2O_3	12.2 [3]	11.7 [4]	
total	99.2	97.7	94.3

[1] Analyst, K. Gram Jeppesen.

[2] Analyst, A. Thorboe.

[3] Total Fe determined by A. Thorboe, and the Fe^{2+}/Fe^{3+} ratio determined by Mössbauer spectroscopy (cf. section 5.11).

[4] Total Fe determined by microprobe, and the ratio by Mössbauer spectroscopy.

It has been possible to regenerate OH groups in heat-treated iron-containing amphiboles that resembles arfvedsonite[53, 54, 55]. This was also tried in the present investigations. The reductions were carried out during a 4-hour period at 600°C in an atmosphere of 50% hydrogen and 50% argon.

These samples were used in the structural studies (cf. section 5.8-5.11).

5.6. Results

5.6.1. Heat-treatment Experiments

DTA-TG curves are shown in fig. 5.2 for the grain size fraction 56-400 microns. There is a minor weight loss in the interval 100-450°C and a minor weight increase in the interval > 500°C. The weight increase increases for decreasing grain size.

The colour changes from bluish-green to brown on heating the mineral to 400°C. The grains take on a reddish tinge on heating the fine-grained fraction to 700°C in one hour. For the coarse-grained fraction this colour is first obtained after several hours of heating.

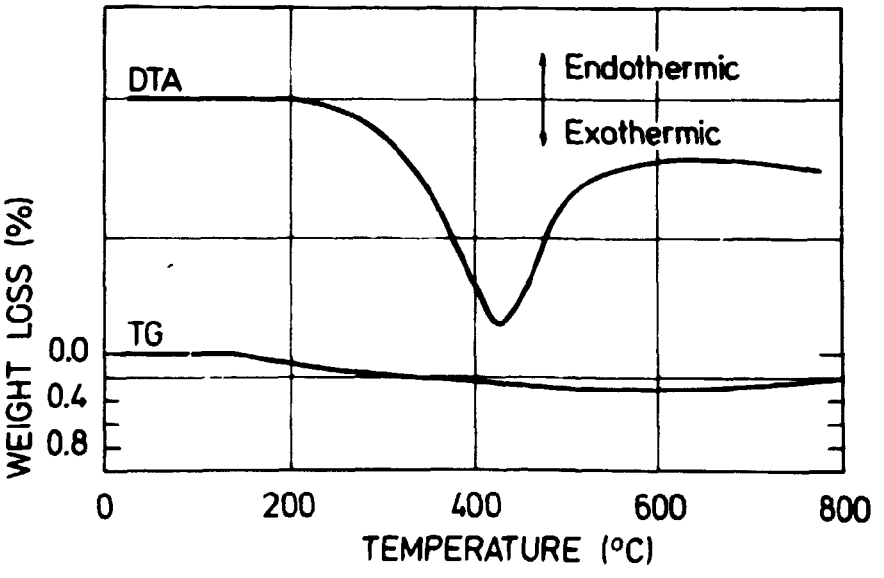

Fig. 5.2. DTA and TG curves of arfvedsonite.

In one experiment the fine-grained sample was heated to 700°C for 40 hours. Table 5.2 gives the weight increase and the calculated percentage of Fe^{2+} that was oxidised to Fe^{3+}. This is the only reaction that can explain the weight increase.

Table 5.2

Heat-treatment of a fine-grained sample at 700°C

Heat-treatment at 700°C, (hours)	Weight increase, (per cent)	Per cent of original Fe^{2+} oxidised
1	0.35	14.5
5	0.65	26.8
10	0.90	37.0
20	1.25	51.5
40	1.80	74.2

Thus most of the Fe^{2+} was oxidised in the 40-hour heat-treatment and hence the original crystal structure must have been almost destroyed.

5.6.2. Sulphatising Roasting Experiments

In fig. 5.3 the weight increase versus time is shown for the roasting of a coarse-grained fraction and a fine-grained fraction at 700°C by 5 volume % SO_2 in atmospheric air.

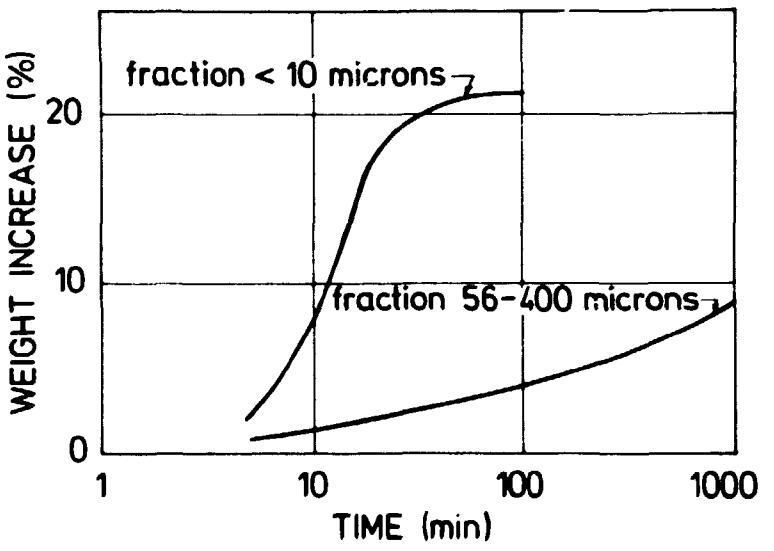

Fig. 5.3. Sulphatising roasting of arfvedsonit at 700°C by 5% SO_2 in atmospheric air.

The fine-grained sample reached a constant maximum weight increase of approximately 21-22 per cent within one hour of roasting. The maximum weight increase increases on decreasing the temperature in the interval 600-750°C. It is approximately 20% at 750°C and 40% at 600°C. These two values are almost independent of the SO_2 partial pressure in the investigated

range 5-15 vol. % SO_2, while it is more dependent in the interval 650-700°C. A sample roasted to a maximum weight increase at one temperature, and then cooled or heated to another temperature with continued SO_2 supply, will reach the same maximum weight increase as if it was roasted at the new temperature. The maximum weight increase as a function of temperature is shown in fig. 5.4. A similar dependence between weight increase, temperature and SO_2 partial pressure is also seen for samples roasted to smaller weight increases.

There is a $Fe_2(SO_4)_3 \rightleftharpoons Fe_2O_3 + 3\ SO_2$ equilibrium in this temperature interval, as discussed in section 5.12.3.

Water vapour in the roasting gas had no effect on the roasting rate at 580 and 700°C.

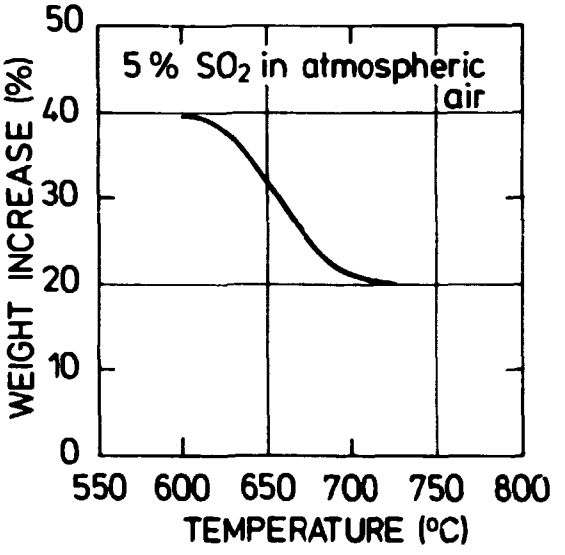

Fig. 5.4. The maximal weight increase versus temperature.

5.7. Microscope Investigations

The raw material, heat-treated and roasted samples were investigated in plane polished samples. One roasted sample was investigated in a thin section.

The raw material was homogeneous.

There were many cracks in the heat-treated and in the roasted samples, and most of them were parallel to the cleavage directions of the arfvedsonite. Samples heat-treated at 700°C for a couple of hours or more were clearly altered along the surface and the cracks. These areas had a red shine in dark field illumination.

Samples roasted from a few per cent to maximum weight increase were

investigated. It was possible to distinguish between three different layers, a sulphate layer situated on the surface of the original arfvedsonite grain, an altered layer unevenly distributed along the surface and in cracks of the arfvedsonite grains, and an apparently unaltered core that was anisotropic. The three layers are outlined in fig. 5.5.

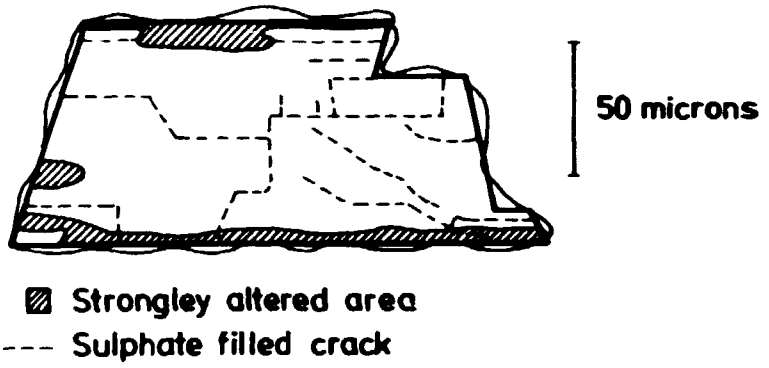

Fig. 5.5. Sketch of a roasted arfvedsonite grain.

The sulphates were unevenly and apparently randomly distributed on the surface. Fine hematite grains were dispersed in this phase.

The altered layer had a reddish shine probably because of precipitated hematite. The thickness of the layer varied but it did not grow along special crystallographic directions. The most altered areas were rich in cracks. The altered part of the grains increased with the weight increase, and the samples roasted to maximum weight increase contained no unaltered core.

The altered surface layer was much thicker in the roasted than in the heat-treated samples.

One sample roasted to 10% weight increase at 700°C was heated in a high-temperature microscope. The sulphates began to melt at approximately 640°C.

5.8. X-ray Diffraction Investigations

The raw material and a sample roasted to 12.5% weight increase at 690°C were investigated by high-temperature diffractograms. The samples were heated to 800°C. Some other samples roasted to different weight increases at 690-700°C and the reduced samples were investigated by normal diffractograms.

Two changes were registered on the high-temperature diffractogram of the raw arfvedsonite. At 300-400°C there were some small displacements in a few lines corresponding to a small contraction in the unit cell. Some

new lines appeared at approximately 600°C. A new crystal phase identified as acmite was formed but the arfvedsonite lines did not disappear.

The formation of acmite is discussed in section 5.12.1. In appendix 2 the diffraction lines are given for the raw material before heating, and after heating to 400°C and 700°C, respectively.

The following phases were identified on the diffractograms of the roasted samples, hematite, $Na_3Fe(SO_4)_3$, $NaFe(SO_4)_2$ and arfvedsonite (the lines of the heat-treated sample). Acmite was not identified. Hematite was only identified in samples roasted to more than approximately 6% weight increase. The arfvedsonite lines did not disappear before the sample was roasted to maximum weight increase.

The $Na_3Fe(SO_4)_3$ and $NaFe(SO_4)_2$ lines disappeared at 450 and 520°C, respectively, on the high-temperature diffractogram of the roasted sample. No new lines were observed as a result of the heating and the subsequent cooling of the sample. The diffraction lines before the heating are given in appendix 2.

The diffractograms of the samples that were heat-treated or roasted and then reduced were almost identical to the original arfvedsonite diffractogram. There were some small differences of 0.01-0.02 Å in some lattice parameters. An average diffractogram is given in appendix 2, and the slight shifts are indicated.

5.9. Electron Microprobe Investigations

These investigations were mostly carried out on the pegmatite arfvedsonite, but a roasted sample of the lujavrite arfvedsonite from drill core 16 was also investigated. Raw material, heat-treated and roasted samples of the pegmatite arfvedsonite were investigated.

The raw material and a sample heated to 700°C were homogeneous. The altered surface layer was too thin to be detected.

The following roasted samples were investigated. The pegmatite arfvedsonite: a fraction of 40-100 microns roasted to 3.1 and 8.6% weight increase, respectively, a fraction of 56-400 microns roasted to 9.0%, and the lujavrite arfvedsonite: a fraction of 40-100 microns roasted to 6.2% weight increase. The roastings were performed at 700°C with 5% SO_2 in atmospheric air.

The mechanism of sulphatising roasting in the lujavrite and the pegmatite samples is undoubtedly identical in both.

The three phases, which were already mentioned in connection with the microscope investigations, were also found here. Outside the original

arfvedsonite grains were the sulphates with dispersed hematite grains. The sulphates were also found in the cracks in the grains. Na and Fe were the dominant metal ions in this phase, but small amounts of the others were also found. Usually Si was not detected in the sulphates, except for the most roasted samples. It is supposed to be present as fractions broken away from the silicate structure and not as dissolved SiO_2.

The borderline between the sulphates and the silicate structure was very well-defined. The altered surface layer was depleted with respect to most of the cations found in the sulphates. Al moved slower than Na, K and Fe. A higher concentration of Si was measured in the surface layer, probably as a result of the depletion of the other ions. The layer was very inhomogeneous.

Na, and to a small extent K, move to the sulphates from the unaltered core of the grains. The movement from the core was very small in the sample roasted to 3.1%, while it was considerable in the coarse-grained fraction roasted to 9.0%. In the last-named sample the Na concentration

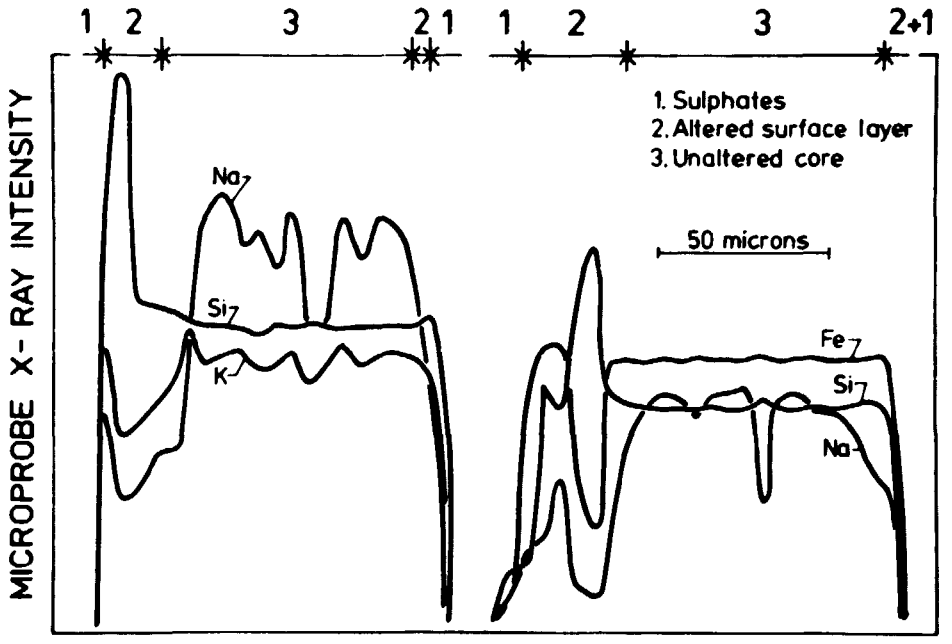

Fig. 5.6. Microprobe X-ray intensity profiles through roasted arfvedsonite grains.

fell to a lower and rather constant value in the core. The Na concentration varied in the two samples roasted to 6.2 and 8.6%. This is shown in fig. 5.6, where some typical X-ray intensities measured for different elements are shown versus distance for the last-named sample. The large variations in the Na concentration show that the reaction is not controlled by bulk dif-

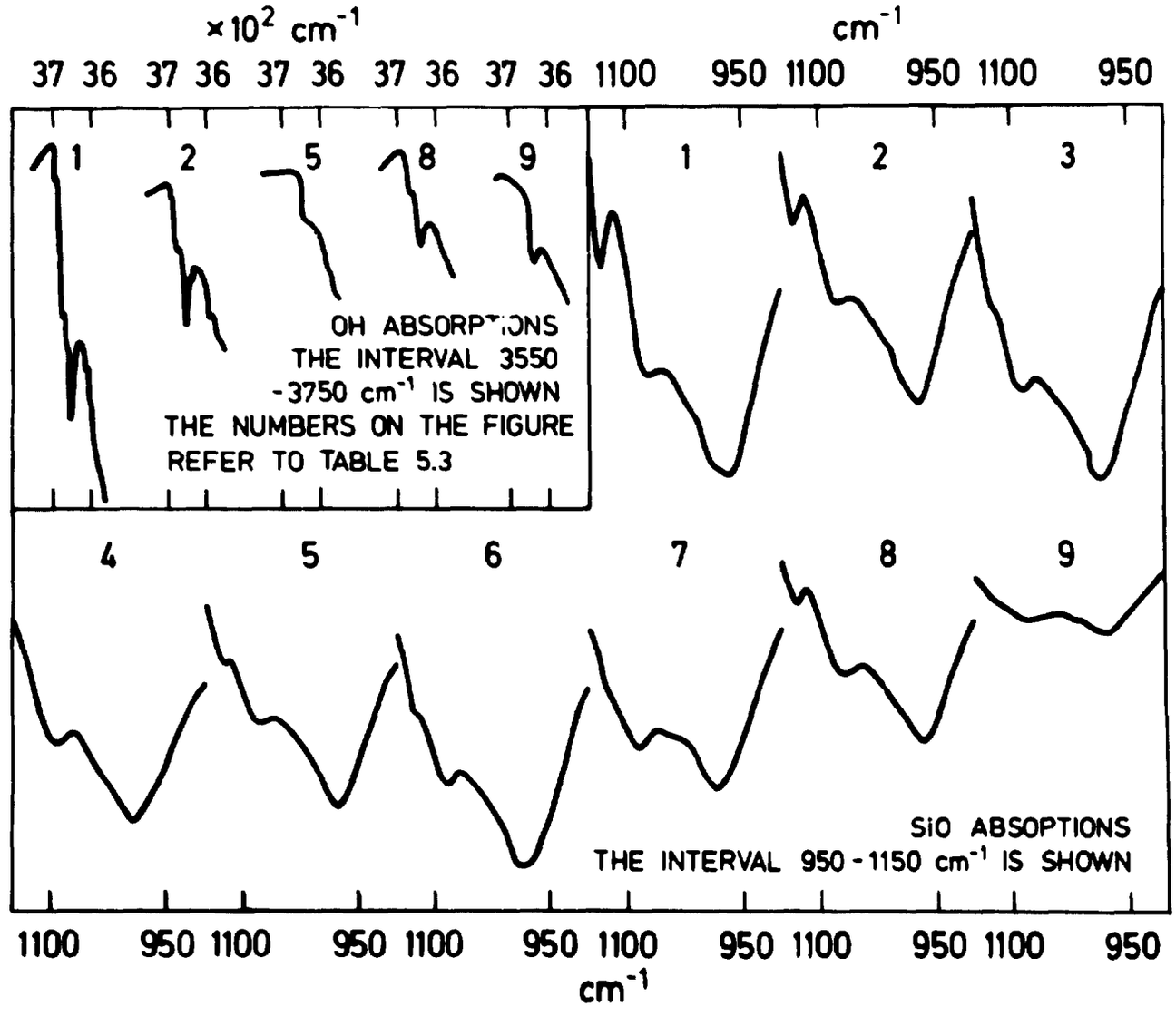

Fig. 5.7. IR spectra of some arfvedsonite samples.

fusion from the interior of the grains to the surface, but instead by short-range diffusion in the silicate structure to sulphate-filled cracks, in which the further transport to the surface takes place.

5.10. Infrared Spectroscopical Investigations

Infrared spectra were made from the raw material, the heat-treated, the roasted and the reduced samples.

In the interval 3600-3700 cm^{-1} there was a OH absorption band and in the range 600-1700 cm^{-1} there were silicate ring and chain absorption bands.

The absorption peaks of the investigated samples are given in table 5.3, where the preceding treatment of the samples is also described. The spectra of arfvedsonite resemble those of other amphiboles such as crocidolite (cf. Patterson and O'Connor[56]). In the interval 700-1600 cm^{-1} the spectrum may be resolved in 5 peaks. In the OH absorption band there is one very strong and some very weak absorptions. Some parts of the spectra are shown in fig. 5.7.

The OH groups are coordinated to 2 M_1 and 1 M_3 lattice positions. Different cation combinations in these positions will give different absorptions, so these positions are mainly occupied by the same cation which is Fe^{2+}, as shown by the chemical analysis in section 5.4.

The first change was observed at 300-500°C by heat treating arfvedsonite in oxidizing atmosphere. The OH absorptions and the absorption at 1132 cm^{-1} disappeared. Simultaneously, the silicate absorptions were displaced towards higher figures. This displacement continued on further heating to 700°C.

The sample heated in an argon atmosphere to 700°C showed some weak traces of the original OH absorption band. The OH groups were therefore not completely lost.

The spectra of the roasted samples had weaker and broader absorptions than those of the heat-treated samples.

The spectra of the samples that had been heat-treated and then reduced were similar to those of the original arfvedsonite. The absorption at 1132 cm^{-1} was regenerated, but a couple of the original very weak OH absorptions were missing. The absorptions of the spectrum of the roasted and reduced sample were much weaker than of the heat-treated and reduced sample.

Table 5.3

Preceding treatment of arfvedsonite samples from which IR spectra were made and the measured IR absorption peaks

Sample	Heat treatment/ Roasting temp. (°C)	Atmosphere	Grain size fraction, microns	Weight increase by roasting (%)
1	Untreated			
2	300	Atmospheric air	< 20	
3	500	" "	< 20	
4	700	" "	< 20	
5	700	Argon	< 20	
6	695 for 2 hours	Atmospheric air	56-400	
7	695 " 2 "	Roasting	56-400	6%
8	Sample number 6 reduced for 4 hours at 600°C			
9	" " 7 " " 4 " " 600°C			

Sample number	Absorptions cm^{-1}								
1	743	968	1075	1132	1580	3627	3640	3655	3669
2	746	969	1075	1132	1580	3629	3644	3655	3670
3	751	984	1086	1125	1580				
4	755	998	1090		1580				
5	750	980	1082	1127s	1580		3646s		
6	755	985	1085	1125s	1580				
7	753	986	1083		1580				
8	743	966	1070	1130	1580		3643		3670
9	745	978	1083		1580	3630	3641		

The absorptions showing an s are much diminished compared to the original ones.

5.11. Mössbauer Spectroscopy Investigations

Mössbauer spectra were made on raw material, on heat-treated, on roasted and on reduced samples.

Roasted arfvedsonite shows a complicated Mössbauer spectrum composed of the hematite and the arfvedsonite residual spectra. The hematite is situated on the surface of the grains and is easy to dissolve in concentrated hydrochloric acid, in which the arfvedsonite is insoluble. This was done to all the roasted samples.

A Fe^{2+}/Fe^{3+} ratio was determined from the Mössbauer spectrum. The concentration was proportional to the absorption area. A correction was required, since the fraction of Fe^{2+} and Fe^{3+} that absorbs and emits the gamma quanta without recoil differs for different lattice positions. For arfvedsonite, the measured Fe^{2+}/Fe^{3+} absorption area ratio has to be multiplied by a factor of 1.17 (cf. E.B. Andersen, J. Fenger, and J. Rose

Hansen[50]). This value was also used for the heat-treated and roasted samples. Its use is justified in appendix 1.

Appendix 1 also shows some of the spectra. Mention is made of the criteria after which they are resolved, and the calculated parameters are given.

The spectrum of the raw material is similar to other arfvedsonite spectra[50]. It may be resolved in three doublets of which two refer to Fe^{2+} in the lattice positions M_1 and M_3 and the third to Fe^{3+} in the M_2 position. The absorption areas of the two Fe^{2+} absorptions overlap very much. The standard deviation (s.d.) on the Fe^{2+} contents in these positions is therefore large. The s.d. on the Fe^{3+} absorption is, on the other hand, small and thus the total Fe^{2+} and Fe^{3+} contents may be determined with a s.d. of approximately 2%. The contents in the lattice positions are given in table 5.4.

Table 5.4

Fe^{2+} and Fe^{3+} contents in lattice positions of arfvedsonite

Absorption	% of total absorption	Standard deviation %	Corrected Fe^{2+} and Fe^{3+} contents
Fe^{2+} in M_1	50.8	9.0	69.4
Fe^{2+} in M_3	15.2	12.0	
Fe^{3+} in M_2	34.0	1.5	30.6

This solution of the arfvedsonite spectrum is statistically acceptable according to the computer program.

The absorption of Fe^{2+} in M_3 is rather broad. This indicates an overlap of another absorption, perhaps Fe^{2+} in M_2. The Fe^{2+} in M_1 absorption is therefore rather large compared to the Fe^{2+} in M_3 absorption. The M_1 position is supposed to be completely occupied by Fe^{2+}, while the M_3 position is only partly filled.

The Mössbauer spectrum of arfvedsonite changes if the sample is heated to temperatures higher than 300°C. In fig. 5.8 the total Fe^{2+} content is shown versus temperature. There is a remarkable decrease in the interval 300-500°C, and a much smaller decrease at higher temperatures.

The spectra of the heat-treated samples may be resolved in 4 doublets, 3 of them have almost the same parameters as the untreated arfvedsonite. A new doublet is supposed to originate from Fe^{3+} in the M_1 position, as described in appendix 1. The parameters of some heat-treated samples are also given in appendix 1.

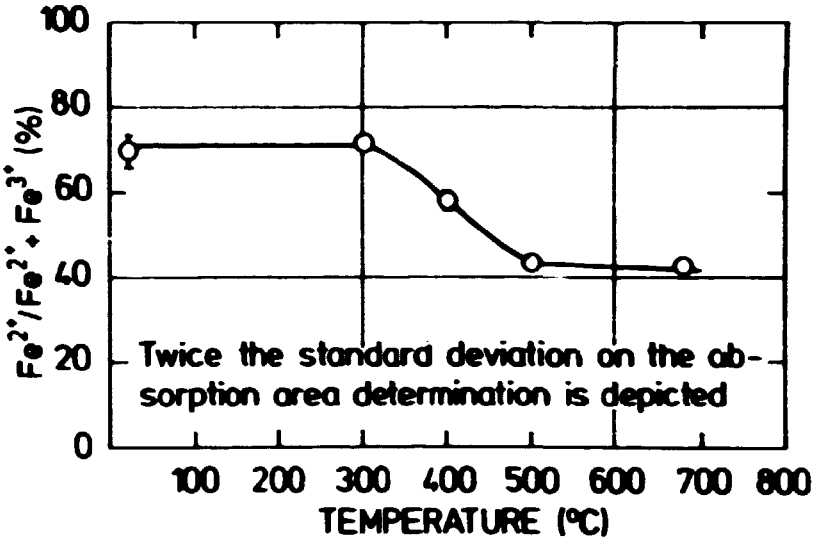

Fig. 5.8. Fe^{2+} content in arfvedsonite as function of heat-treatment temperature.

The two Fe^{2+} and the two Fe^{3+} absorptions overlap mutually, so the s.d. on the absorption area determination is very large. However, the total Fe^{2+} content is determined with a s.d. of approximately 2%.

Except for the new Fe^{3+} in M_1 absorption, it is difficult to see what has happened at the single lattice positions, because of the overlap.

Ernst and Wai[57] investigated the heat treatment of ribeckite ($Na_2Fe^{3+}{}_2Fe^{2+}{}_3Si_8O_{22}(OH)_2$). The Mössbauer spectra of this amphibole and heat-treated samples are in principle identical to the similar ones of arfvedsonite. However, there are differences in the interpretation by Ernst and Way of the heat-treated spectra of ribeckite and of arfvedsonite in the present investigation. These differences are shown in appendix 1, where arguments are put forward for the correctness of the present interpretation.

The spectra of the roasted samples (the hematite formed by the roasting was dissolved before the spectra were made) were identical to those of the heat-treated ones. In table 5.5 the Fe^{2+} contents in heat-treated and roasted samples are compared.

The differences between the Fe^{2+} contents in the two compared samples are in all cases within the s.d. of the measurement.

In appendix 1 two spectra of heat-treated and roasted samples are shown. They are identical.

Four of the samples used in the comparison of the heat-treated and roasted samples were reduced for 4 hours at 600°C. Two of the spectra and the parameters are given in appendix 1.

Table 5.5

A comparison of heat-treated and roasted samples

Sample number	Grain size fraction (microns)	Heating/ roasting-temperature (°C)	Heating/ roasting (hours)	Weight increase (%)	Fe^{2+} absorption area (%)
1	20	690	0.5		35.0
2	20	690	0.5	18.0	37.2
3	56-400	695	2.0		42.4
4	56-400	695	2.0	6.0	39.2
5	20	695	1.0		35.0
6	20	695	1.0	6.0	37.6

The spectra were resolved in the same way as those of the untreated arfvedsonite. The following contents were measured in the single lattice positions as given in table 5.6.

The reduction was not complete for samples 4 and 5. The broadness of the Fe^{3+} absorptions indicates an overlap of another absorption, probably Fe^{3+} in M_1. Samples 3 and 6 are more reduced than the original arfvedsonite. This is probably because some O_3 positions in the arfvedsonite were occupied by O^{2-}.

Table 5.6

The Fe^{2+}-Fe^{3+} contents of the different lattice positions in reduced arfvedsonite samples

Sample number (table 5.5)	Fe^{2+}-Fe^{3+} at lattice position (%)		Standard deviation (%)	Corrected Fe^{2+} content
3	Fe^{2+} in M_1	51.8	3.7	74.9
	Fe^{2+} in M_3	20.2	5.2	
	Fe^{3+} in M_2	28.2	1.2	
4	Fe^{2+} in M_1	37.6	2.8	67.3
	Fe^{2+} in M_3	26.2	3.8	
	Fe^{3+} in M_2	36.2	1.1	
5	Fe^{2+} in M_1	37.8	7.4	69.7
	Fe^{2+} in M_3	28.4	10.2	
	Fe^{3+} in M_2	33.7	1.2	
6	Fe^{2+} in M_1	47.6	2.8	72.9
	Fe^{2+} in M_3	22.0	4.0	
	Fe^{3+} in M_2	30.2	0.8	

5.12. Discussion

The discussion of the present results may be divided into three parts.

1. Heat treatment of arfvedsonite.
2. Sulphatising roasting of arfvedsonite.
3. The sulphates formed by the roasting.

5.12.1. Heat-treatment of Arfvedsonite

The changes that are observed in arfvedsonite as a result of heat-treatment in an oxidizing atmosphere are given in table 5.7.

A corresponding set of reactions is known for similar amphiboles such as crocidolite and riebeckite[53,54,55,56,57,58,59,60,61,62]. Uncombined water is lost in the interval 100-400°C. A dehydrogenation takes place at 300-500°C. This may be described by the reactions:

1. In the mineral:

$$Fe^{2+} + OH^- \simeq Fe^{3+} + O^{2-} + H^+ + e^-.$$

2. At the surface:

$$H^+ + e^- + 1/4\ O_2 \simeq 1/2H_2O.$$

Hydrogen ions and electrons are supposed to move to the surface during the dehydrogenation[55], because the electron movement may occur through the Fe^{3+} atoms.

A continued oxidation of Fe^{2+} takes place at temperatures above 500°C. This is a surface oxidation in which acmite and, in long-time heat treatment, also hematite are formed.

The dehydrogenation only occurs in oxidizing atmospheres. A dehydroxylation was observed at 600-700°C in neutral or reducing conditions. The crystallographic changes were small in dehydrogenation. The coordination numbers were unchanged, but the unit cell parameters were diminished approximately 1%, because the Fe^{3+} ion is smaller than the Fe^{2+} ion.

Dehydroxylation is a much more destructive process than dehydrogenation because oxygen ions are removed from the lattice.

The continued oxidation of arfvedsonite above the dehydrogenation temperature is characterized by acmite formation and, if heat-treatment continues for many hours, also by hematite formation. Acmite is formed first because there are considerable structural similarities between the arfvedsonite and the acmite structure. The transformation demands in principle only some displacements in the Si-O tetrahedrons, but no long-range diffusion.

An incipient thermal decomposition of the arfvedsonite structure might be expected at 700°C. It is probably seen as a less intense Si-O band in the IR spectra. Patterson[60] investigated the decomposition of the mineral crocidolite (a). At 800°C it is decomposed into hematite (h), a spinel (s), acmite (p) and cristoballite (c). The decomposition products are oriented in proportion to the original structure after the following planes:

$$(100)_a \,||\, (100)_p \,||\, (0001)_h \,||\, (111)_s \,||\, (011)_c \,,$$

and the following directions,

$$c_a \,||\, c_p \,||\, c_h \,||\, \{211\}_s \,||\, a_c \,.$$

Table 5.7

Heat treatment of arfvedsonite in oxidizing atmosphere

Temperature (°C)	Change
100-400	A minor weight decrease on the TG curve.
300-500	Loss of the OH band in the IR spectrum. An exothermal reaction is observed on the DTA curve. The Fe^{2+} fraction of total Fe is decreased from 70 to 42%. There is a small contraction in the unit cell parameters on the X-ray diffractogram. The colour of the grains alters from bluish-green to brown.
> 500	A minor weight increase is observed on the TG curve, especially for fine-grained samples. The Fe^{2+} fraction of total Fe still decreases but at a much slower rate.
600	Acmite is observed on the X-ray diffractogram.
700	Hematite is formed if roasting continues for a few hours.

Acmite is formed very easily, while the formation of the other crystalline compounds demands more transformations and more diffusion. Cristobalite formation is especially difficult. Spinel and cristobalite were not identified in the present investigation.

It was possible to almost regenerate the original arfvedsonite structure in a sample heated to 700°C by reduction. The small changes in Mössbauer parameters and in lattice parameters indicate a slightly different structure.

The structure of the oxyamphibole at 700°C is therefore rather unchanged from the original. A surface oxidation takes place and probably a thermal decomposition of the structure begins, but these are rather slow processes compared to the roasting time.

5.12.2. Sulphatising Roasting of Arfvedsonite

Roasting is a surface process taking place both at the outside surface of the grains and in the many cracks in the structure. We may distinguish between three layers in the roasted grains. The sulphates are situated on the surface of the grains and in the cracks. The silicate structure, which is nearest to the sulphates, is strongly altered, while the rest of the structure is almost unaltered. The altered layer has a red colour indicating hematite formation, and the layer is depleted with respect to metal ions, especially Na.

The unaltered part of the grains is almost unchanged, althouth in some areas it is depleted with respect to Na. The majority of the metal ions in the sulphates originate from the altered layer.

We may distinguish between the following processes taking place during roasting.

1. Na diffusion from the unaltered areas of the grains.
2. Surface alteration.
3. Metal ion diffusion from the altered areas.

These processes are undoubtedly connected to each other.

The cracks are an important factor both in the alteration - there are always numereous cracks in the most altered areas - and in the movement of Na from the unaltered areas and metal ions from the altered areas, because the metal ions diffuse through the silicate structure to the sulphate-filled cracks and through these to the surface. The diffusion in the silicate structure is therefore short-ranged compared to the dimensions of the grains.

The diffusion in the altered area must be a rapid process compared to the diffusion in the unaltered areas because the original silicate structure must have broken down. Na in the A position of arfvedsonite is labile compared to the other cations in the structure, because the A positions form a channel-like system. Papike et al.[63] exchanged Na for K in this position in the amphibole richterite $(Na,K)_2(Mg,Mn,Ca)_6Si_8O_{22}(OH)_2$ by heating the mineral to 850°C in a salt melt.

Asmund[1] proposed a roasting mechanism composed of the following two reactions:

1. a) diffusion : $2Me^+ + O^{2-}$ to the surface,
   b) surface reaction : $2Me^+ + O^{2-} + SO_2 + \frac{1}{2}O_2 \rightleftharpoons Me_2SO_4$.
2. a) in the lattice . $2Fe^+ \rightleftharpoons 2Fe^{3+} + 2e^-$,
   b) diffusion : $2Me^+ + 2e^-$ to the surface,
   c) surface reaction : $2Me^+ + 2e^- + SO_2 + O_2 \rightleftharpoons Me_2SO_4$.

The present Mössbauer investigations clearly showed that Fe^{2+} is not oxidized in the unaltered parts of the grains. However, it is undoubtedly oxidized in the altered surface layer; as proved by the red colour of the hematite and by the Mössbauer investigations of Asmund[1]. The second reaction might therefore occur in the surface layer. The oxide ion might, on the other hand, have a sufficiently large mobility in the altered layer for the first reaction to occur, perhaps as a pore diffusion through micro-cracks.

We cannot explain the Na diffusion in the interior of the grains by an oxidation of Fe^{2+}. An oxygen ion bulk diffusion, as proposed in the first reaction of Asmund, must be impossible. If a diffusion coefficient of 10^{-14} cm^2/s is supposed for the oxygen ion diffusion in the lattice (the real value is undoubtedly much lower), the penetration of the diffusion profile for a diffusion time of 15 min should be $(Dt)^{\frac{1}{2}} = (10^{-14} \times 900)^{\frac{1}{2}}$ cm = 0.03 microns.

The Na diffusion in the interior of the grains must therefore be explained either by pore diffusion of oxygen ions or by a counter diffusion of another cation such as H^+. The counter diffusion is unlikely because the reaction rate did not depend on the amount of water vapour in the roasting gas, in contrast to, for instance, natrolite (cf. section 7.3).

5.12.3. The Sulphates Formed by the Roasting

Arfvedsonite, hematite, $Na_3Fe(SO_4)_3$ and $NaFe(SO_4)_2$ were identified on the diffractograms of the roasted samples. Na and Fe are the main cations in the sulphates. The maximum weight increase decreases with increasing temperature in the range 650-750°C. An equilibrium must exist between the sulphates and SO_3 in this interval.

Theoretically, there is a possibility of pyrosulphates, sulphates, basic sulphates or oxides in the sulphates, depending on the equilibrium conditions in this very complicated multicomponent system.

A general view of the system can be obtained by considering the main component system, Na_2SO_4-$Fe_2(SO_4)_3$-Fe_2O_3-SO_3. Literature on this system is sparse. The Na_2SO_4-$Fe_2(SO_4)_3$ system has been investigated by Bolshakow et al.[64]. The phase diagram is shown in fig. 5.9.

Vickert investigated the stability of the two above-mentioned double sulphates in the presence of SO_3. His results are shown in fig. 5.10. Basic sulphates, such as $6Na_2SO_4$, Fe_2O_3, $Fe_2(SO_4)_3$, may be formed by the decomposition. The stabilities of some Na_2SO_4-$Fe_2(SO_4)_3$ mixtures are shown in fig. 5.11. $Fe_2(SO_4)_3$ is stabilised by the presence of Na_2SO_4.

The diffractions of $Na_3Fe(SO_4)_3$ and $NaFe(SO_4)_2$ disappeared at 520

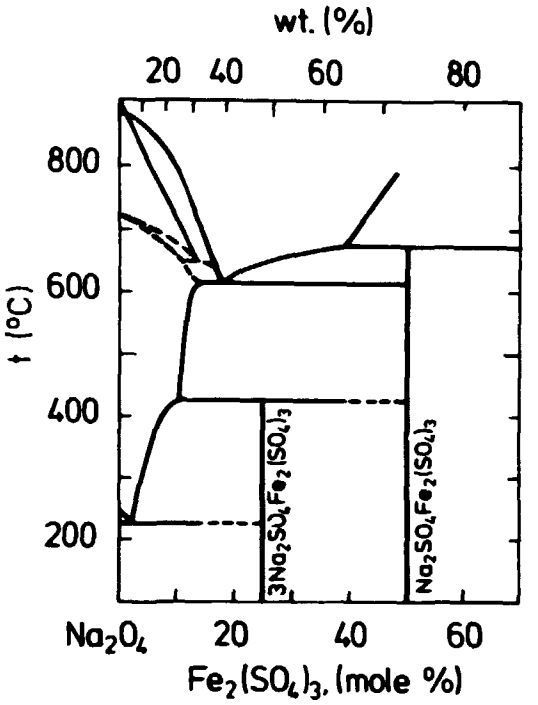

Fig. 5.9. The Na_2SO_4 - $Fe_2(SO_4)_3$ phase diagram, after Bolshakow et al.[64].

and 450°C, respectively, on a high temperature X-ray diffractogram. The phase diagram of Bolshakow et al.[64] gives 420 and 680°C, respectively, so the agreement is very poor. This might be a consequence of the occurrence of other cations in the present system.

The two double sulphates are present on the X-ray diffractograms of the samples roasted at 700°C, so the Na to Fe ratio in the sulphates must lie in the range 3:1 to 1:1. The ratio must be a function of gas composition,

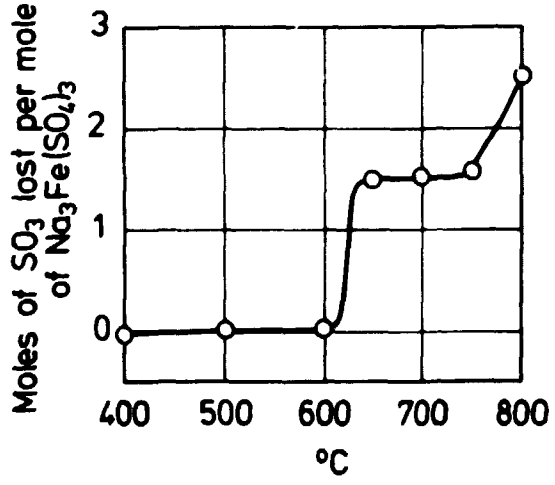

Fig. 5.10. Decomposition of $Na_3Fe(SO_4)_3$; the SO_3 loss was determined after 6 h of heating in an atmosphere of 0.7 vol% SO_3 in atmospheric air.

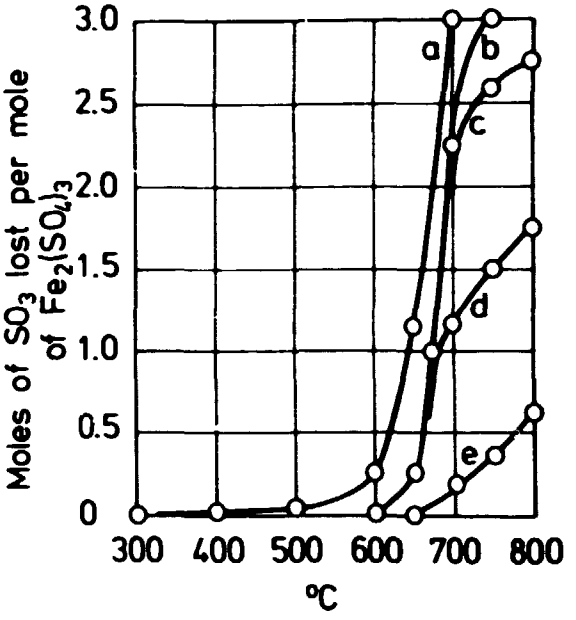

Fig. 5.11. The decomposition of some Na_2SO_4 - $Fe_2(SO_4)_3$ mixtures.
a) $Fe_2(SO_4)_3$ in atmospheric air,
b) $Fe_2(SO_4)_3$ in atmospheric air with 9 vol% SO_3,
c) $Fe_2(SO_4)_3/Na_2SO_4$ mole ratio 1/1 in the atmosphere of "b",
d) $Fe_2(SO_4)_3/Na_2SO_4$ mole ratio 1/3 in the atmosphere of "b",
e) $Fe_2(SO_4)_3/Na_2SO_4$ mole ratio 1/8 in the atmosphere of "b".

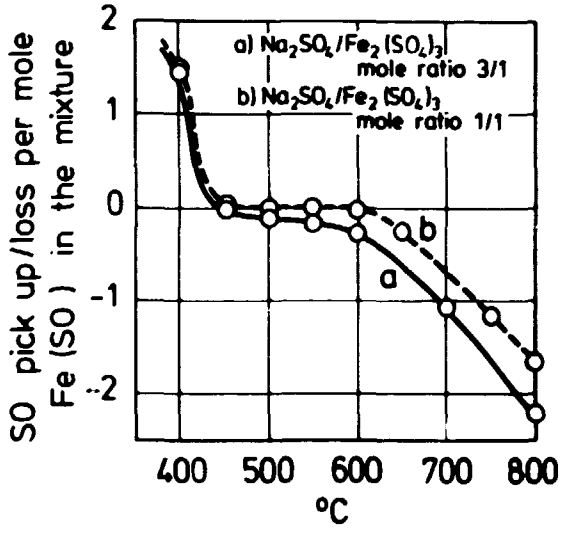

Fig. 5.12. SO_3 pick up and loss by heating a mixture of Na_2SO_4 and $Fe_2(SO_4)_3$ in a flow of 9 vol% SO_3 in atmospheric air.

temperature, and cooling conditicns (slow cooling rates with a continued SO_2 supply give equilibrium at lower temperatures, while a rapid cooling might maintain the high temperature equilibrium).

The samples roasted to maximal weight increase at 650°C still contained hematite in the sulphates, thus it is impossible to roast all the hematite to sulphate. This agrees with the results of Vickert[65], who roasted a mixture of Na_2SO_4 and Fe_2O_3 at different temperatures. The theoretical SO_3 uptake was not obtained at temperatures above 400°C.

Vickert also investigated the presence of pyrosulphates in the Na_2SO_4-$Fe_2(SO_4)_3$ system. As shown in fig. 5.12, there is no pyrosulphate present above 450°C. So the presence of $Fe_2(SO_4)_3$ decreases the stability range of pyrosulphates. A mixture of Na_2SO_4, $Fe_2(SO_4)_3$ and hematite is an SO_3 catalyst at these temperatures[66]. Presumably it is the sulphates, rather than the arfvedsonite, that catalyze SO_3 formation during most of the roasting period.

6. STRUCTURAL STUDIES OF STEENSTRUPINE

Steenstrupine might be described as a Na-Ca-Fe-Mn-rare earth-silico-phosphate that contains small amounts of U and Th. The composition can vary within wide limits. The most important property in relation to the sulphatising roasting is its degree of alteration. The recovery of uranium from lujavrite samples containing different types of steenstrupine is reported in chapter 9. The recovery is shown to depend on the degree of alteration, as the best recoveries are obtained from the most altered samples and the poorest from the homogeneous ones. Most of the uranium not recovered by the sulphatising roasting is thus contained in the homogenous and the partly altered steenstrupine.

A perfect steenstrupine for an investigation of the mechanism of the sulphatising roasting should be homogeneous and all grains should have the same composition. Probably such a steenstrupine does not exist, because there are always variations between the grains.

Investigations of two different steenstrupines are reported in this chapter. Most of the experiments were carried out on a pure sample hand-picked under the microscope from a steenstrupine vein in drilling core number 1 at a depth of 44 m. A few microprobe investigations were made on steenstrupine grains in a lujavrite sample from drilling core 24 at a depth of 86.50-86.75 m. (This sample is also described in section 9.3).

6.1. Raw Material Investigations

A microscopic investigation of the steenstrupine from the vein showed it to be isotropic, the colour yellow-brown in transmitted light. The natural grain size is $\rangle$ 100 microns, so the grains are free of each other in the fraction of $\langle$ 56 microns used for the experiments.

The X-ray diffractogram showed some very weak lines that were identified as originating from acmite. As expected, there were no steenstrupine lines because the mineral is metamict.

The fraction was supposed to be at least 90% pure. By microprobe investigation, the following elements were detected: Ca, Si, Y, P, La, Ce, Nd, Pr, Mn, U, Th, Na, and traces of K, Sm, Al, Ti, and Zr. The grains were not completely homogeneous and there were variations from grain to grain.

The U content was 1.04% determined by a chemical analysis. A complete analysis was impossible because the amount of steenstrupine was too small. The variations in composition made a microprobe analysis very

difficult. A qualitative microprobe investigation showed a composition that was not abnormal. The average ratio of Si to P was between 2:1 and 3:1. The Th/U ratio was about 4:1.

6.2. Heat-treatment Experiments

TG - DTA curves are shown in fig. 6.1. The weight loss below 700°C was approximately 8 per cent. Most of the water was lost below 300°C.

The following peaks were registered on the DTA curve:

Peak maximum 120°C (interval 60-180°C): Endotheric reaction.
Peak maximum 300°C (interval 290-310°C): Very weak endothermic reaction.
Peak maximum 600°C (interval 590-610°C): Very weak endothermic reaction.
Peak maximum 660°C (interval 650-665°C): Exothermic reaction.
Interval 760-900°C: Endothermic reaction.

The last-named endothermic reaction might be composed of two reactions, the first in the interval 670-680°C and the second in the interval 690-900°C.

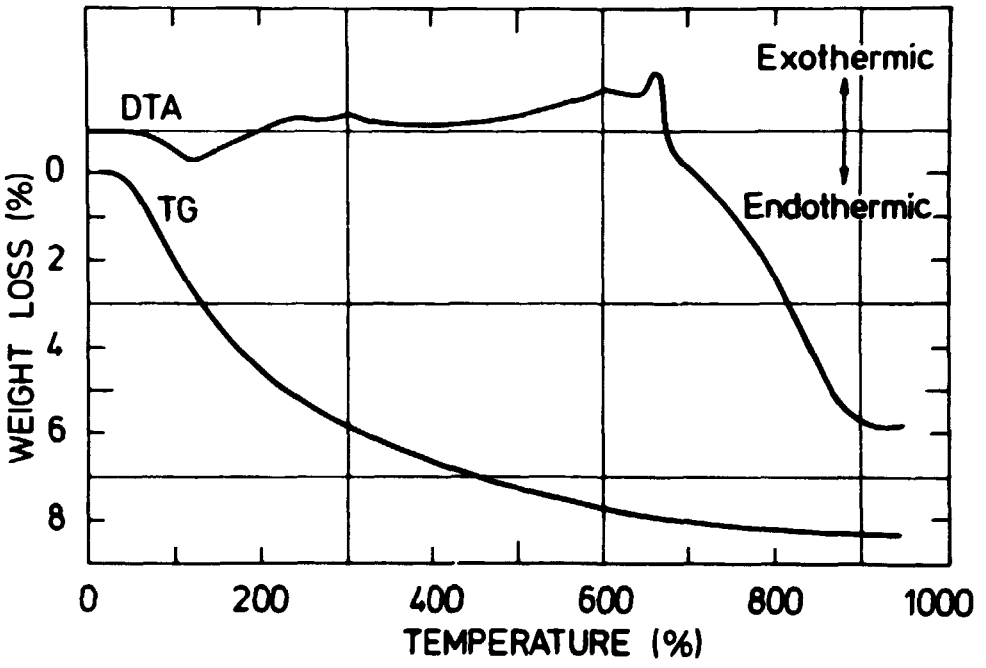

Fig. 6.1. TG-DTA curves of steenstrupine.

An X-ray diffractogram of a sample heated to 700°C for two hours showed only one weak and very broad line, which might be the strongest line of monazite.

Monazite and a (U, Th)O_2 compound were identified on diffractograms

of samples heated to 800 and 960°C. The diffraction lines are given in appendix 3. Thorianite was found by heat treatment of another steenstrupine sample[71].

The sample heated to 700°C was investigated in the microprobe. The grains were more inhomogeneous than in the raw material, but it was not possible to detect a monazite or a silicate phase.

6.3. Sulphatising Roasting

A steenstrupine fraction of < 56 microns was used in the sulphatising roasting experiments. The fraction was roasted to different weight increases with and without a Pt catalyst at 700°C. The roasting gas was usually 5 volume per cent SO_2 in atmospheric air. The weight increase versus time for the two experiments is shown in fig. 6.2. The initial

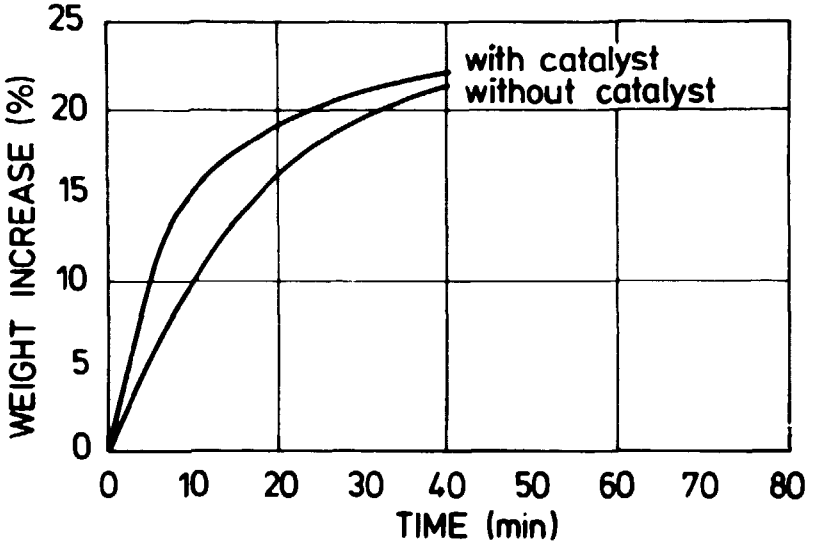

Fig. 6.2. Sulphatising roasting of steenstrupine, influence of a Pt-catalyst.

roasting rate was increased by the presence of the catalyst, but the maximum obtainable weight increase was the same. The maximum obtainable weight increase depended on temperature and SO_2 partial pressure. It was, for instance, 28% when roasting at 700°C with 5 volume% SO_2 in the gas, but 33% at 600°C with 15% SO_2.

X-ray diffractograms were obtained from samples roasted to different weight increases. The sulphates were first extracted by a 0.1 n sulphuric acid. Monazite was identified on all the diffractograms. No other phases except for $Ce_2(SO_4)_3$ were identified. This phase was very difficult to dissolve and something remained insoluble after extraction of 100 mg sample with 5 ml of the acid solution.

The recovery of uranium versus the weight increase is shown in fig. 6. 3. The recovery is below 60 per cent at the maximum weight increase.

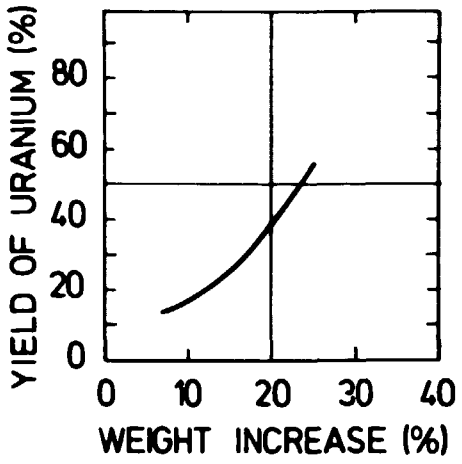

Fig. 6. 3. Sulphatising roasting of steenstrupine, yield of uranium.

When steenstrupine was roasted at 580°C and 700°C, the roasting rate was increased by increasing the amount of water vapour in the roasting gas, but the effect was small at 700°C.

Some samples roasted to weight increases below 15% were investigated by microprobe. An altered surface layer was depleted with respect to metal ions, especially Na. U and Th seemed to be rather unchanged. This sample was, however, unsuitable for an investigation of the mechanism of sulphatising roasting because of the differences between and inside the grains.

Some microprobe investigations were instead performed on steenstrupine grains from the lujavrite sample from drilling core 24. The steenstrupine grains were almost homogeneous, but there were, of course, variations from grain to grain. A lujavrite sample was roasted. A fraction of > 75 microns was magnetically separated in a predominantly arfvedsonite and a predominantly white mineral fraction. In one experiment the latter fraction was roasted to 3. 5% weight increase at 700°C. A steenstrupine grain was

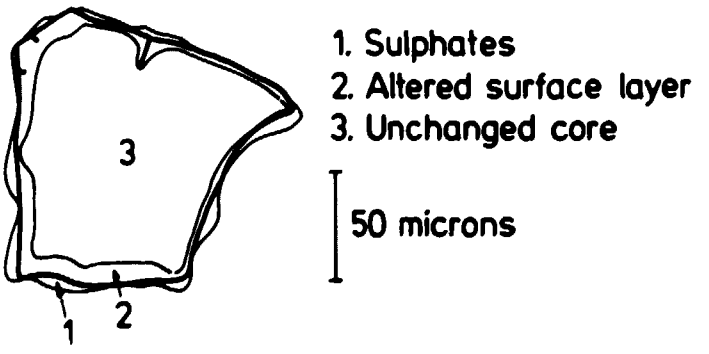

Fig. 6. 4. Sketch of a roasted steenstrupine grain.

investigated in a polished sample. In a microscopic and microprobe examination three layers may be distinguished, as outlined in fig. 6.4. Outermost there was a sulphate layer that gradually changed into a silicate-phosphate-sulphate layer. The core in the interior of the grain was unchanged and the borderline between this and the mixed phase was quite well-defined. In dark field illumination the mixed phase was characterised by a red colour.

Profiles of the measured X-ray intensity versus distance are shown in fig. 6.5, where the three zones are marked. In a few profiles there was

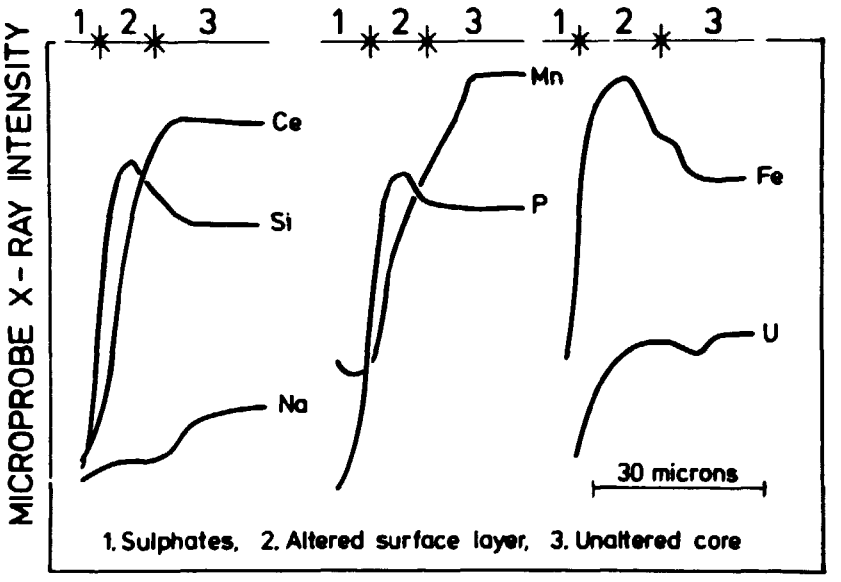

Fig. 6.5. Microprobe X-ray intensity profiles through a roasted steenstrupine grain. The profiles are made perpendicular to the surface with intervals of a few microns.

an indication of a fourth layer between the unaltered core and the silicate-phosphate-sulphate layer, as shown in fig. 6.6. This new layer was very thin and rich in Na and S, but poor in Si and P. It may, however, have represented a sulphate-filled crack, although a similar layer was seen when roasting sodalite (cf. section 7.2). The sulphate-filled cracks were few in number compared to arfvedsonite.

A higher X-ray intensity was measured for the elements Si, Fe, and K in the silicate-phosphate-sulphate layer. The higher Fe and Si intensities could be caused by a change in matrix effect owing to lower concentrations of other cations, while there was probably a real enrichment in K in this layer. Fe was undoubtedly found as hematite, because of the red colour of the layer.

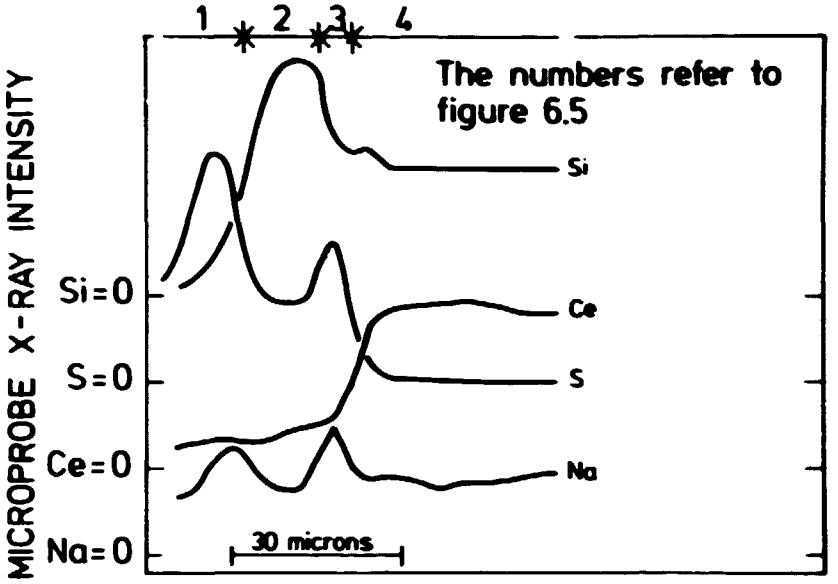

Fig. 6.6. Microprobe X-ray intensity profiles through a roasted steenstrupine grain.

The altered surface layer was depleted with respect to some metal ions, especially Na and Ca, while there was no sign of a depletion in the unaltered core, except for a Na diffusion from the outer few microns.

6.4. Some Investigations on the Raw Material Used by Asmund

A few investigations were made on this raw material. The fraction used by Asmund in his experiments was less contaminated with other minerals than the fraction investigated here. The analysis of Asmund's steenstrupine[1)] is distinguished from other analyses by an Al_2O_3 content of 6.23%, where it is usually below 1%. A microprobe investigation showed a much lower Al_2O_3 content in the steenstrupine grains. Albite was detected on an X-ray diffractogram, and a microscopic investigation showed other impurities in the sample, so this steenstrupine fraction must have contained an essential proportion of impurities.

A cursory investigation of a number of the steenstrupine grains was made by microprobe; some grains were homogeneous but most were partly altered. A definition of this type is given in section 8.3.

Asmund's original X-ray diffractograms of heat-treated and roasted steenstrupine were examined, too. Monazite was detected and the intensities of the diffraction lines were increased by higher weight increases. Besides these lines, there were others that were impossible to relate to any mineral in the ASTM card file. The intensity of these diffractions varied.

6.5. Discussion

Little is known of equilibrium conditions in the multicomponent system of steenstrupine composition. One sample was investigated here, but because of the variations in the compositions of different steenstrupines it is not likely that they all react exactly as the present one.

The investigated steenstrupine began to melt at 680°C and at 700°C it was composed of a fine-grained monazite phase, an amorphous phase, perhaps a (U, Th)O_2 phase and a minor amount of melt. When heated to higher temperatures, the amount of melt increased, so the grain size of the monazite and the (U, Th)O_2 compound was definitely identified.

The amounts of rare earths and phosphorus usually correspond to the composition of monazite, so it is most likely that these elements were concentrated in this phase. The amorphous phase and the melt were therefore prevailing silicates.

Asmund[1] found that the roasting rate for steenstrupine at 700°C depended on the amount of water vapour in the roasting gas. The roasting rate, for the steenstrupine sample investigated by the present author, showed a similar dependence at 580°C, but at 700°C the rate only slightly depended on the amount of vapour. The difference was not further investigated, but it might be caused by different compositions of the steenstrupine samples or by a higher degree of impurity minerals in the sample investigated by Asmund.

The reaction between SO_2 or SO_3 and NaO - Al_2O_3 - SiO_2 and NaO - CaO - SiO_2 glasses also depends on the amount of water vapour in the roasting gas[76,77,78]. At 100-600°C, the reaction with water involves the exchange of sodium ions by hydrogen ions and the reaction was limited by the diffusion of Na ions through a compacted layer of glass at the surface that arises from a secondary dehydration reaction. The reaction between SO_3 and glass may be described by the equation

$$SO_3 + \text{glass}\begin{matrix}Na^+ \\ Si^{4+} \\ \text{etc.}\end{matrix}{}_{O^{2-}} + H_2O \rightleftharpoons \text{glass}\begin{matrix}Si^{4+} \\ O^{2-} \\ \text{etc.}\end{matrix}{}_{H^+} + Na_2SO_4$$

With anhydrous reagents, the SO_2 or SO_3 reaction involves the simultaneous diffusion of Na^+ and O^{2-} ions to the glass surface and the speed is limited by the rate of diffusion of oxygen ions; above 700°C this process

predominates over the ion exchange, also when roasting in atmospheres containing water-vapour.

The effect of water vapour is undoubtedly the same in steenstrupine. Sodium ions and perhaps also calcium ions may be exchanged by hydrogen ions.

A sulphate and a combined silicate-phosphate-sulphate layer were formed by the roasting of steenstrupine. Metal ions diffuse from the combined layer and Na also from the outer layer of the unaltered core out to the sulphate layer, while SO_4^{2-} or SO_3 diffuse into the combined layer. Diffusion of uranium and thorium was only demonstrated from the outer few microns of the combined layer.

The roasting rate at 700°C of the steenstrupine investigated by the present author is probably limited both by a combined diffusion of cations, especially sodium, and oxygen ions and by a disintegration of the surface layer as the sulphates penetrate into this layer. Asmund[1] found that sodium and calcium were the dominant cations in the sulphates when roasting to smaller weight increases, whereas, for instance, a high recovery of uranium was found only when roasting to high weight increases. The recovery of uranium is therefore limited by the disintegration process.

The combined diffusion of cations and oxygen ions must be limited by the low mobility of the oxygen ion. Steenstrupine is metamict and it is partly melted at 700°C. The diffusion coefficient of the oxygen ion might therefore be rather high compared to the coefficient in the other minerals investigated. It is not possible to decide whether it is a bulk diffusion or a kind of pore diffusion as suggested by Asmund[1].

The recovery of uranium is only approximately 50 per cent as a result of roasting to maximal weight increase. Thus it must be bound in a phase that is not roasted. The most likely explanation is that, during the transformations accompanying the heating and roasting, some of the uranium enters the monazite phase.

7. STRUCTURAL STUDIES OF ANALCIME, SODALITE, NATROLITE, AEGIRINE, MONAZITE, MICROCLINE, AND ALBITE

Some of these minerals are among the fast-reacting ones in connexion with sulphatising roasting; however, this discovery was made rahter late in the present work, so they have not been investigated as thoroughly as desired.

7.1. Analcime

The TG-DTA curves of pure analcime are shown in fig. 7.1. Two endothermic reactions were observed:

435°C (peak top) strong endothermic reaction,
630°C (peak top) weak endothermic reaction.

The strong endothermic reaction is due to a loss of structurally bound water of approximately 8.4%.

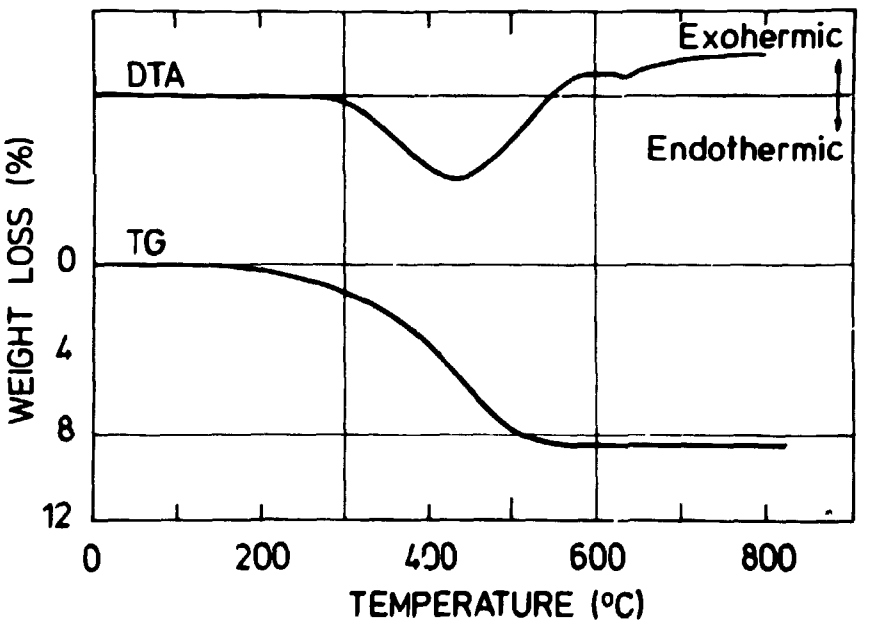

Fig. 7.1. DTA-TG curves of analcime.

X-ray diffraction patterns were almost identical for the raw material and for samples heated to 700°C. The crystal structure is therefore rather unchanged by the heat-treatment and the dehydroxylation.

The weight increase versus temperature is shown in fig. 7.2 for the sulphatising roasting of analcime at 700°C with 5% SO_2 in atmospheric air and different heating rates up to the reaction temperature. The connexion between heating rate and weight increase is not completely understood. There are probably two reaction mechanisms, one in which the rate of the weight increase is directly proportional to time and one in which it decreases with time. The rate increases by increasing the heating rate. It is, however, rather slow if the sample is heated rapidly to 350°C and kept at this temperature for 40 minutes before the heating is continued. These differences might be a consequence of the alteration of the crystal structure as a result of the dehydroxylation. A fast heating rate must destroy more of the crystal structure and form more cracks than a slow rate, and the roasting rate must thereby be increased. However, the differences in alteration were not detectable on X-ray diffractograms.

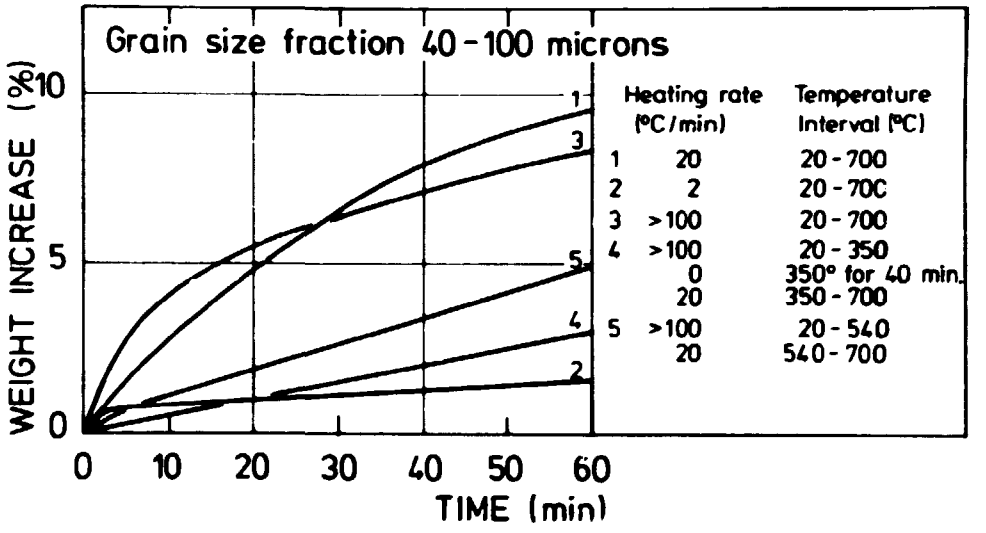

Fig. 7.2. Sulphatising roasting of analcime; the dependence of the reaction rate on the heating rate up to the reaction temperature, 700°C.

When analcime was roasted at 580°C, the roasting rate was increased by increasing the amount of water vapour in the roasting gas, while there was no effect at 700°C.

The diffractogram of a sample roasted to 14% weight increase showed the same diffractions as the heat-treated samples.

In a microscopical and microprobe examination it was possible to distinguish between three layers, as outlined in fig. 7.3. Outermost, there was a sulphate layer followed by a silicate-sulphate layer rich in Al but poor in Na. The core of the grains seemed unchanged. Some microprobe X-ray intensity profiles through a grain in a sample roasted to 9.1% weight increase are shown in fig. 7.4. It is possible to distinguish between the unchanged core and the silicate-sulphate layer in the roasted grains, if the plane polished sample is etched by hydrofluoric acid vapour. The silicate-sulphate layer is very unevenly distributed along the surface of the original analcime grain. There are no distinct borderlines between the three layers. The S concentration is low in most of the silicate-sulphate layer.

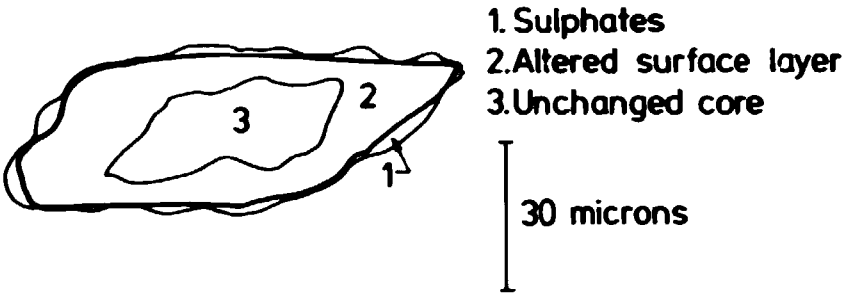

Fig. 7.3. Sketch of a roasted analcime grain.

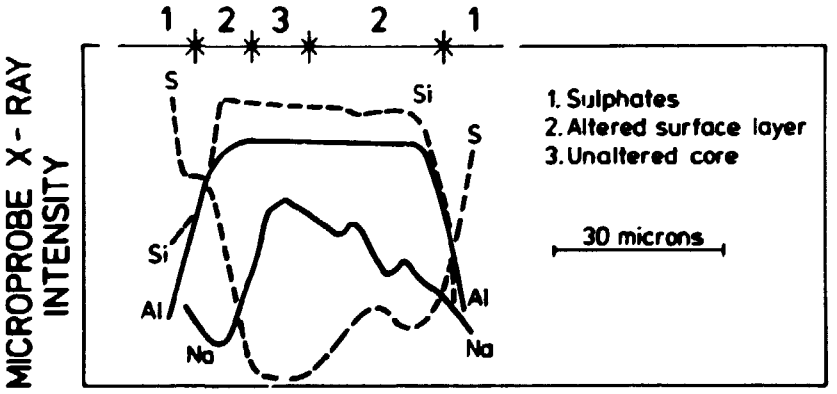

Fig. 7.4. Microprobe X-ray intensity profiles through a roasted analcime grain.

7.2. Sodalite

There was no reaction on the DTA curve of sodalite, and an X-ray diffractogram of a sample heated to 700°C was similar to that of the raw material.

When sodalite was roasted at 580°C, the roasting rate was increased by increasing the amount of water vapour in the roasting gas, while there was no effect at 700°C.

A sample roasted to 10.2% weight increase at 700°C with 5% SO_2 in atmospheric air was investigated in the microscope and in the microprobe.

Four layers could be distinguished, as outlined in fig. 7.5. Outermost, there was a sulphate layer followed by a silicate sulphate layer rich in Al

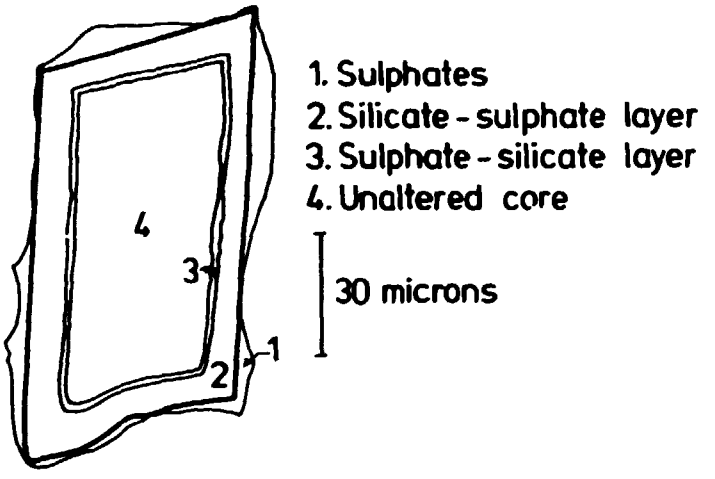

Fig. 7.5. Sketch of a roasted sodalite grain.

but poor in Na and Cl. The third layer was a very thin sulphate silicate layer that was rich in Na and S and poor in Al and Si compared to the second layer. The interior of the grains seemed unchanged except for a Na depletion in the outer few microns. Some average X-ray intensity profiles are shown in fig. 7.6. The borderlines between the Na-rich, sulphate-silicate layer and the two surrounding layers are well-defined in contrast to the other borderlines. The zone that has been attached by the roasting is of uniform thickness in sodalite, in contrast to the minerals analcime and natrolite (cf. section 9.1, and 9.3).

The ion movements through the layers, which must have taken place during the roasting, are outlined in fig. 7.7. Transport must be bulk diffusion or diffusion through microcracks, because it was not possible to detect sulphate-filled cracks in, for instance, the second layer. It is not

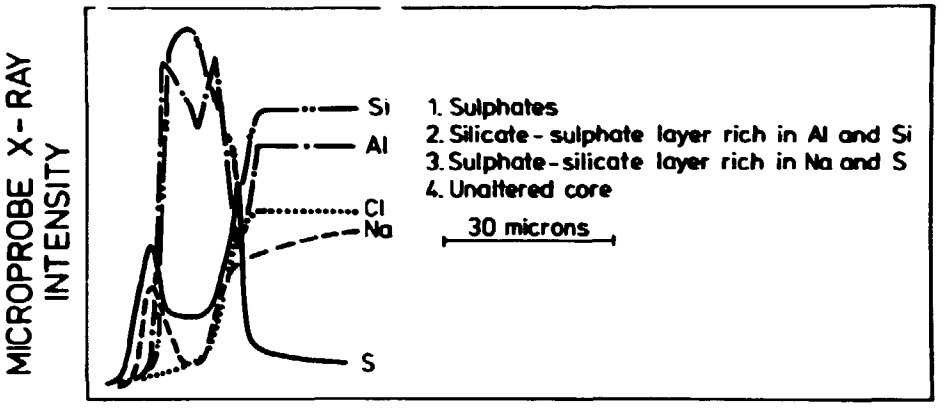

Fig. 7.6. Microprobe X-ray intensity profiles in a roasted sodalite grain.

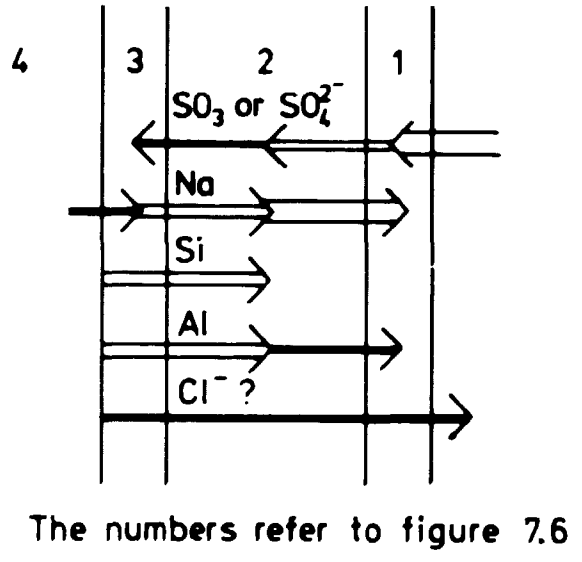

Fig. 7.7. Ion diffusion during the sulphatising roasting of sodalite.

known how Si and Al move through the third layer. The most likely explanation is that the silicate structure is dissolved in the sulphate-silicate layer and precipitated as the silicate-sulphate layer rich in Al and Si.

There seems to be a loss of the Cl^- ion. It could be lost as Cl_2 or HCl. These compounds may be formed when NaCl is treated by SO_3 [67]. According to the Na_2SO_4-NaCl phase diagram, NaCl should be dissolved in Na_2SO_4 at 700°C [74].

There is a difference between the present sodalite and that seen in most of the lujavrite samples from the drilling cores, because the latter usually turn a blue colour on heating to 700°C. This difference has not been investigated.

7.3. Natrolite

The DTA-TG curves are shown in fig. 7.8. There is only one endothermic reaction on the DTA curve, i.e. at 350°C (the peak top), and it is caused by a 9.8% loss of structurally bound water. The water is lost in a temperature interval that is narrow compared to that of analcime. It is therefore possible on a TG curve to roughly distinguish between the water lost by these two minerals, and hence to give an estimate of the amounts of the two minerals in mixtures.

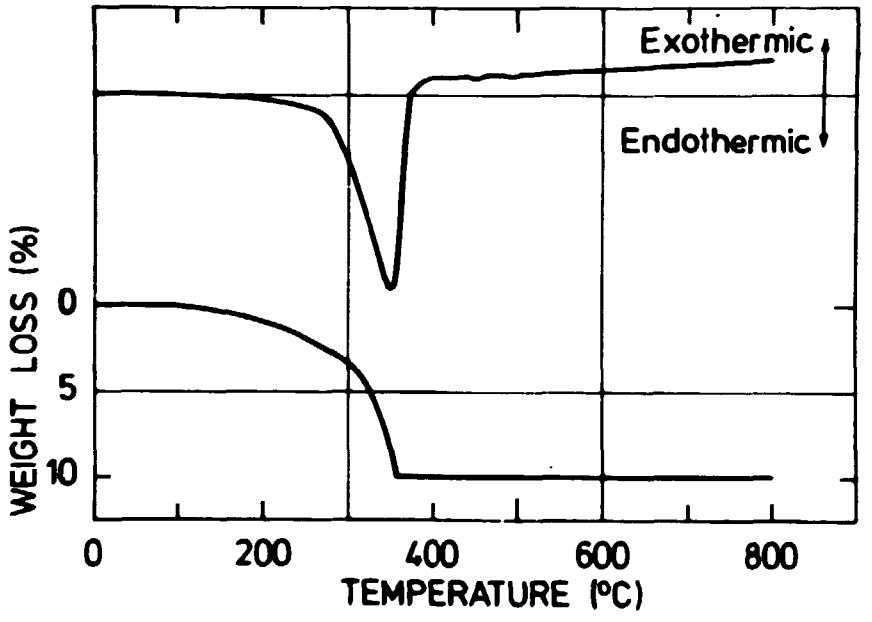

Fig. 7.8. DTA-TG curves of natrolite.

An X-ray diffractogram of a sample heated to 700°C was almost identical to that of the raw material.

When natrolite was roasted at 580 and 700°C, the roasting rate was increased by increasing the amount of water vapour in the roasting gas.

The roasting rate for natrolite is the highest measured for the minerals investigated, as shown in fig. 4.1.

A sample roasted to 14.0% weight increase at 700°C with 5% SO_2 in atmospheric air was investigated in the microscope and by microprobe. Three layers could be distinguished, as outlined in fig. 7.9. Some X-ray intensity profiles are shown in fig. 7.10. The roasted natrolite grains were quite similar to those of analcime. The altered surface layer was depleted with respect to Na, and S was detected, although in low concentrations in many places. Etching by hydrofluoric acid vapour makes it possible to distinguish the unchanged core from the silicate-sulphate layer.

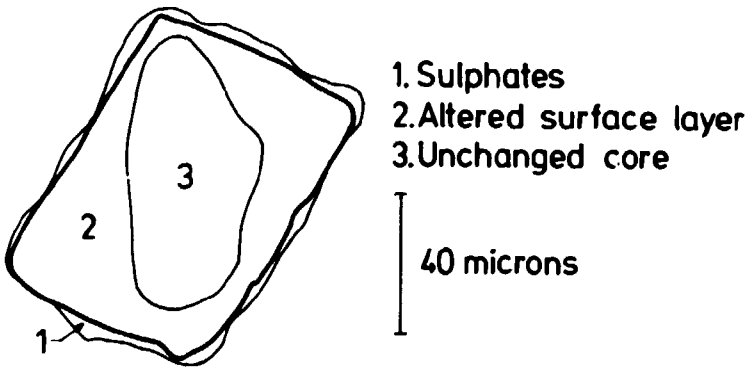

Fig. 7.9. Sketch of a roasted natrolite grain.

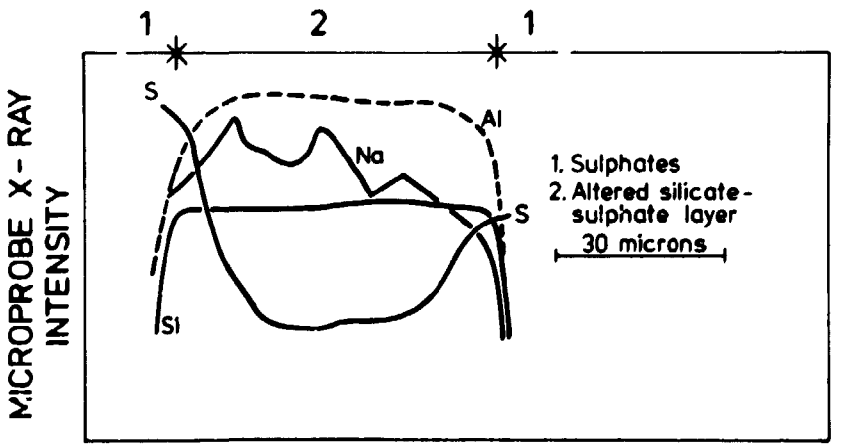

Fig. 7.10. Microprobe X-ray intensity profiles through a roasted natrolite grain.

7.4. Aegirine

This mineral is not particular interesting in connexion with sulphatising roasting because the reaction rate is rather slow.

A few investigations were performed on the sample that Asmund[1] used in his experiments. It was not a completely pure fraction, and there were some impurities of white minerals. Asmund found an Al_2O_3 content of 5.0%, but the major part of this was definitely caused by the impurity minerals. Al was only detected as a trace element in the aegirine by microprobe examination.

A sample roasted to 4.5% weight increase at 700°C with 5% SO_2 in atmospheric air was investigated in the microscope and by microprobe. The colour of the grains changed from green to light red probably because of hematite formation, although this phase was not detected on an X-ray diffractogram. There was no sign of a diffusion of any of the cations, so the roasting process had only attacked a thin surface layer.

Asmund found the reaction rate to increase if roasting continued for many hours; he also found that the X-ray diffractograms altered at the same time. The increased reaction rate is undoubtedly due to a structural decomposition. An X-ray diffractogram shown by Asmund[1] could indicate hematite and cristoballite as the new phases.

7.5. Monazite

According to Asmund[1], monazite from Kvanefjeld is one of the fastest reacting minerals in sulphatising roasting, while monazite from Malaya is a very slowly reacting mineral.

Asmund's Kvanefjeld monazite was investigated by microprobe by the present auther, using a more impure fraction than that used by Asmund. The sample contained 50-60% monazite.

The monazite contained Si as a trace element, but the SiO_2 content was much lower than the 13.9% stated by Asmund. There are many impurity minerals and the high Si content found by Asmund must have originated from these. One of the impurities is uranothorite, in which the major part of the uranium and a considerable part of the Th is contained. The U content in the monazite itself is at most a few parts per thousand.

The impurity minerals were not detectable on an X-ray diffractogram because there are many different minerals.

A sample roasted to 4.2% weight increase was also investigated by microprobe. Some of the impurity minerals were severely attacked by

the roasting, but it was not possible to detect any attack on the monazite.

It may therefore be concluded that monazite is one of the slow-reacting minerals with respect to sulphatising roasting. Uranothorite must, on the other hand, be a fast-reacting mineral, because the recovery of uranium from the roasting of the monazite of Asmund is rather high[1].

7.6. Albite and Microcline

These minerals are among the slowest reacting in sulphatising roasting. They were only investigated by microprobe in a lujavrite sample from drilling core 24 (at a depth of 86.50-86.75 m). The sample was magnetically separated into a predominantly white mineral and a predominantly arfvedsonite fraction. The white mineral fraction was roasted to 3.5% weight increase and investigated by microprobe. There was no sign of an attack on these minerals as a result of the roasting.

7.7. Discussion

The minerals albite, microcline, aegirine, and monazite are among the slowest reacting minerals with respect to sulphatising roasting. They are therefore of limited interest in this connexion.

Natrolite and sodalite are two of the fastest reacting minerals, while analcime reacts at a medium speed. The reaction rate of analcime depends on the heating rate up to the roasting temperature. A fast rate is obtained by a fast heating rate, probably because the structure of the mineral is much more destroyed hereby.

There are some points of resemblance between the roasted grains of analcime, natrolite, and sodalite. Roasting is a surface process in which a sulphate phase is formed on the outside of the grains. The surface layer of the original grains is a mixed silicate-sulphate layer rich in Al and poor in Na. The interior of the grains is rather unchanged. In the case of sodalite there is a fourth layer separating the mixed silicate-sulphate layer and the unchanged core. This very thin layer is a mixture of silicate-sulphate, rich in Na and S but poor in Si and Al. The borderline between this layer and the unchanged core is very well defined in contrast to the other borderlines in this and the other minerals.

The cations in the sulphates originate mainly from the mixed surface layer. This is of a uniform thickness in the case of sodalite, while it varies very much in the case of analcime and natrolite.

The mixed silicate-sulphate layer might be regarded as an aluminium-silicate phase where SO_3 or the sulphates have diffused into the phase and

Na out of the phase. We do not know the structure of this phase but it is most likely to be amorphous. Nevertheless, we cannot exclude the possibility of a crystalline silicate-sulphate phase. We know, for instance, of a $(2CaO, SiO_2)_2 \cdot CaSO_4$ phase in the $CaSO_4$-CaO-SiO_2 system[68]. A small but distinct solid solution of $CaSO_4$ is also seen in alpha 2 $CaO \cdot SiO_2$ at 1000°C[68].

The roasting rates for analcime, sodalite and natrolite were all increased by increasing the amount of water vapour in the roasting gas, when roasting at 580°C and the rate of natrolite was also increased at 700°C. The effect of water vapour was discussed for glasses[76, 77, 78] and for steenstrupine in section 6.5. The reaction involves the exchange of sodium ions by hydrogen ions, and the reaction is limited by the diffusion of the sodium ion. At 700°C the roasting rates of analcime and sodalite were not affected by water vapour and the rate of natrolite was very fast with anhydrous reagents. The cation diffusion into the sulphates must therefore be controlled by a simultaneous diffusion of oxygen ions. We do not know much about the diffusion coefficients of the metal ions and the oxygen ions in these minerals. Sodium self-diffusion coefficients have been determined in some minerals by Sippel[69]. His results are shown in fig. 7.11. The

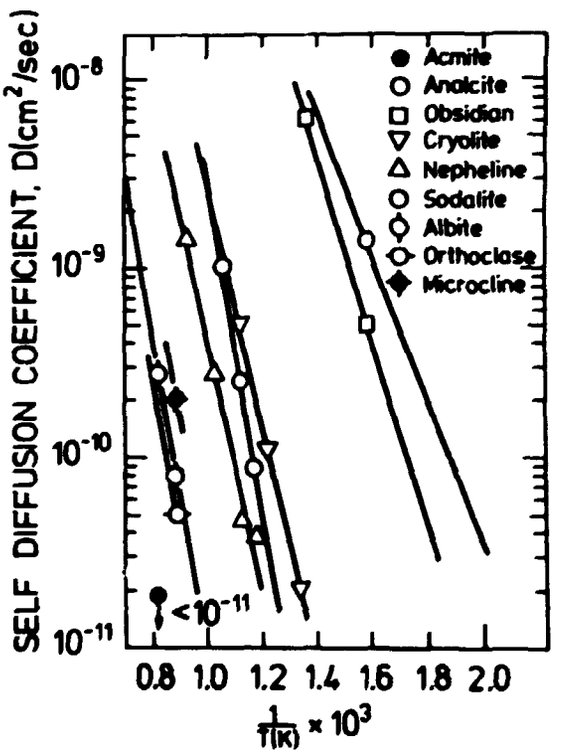

Fig. 7.11. Na self-diffusion coefficients in some minerals, after Sippel[69].

coefficient is rather high for analcime but low for the other minerals. The oxygen ion self-diffusion coefficient must be extremely low in the minerals, so a bulk diffusion of this ion cannot explain the sodium ion diffusion. A kind of pore diffusion is likely.

The roasting mechanisms are supposed to be similar for natrolite and analcime. These minerals are similar in composition to albite, but they roast much faster. The most important difference between them is the crystal water in the first two, so it is likely that there is a connexion. between these two relations. Water is lost on heating to the reaction temperature and the crystal structure must be partly destroyed hereby and microcracks formed. SO_3 or SO_4^{2-} may diffuse into the structure through these cracks and Na^+ and O^{2-} may diffuse out. The diffusion taking place in the silicate structure is therefore short-ranged compared to the diffusion in the cracks. These were not identified in the microscopical and microprobe examinations, probably because they are too thin. In natrolite a counter diffusion of hydrogen ions might be of some importance, as the reaction rate depends on the amount of water vapour in the roasting gas.

In the case of sodalite, the reaction is supposed to be controlled by the dissolution of the mineral grains by the inner sulphate-silicate phase. Al and Si have to be moved through this phase to the other silicate-sulphate phase.

It may be difficult to extract the sulphates from the mixed silicate-sulphate layers in analcime, sodalite, and natrolite, as discussed in section 9.4.

Al is closely related to the mixed phase and is only found in small amounts in the sulphates. According to the $Na_2SO_4 - Al_2(SO_4)_3$ phase diagram[70], a considerable amount of Al could be expected in the sulphates. The lower mobility of Al compared to Na might explain the lack of Al in this phase.

8. URANIUM MINERALISATION IN DIFFERENT LUJAVRITE SAMPLES

8.1. Introduction

As already mentioned in chapter 2, there is a considerable difference between lujavrite samples from different places in Kvanefjeld. The mineralogical composition and the uranium mineralisation may vary.

Twenty-six lujavrite samples from the mine material, the drilling cores and from outside the drilled areas of Kvanefjeld were investigated in order to see how the recovery of uranium depends on the mineralisation. A geological description of the samples is given in appendix 4. Some characteristic uranium minerals were investigated and characterized by an electron microprobe investigation. These results were compared to the recovery of uranium by sulphatising roasting. The results from the roasting experiments are reported in chapter 9, while a survey of the uranium mineralisation is given below.

Uranium mineralisation proved to be the property determining the recovery of uranium.

Steenstrupine and pigmentary material occur in almost all the 26 samples investigated. Steenstrupine is the most important uranium mineral in most samples, while pigmentary material is in a few samples. Monazite/thorite occur in some samples, but are usually of minor importance. Monazite is U-deficient and the uranium is usually contained in associated thorite or uranothorite. U-Nb mineralisations were found in a few samples.

8.2. Steenstrupine

Bøggild[10] and Sørensen[11] investigated the occurrence of steenstrupine and classified it into a few groups according to mineralogical criteria.

In connexion with the sulphatising roasting of steenstrupine, one property is of most significance, namely the degree of alteration. This will appear from the results given in chapter 9.

The steenstrupine may vary from a homogeneous to a strongly altered mineral[11]. In the present investigation, the steenstrupine is divided into three groups.

1. Homogeneous or almost homogeneous steenstrupine.
2. Partly altered steenstrupine.
3. Strongly altered steenstrupine.

A short description of these types and of some microprobe investigations of the types is presented below.

8.2.1. Homogeneous and Almost Homogeneous Steenstrupine

The single grains are homogeneous or almost homogeneous in this type. There are samples where the steenstrupine grains are altered in some areas, for instance along the surface, but significant areas of the steenstrupine grains are homogeneous. These steenstrupines are included in the homogeneous group.

The colour of the steenstrupine grains in these samples varies from colourless to yellow and to red-brown. The composition varies from grain to grain in a thin section. A 50% variation can be seen in the elements Na, Ca, Fe, and Mn, while Si, P, and the rare earths are more constant. Some analyses are given in table 8.1.

This type of steenstrupine was found in seven of the samples investigated. A description of the samples is given in table 9.1 and in appendix 4, to which the sample numbers given in this chapter refer.

It is a matter of discussion whether the steenstrupine in samples 24 and 26 is homogeneous or not. Many of the grains, especially in sample 24, are altered along cracks and at the surface. This is shown in the microprobe distribution pictures described below. This might be another kind of alteration than that described in section 8.3 for the partly altered type where the whole grain is altered. Samples 24 and 26 are surface samples, so a weathering process might have caused the alteration.

Plates 1 and 2 (pictures 1-15) show microprobe back-scattered electron pictures (abbreviated B-S-E) and element distribution pictures of a steenstrupine grain from sample number 24. The grain is approximately 250 x 400 microns. The first B-S-E picture shows most of the grain, while the second shows a magnification of the central part of the first picture. The dark bands on the pictures are due to cracks in the thin section. The grey areas are the homogeneous parts of the grain. The inhomogeneous (or altered) areas are dark and composed of a Na-Al-silicate, a Na-Fe-silicate (arfvedsonite or aegirine), a Ca-Mn-silicate and a Zr-silicate. A very light area to the right in the picture is a rare earth phosphate. Some of the phases identified in the inhomogeneous areas are probably inclusions while others are alteration products.

Plate 3 (pictures 1-5) shows some element distribution pictures from a rather inhomogeneous grain from sample number 26. U, Th, and Zn seem to be homogeneously distributed, while Si and P may vary. They partly substitute for one other.

8.2.2. Quantitative Microprobe Analysis

Steenstrupine grains were analyzed from the following samples: number 2 (mine sample), 13, 19, 20 (from drilling cores 4, 24 and 28) 24 and 26 (from outside the drilled areas of Kvanefjeld). In addition, a sample from Tugtup agtakorfia, kindly provided by H. Sørensen, was analysed. This is a homogeneous anisotropic steenstrupine having the GGU (Geological Survey of Greenland) number 21063.

Steenstrupine is a very difficult mineral to quantitatively analyze by microprobe. There is usually a considerable loss of Na when the sample is hit by the electron beam and the structure is in some cases destroyed, whereby a crater is formed in the sample. Point analysis (equal to the resolution of the microprobe, 3 microns) was impossible. Instead, areas of 90 x 90 or 45 x 45 microns were analyzed by scanning the electron beam. Nevertheless, it proved impossible to avoid a minor Na loss, especially in the sample from drilling core 4. A crater was made by the electron beam in the sample from outside Kvanefjeld, number 26. A loss in Na usually increases the other X-ray intensities, but crater formation does not seem to change them very much. The operating voltage was 10kV when determining Na, and 15kV in all other analyses.

The analyses are given in table 8.1. Y analysis was not performed because no Y standard was available. The measured Y intensity, given in counts/10 s,is instead listed in table 8.1. The background is subtracted For comparison, the measured intensity is given for a monazite standard containing 0.11 per cent Y_2O_3. This standard was kindly provided by J. Rønsbo.

Analysis numbers 7 and 8 differ very much from the others. Si and Na are low, while U is high. F was not detected by microprobe examination of these two grains, and Be, Li and B were only found as trace elements by an emission spectrographical examination on a separated steenstrupine fraction. This also confirmed the low Na content. An X-ray powder diffraction examination was performed by J. Rose-Hansen, but the lines were too weak to determine the structure of the mineral. The unusual composition might indicate a new mineral.

Analyses 1, 3, 4, 5, and 6 are similar, although there is some variation in the Na_2O content. The total is very high in analysis 2, so the H_2O content in this sample must be low. Analyses 1-6 are similar to other steenstrupine analyses from Ilimaussaq[10,11]. Analysis number 6 was made on a homogeneous grain. A qualitative analysis of two homogeneous areas in altered

Table 8.1

Microprobe analysis of steenstrupine

Analysis number	1	2	3	4	5	6	7	8
Sample number	2	21063	19	13	20	24	26	26
SiO_2	30.9	28.2	24.7	29.2	28.6	28.2	10.8	8.3
P_2O_5	9.0	12.4	10.4	10.4	9.6	9.2	12.0	11.7
UO_2	1.03	0.13	1.03	0.90	0.84	0.86	1.82	1.67
ThO_2	4.8	0.73	4.1	3.8	3.5	3.6	4.1	4.2
La_2O_3	8.7	8.8	10.1	9.1	10.6	10.2	11.3	11.5
Ce_2O_3	14.5	19.4	13.7	15.6	15.1	15.0	17.6	18.6
Pr_2O_3	2.2	2.4	2.5	2.2	2.5	2.4	2.6	2.6
Nd_2O_3	4.2	5.2	4.3	4.7	4.0	4.0	5.3	4.8
CaO	3.1	1.0	2.3	1.8	2.5	2.1	0.5	0.9
MnO	4.3	5.6	3.4	4.0	3.2	4.8	1.3	4.1
Na_2O	2.3	14.2	8.9	6.3	8.0	3.2	0.2	-
Fe_2O_3	3.8	3.2	3.9	4.2	4.7	4.2	4.4	4.1
Al_2O_3	1.1	-	-	-	-	-	0.2	1.5
K_2O	-	-	-	-	-	-	0.3	0.3
ZnO	-	-	-	-	-	-	.0	0.6
total	90.5	101.3	89.3	92.2	93.1	87.8	73.4	74.9
Y (counts)	204	83	394	436	425	361	783	307
Y standard (0.11% Y_2O_3)	25							

grains in this sample showed a much lower Si/P ratio, which lay between the "normal" one and that of analyses 7 and 8. It was not investigated whether there was any connexion between alteration and Si/P ratio in this sample.

A few per cent Nb_2O_5 has been determined in most of the previously reported analyses of steenstrupine, but it was not detected in the present investigations of both homogeneous and altered steenstrupine. There were inclusions of a Nb-Ti-rare earth (Ce part)-U mineral in the steenstrupine grains from GGU 21063. Steenstrupine is therefore not a Nb-containing mineral, but Nb may be found in the inclusions.

8.2.3. Partly Altered Steenstrupine

This type of steenstrupine was found in ten of the samples investigated. The grains have a varied appearance in thin sections. Some areas are anisotropic and others are isotropic. The colour may also vary within a

grain; usually it is yellow, brown or grey. The refractive index is seen to vary within the grains when they are observed in reflected light.

An incipient decomposition into a predominant silicate and a predominant phosphate phase has occurred in this type of steenstrupine. In fig. 8.1 some concentration profiles (uncorrected measured X-ary intensity)

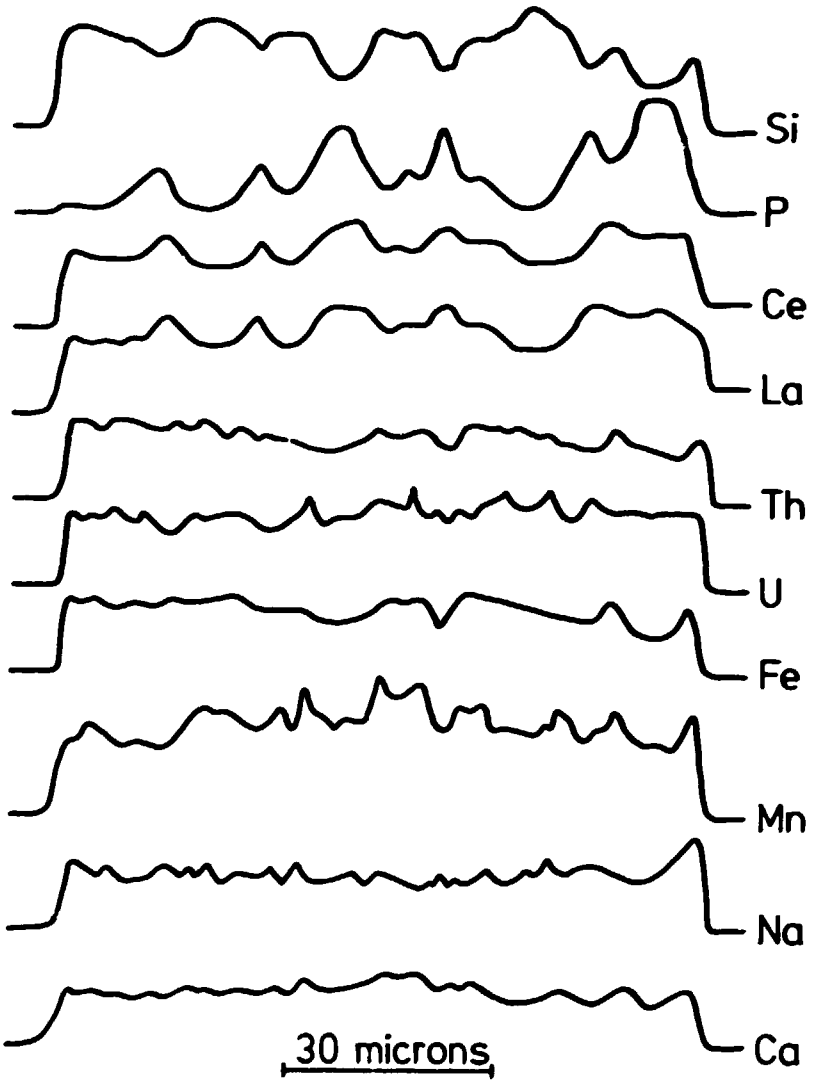

Fig. 8.1. Microprobe X-ray intensity profiles through a steenstrupine grain of the partly altered type.

are shown through a grain from a sample from drilling core 16 (sample number 8). All the profiles are made in the same track.

The rare earths are concentrated in the phosphate-rich phase, while the other metal ions are concentrated in the silicate-rich phase. Although not evident from fig. 8.1, a partial separation has occurred between the

Ce part and the Y part of the rare earths. Y is concentrated in the silicate-rich phase. The small differences in ionic radii must explain this separation.

This description applies in general for this type of steenstrupine. The degree of separation between the phosphate- and the silicate-rich phases may vary and so may the "grain size" of the separated areas. The connexion between isotropic/anisotropic areas, the uranium content and the silicate/phosphate rich phases was not investigated.

8.2.4. Strongly Altered Steenstrupine

This type was only found in three of the samples investigated, so it is probably more rare than the other two.

A complete separation in several silicate phases and usually only one phosphate phase occurred in this type. The grains are very inhomogeneous.

Plates 3-5 (pictures 1-14) show microprobe element distribution pictures of a part of a grain from a naujakasite lujavrite from sample number 17. The grain is most clearly demarcated by the light areas on the Ce picture. The dark areas on the back-scattered electron picture are microcline. The P and Si pictures clearly indicate a complete seperation in several silicate and two phosphate phases. The Ce part of the rare earths is bound in a phosphate phase (a monazite or a monazite-like phase). The Y part of the rare earths is bound in a very fine-grained Th-Y-(Mn) phosphate phase. A complete separation of Ce and Y occurred.

It was not possible to make a quantitative microprobe analysis on these grains but a qualitative estimate gave a rather high P content compared to the homogeneous steenstrupines analyzed.

There is a low concentration of a few per cent Th in the "monazite" phase, while the U-concentration is much lower. The major part of the uranium is bound in a very fine-grained phase, probably an oxide one. The other metal ions, Ca, Mn, Fe, and Na, are bound in different silicate phases.

Plate 5-6 (pictures 1-11) show microprobe element distribution pictures of a part of a large steenstrupine grain from an arfvedsonite lujavrite from sample number 23. The grains in this sample are generally very large, 500 microns or more.

On the back-scattered electron picture there is a very bright area resulting from a Th-U silicate. This area is weakly anisotropic, and has a faintly yellow colour. The ratio of Th to U in the grain is approximately 2:1. This might be uranothorite, although the uranium concentration is very high for this mineral.

Ce was mostly found in a phosphate phase but occasionally it was also found in the silicate one. Na, Al, and K were bound in felspars, and Fe in arfvedsonite. There was a minor amount of Zr in a silicate phase. Some of these phases might be of primary origin.

This steenstrupine grain is unusual because of the large area of uranothorite. The same phase is found in other grains but in much smaller areas. A few concentration profiles were made on the uranothorite grain, which is not homogeneous and the variations are pronounced, especially for Si.

8.3. Pigmentary Material

The term "pigmentary material" is here used to denote altered Zr-containing silicate minerals, which contain a minor amount of uranium. The altered minerals have not been identified, but they might, for instance, be eudialyte ($(Na, Ca, Fe)_6Zr(OH, Cl)(Si_3O_9)_2$), lovozerite ($(H, Na, K)_2O$, $(Ca, Mg, Mn)O$, $(Zr, Ti)O_2$, $6SiO_2, 3H_2O$), and katapleite ($Na_2ZrSi_3O_9, H_2O$). The grains are usually grey or yellow in thin sections and they look crackled. In some cases the pigmentary material looks like strongly altered steenstrupine. The pigmentary grains are usually smaller than 100 microns in size, but larger grains may be found. They are often found in grain boundaries in connexion with arfvedsonite, but they may also be found as inclusions in, for instance, analcime and microcline. Small grains of neptunite are often found in connexion with the pigmentary material.

Plates 7-8 (pictures 1-10) show microprobe element distribution pictures of a pigmentary material grain from a medium- to coarse-grained arfvedsonite lujavrite, sample number 3. This is a rather large pigmentary grain of 150 microns in size that lies between grains of analcime and microline. There are two small arfvedsonite grains at the lower right corner.

The main elements in the grain are Si, Zr, Mn, and Ca with minor amounts of Y, Ti, Fe, U, Na, and Al. The grain is of silicate which is decomposed into several phases as seen on the B-S-E picture. There are 3 or 4 homogeneous areas in which Si, Zr and a little U are found. These areas are anisotropic. The highest uranium concentration, approximately 1 per cent, is found at the lower left corner of the grain. The more diffuse areas on the B-S-E picture are mainly composed of a Ca-Mn-Y silicate phase. The other elements are found outside these phases and are more scattered.

Plates 8-9 (pictures 1-14) show microprobe element distribution pictures of a pigmentary material grain from a medium- to coarse-grained arfvedsonite lujavrite, sample number 2.

This pigmentary grain is found in another sample from the mine material. The grain is approximately 200 x 200 microns. A few small arfvedsonite grains are found to the left at the top and at the lower left corner of the pictures. A neptunite grain lies at the top left corner. The pigmentary grain is surrounded by analcime. Three very bright areas are seen on the B-S-E picture. They result from destruction of the carbon layer with which the samples are coated to secure conductivity and do not indicate any differences in the element distribution.

The main elements in the grain are Si, Zr, Mn, and Ca, with smaller amounts of Na, Al, Nb, Ti, U, Zn, and Y. U, Nb, Ti, and Zn are forming an independent phase. The separation of the grain in several phases is not as distinct as for the previous grain.

The neptunite grain is clearly seen on the Ti picture. The uranium content in the right part of the grain is approximately 3%. Sporadically, it is, of course, higher.

Plates 10-11 (pictures 1-12) show microprobe element distribution pictures of a pigmentary material grain from a arfvedsonite lujavrite, sample number 24. The pigmentary grains in this sample are very small, 6-7 grains are seen in the middle and in the lower part of these pictures. There are two oblong arfvedsonite grains at the top left corner parallel to the borders of the picture. A few of the element distribution pictures are displaced relative to the B-S-E picture.

The main elements in this pigmentary grain are Si, Zr, Mn, and Ca, while U, Na, Fe, K, Zn, and Y are found in small concentrations. A decomposition into a Ca-Mn-Y silicate and a Zr silicate phase has occurred.

Na was problematic in the microprobe examinations of the pigmentary material, because it was extremely easily lost in the electron bombardment. A few investigations were made with a low acceleration voltage to get an estimate of the Na content. It was below 5% in the investigated samples and the concentration was higher in the Ca-Mn silicate phase than in the Zr-silicate phase.

8.4. U-Nb Mineralisations

Probably only a small amount of the uranium is found in these rare compounds in the lujavrites; however, the uranium concentrations in these grains may be as high as 10%.

A steenstrupine-like U-Nb mineral has previously been found[1, 72]. Asmund[1] also mentions a steenstrupine containing 10.2% Nb, and 7.32% UO_2. Another sample contained ~ 50% Nb and 7% UO_2[72]. This sample

was investigated by electron microprobe; besides Nb and U, it contained smaller amounts of Si, Fe, Mn, Ti, Ca, and the Ce part of the rare earths.

Plates 11 and 12 show some element distribution pictures from a medium- to coarse-grained arfvedsonite lujavrite sample from the mine material. The U content is as high as 1700 ppm in this sample, which contains much monazite. This sample was not further investigated.

Some grains of a rather unusual composition were found inside a cluster of arfvedsonite grains. These pictures show a part of a grain that is 75-300 microns in size. There are some dark bands on the B-S-E picture due to cracks in the polished sample.

The main elements in this grain are Si, Mn, Ca, U, Ti, Zr, Nb, and Y. There are small amounts of the Ce part of the rare earths, Na, and Fe. The U-content is approximately 10%, and it is concentrated in a Nb-Ti-U phase. Ca is rather uniformly distributed, while Zr and Y are more sporadically distributed and found as silicates.

Further grains of this type were found within the cluster of arfvedsonite grains. A Nb-Ti-U phase was characteristic for these grains.

These grains may have features in common with the normal pigmentary grains. The cations are the same except for Nb and Ti, which in part replace Zr and Si.

A medium- to coarse-grained arfvedsonite lujavrite from the mine material contained a large piece of pyrochlore and numerous small pyrochlore-like crystals. The uranium concentration in the large piece of pyrochlore was 0.3% at most. An X-ray diffractogram showed the diffraction lines of pyrochlore. The pyrochlore is, however, composed of several Nb-Ce part of the rare earth-Si-phases.

Three of the small yellow grains were investigated by microprobe. They are homogeneous, the uranium content is 1-3 per cent and the SiO_2 and Nb_2O_5 contents are approximately equal. Zr and the elements characteristic of pyrochlore were detected.

U-Nb-Ti compounds were also found in a sample from position 6 on the map in fig. 9.1. The uranium content in this sample is approximately 1%; the phase is very fine-grained and found in a Ca-Mn-Mg phase. There is no Si in the Nb-Ti-U phase, while it appears as a trace element in the other phase.

As already mentioned, U may be found in a U-Nb-Ti phase in the pigmentary grains. Nb-Ti-Si-U inclusions were also found in the steenstrupine grains from the sample from Tugtup agtakorfia (sample GGU 21063).

8.5. Monazite/Thorite

Microprobe investigations were carried out on a few monazites. The mineral is U-deficient in all the samples investigated and it is often associated with grains of uranothorite.

Plate 13 (pictures 1-5) shows microprobe element distribution pictures of a medium- to coarse-grained arfvedsonite lujavrite, sample number 15. A series of light areas on the B-S-E picture are mostly monazite as seen on the element distribution pictures. There is, however, a single uranothorite grain in the upper part of the picture. There is a few per cent Th, but less than 0.2% U in the monazite, while there is approximately 20% UO_2 in the uranothorite.

Plates 13-14 (pictures 1-5) show microprobe element distribution pictures from a medium- to coarse-grained arfvedsonite lujavrite, sample number 2.

A part of a monazite grain is shown. In the middle of the grain there is a uranothorite area where the UO_2 concentration is approximately 12%.

8.6. Discussion

Steenstrupine is the most widespread uranium-containing mineral in the ore. It is usually found in homogeneous or partly altered types. An incipient phase separation into a predominantly phosphate and a predominantly silicate phase has occurred in the partly altered steenstrupine. The strongly altered steenstrupine is more rare; in this type a complete phase separation into silicate phases and usually one phosphate phase (monazite) has occurred.

A separation of the rare earths into the Ce part and the Y part has begun in the partly altered steenstrupine, and the separation of Ce and Y is completed in the strongly altered ones.

Pigmentary material is found in almost all samples but it is the main uranium mineral in only few. It is a silicate "mineral" and the most important metal ions are Zr, Ca, Mn and (Na). U and Y are always found in minor concentrations, while Fe, Al, K, Zn, Nb, and Ti may be found in smaller amounts.

Usually, the material is not homogeneous but decomposed into various phases. Areas of 20-30 microns of an anisotropic Zr-silicate were found in a few cases. The uranium is usually found in this phase, but in Nb-Ti-containing pigmentary material U is always found in a Nb-Ti-U phase. A fine-grained Ca-Mn-Y-(Na) silicate was also seen in some cases.

The composition and the degree of decomposition of the pigmentary material vary, probably because this originates from a few primary minerals that have been altered to different degrees.

The uranium content in the pigmentary material is usually below 2%. In Nb-Ti-containing samples it may be higher.

The pigmentary material is the main uranium mineral in the mine material samples. It is usually widespread in samples where the Th/U ratio is low.

Hansen[16] found hematite in connexion with a kind of pigmentary material from some radioactive veins. Only small amounts of Fe were found in the pigmentary material from these samples, so hematite cannot be characteristic of the pigmentary material from the lujavrites.

Monazite is found in many samples but it is usually U-deficient. Uranothorite is often found in connexion with it, and the main part of the uranium in these areas is bound in uranothorite.

U-Nb mineralisations are found in a few cases. The U content is below 10%. Th is not found in these areas. Both Nb-Ti-U and Nb-Ti-Si-U compounds are found.

9. SULPHATISING ROASTING OF DIFFERENT LUJAVRITE SAMPLES

9.1. Introduction

Twenty-six different lujavrite samples were investigated. The samples were chosen from the mine material, from the drilling cores, and from the areas around Kvanefjeld where a further drilling programme is planned. The positions from which the last-named samples were taken is marked on the map in fig. 9.1. The ore types arfvedsonite lujavrite, medium- to coarse-grained arfvedsonite lujavrite, and naujakasite lujavrite are represented in these samples. 0.2-2.5 m of ore were selected from the drilling cores; pieces with the dimensions of 5-10 cm were selected from the surface samples.

Although the samples were rather arbitrarily chosen, most had an uranium content above the average.

The results from the roastings of these samples were compared to the roastings of some average samples made by mixing samples from many drill cores.

The samples were crushed in a hammer mill and ground in a roller. The fineness was 80-90% below 150 microns, which is the degree which

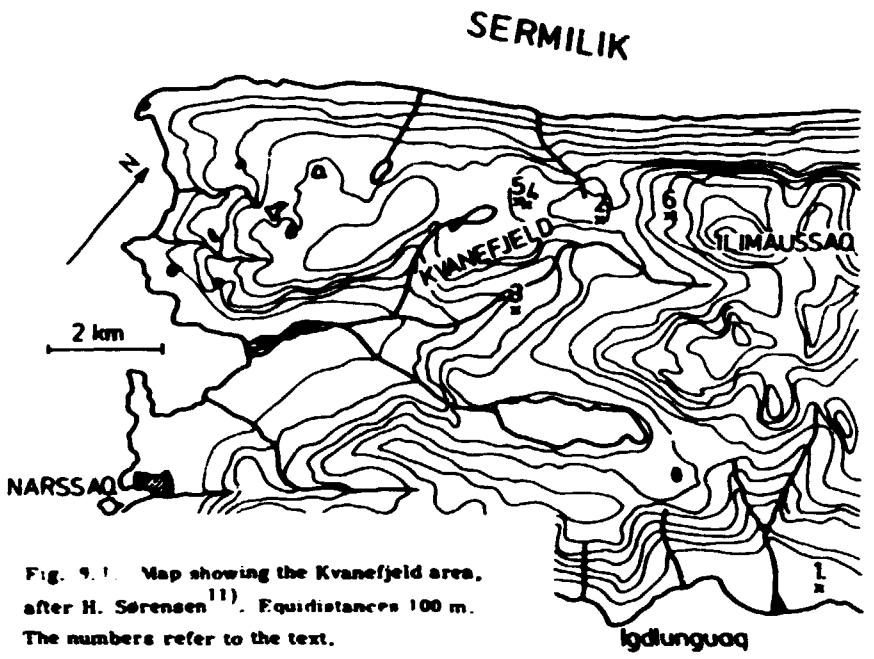

Fig. 9.1 Map showing the Kvanefjeld area, after H. Sørensen[11]. Equidistances 100 m. The numbers refer to the text.

will probably be chosen for an industrial utilisation of the ore. Many of the grains were released hereby.

9.2. Grain-size Distribution

The samples had different natural grain-size distributions as also the ground samples. A few grain-size distribution curves are shown in fig. 9.2.

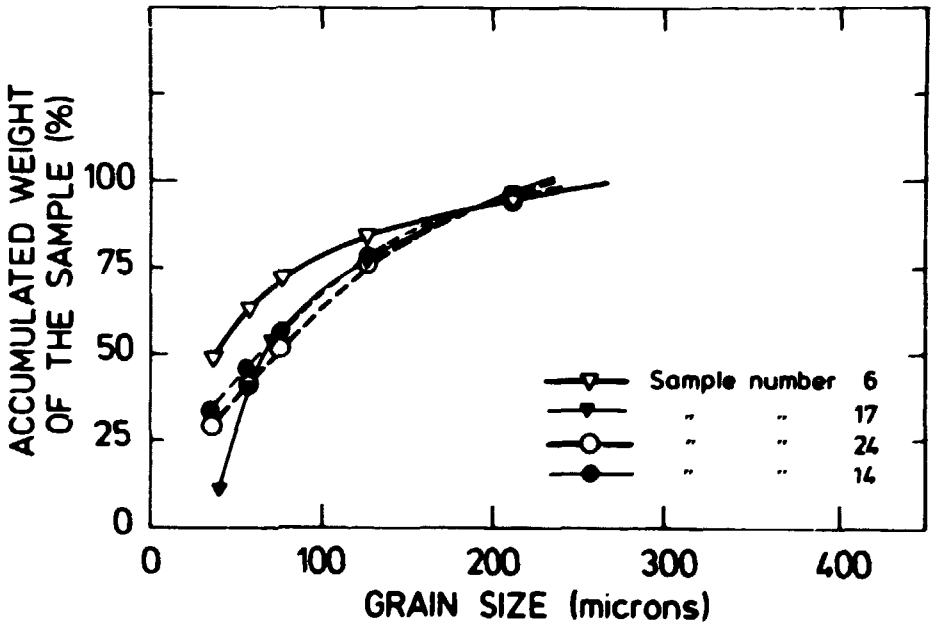

Fig. 9.2. Grain size distribution curves of some of the ground samples.

The samples from drilling cores 30 and 32 are extremes, while the other two are more common.

9.3. Description of the Samples

Table 9.1 gives a very brief description of the samples. A more elaborate one is given in appendix 4.

The following abbreviations are used in table 9.1.

arf	arfvedsonite
anal	analcime
mic	microcline
alb	albite
aeg	aegirine
nef	nepheline
sod	sodalite
nau	naujakasite
nat	natrolite
ste	steenstrupine
pigm	pigmentary material
mon	monazite
tho	thorite

1) the minerals were determined by X-ray diffractogram

2) the minerals were determined by X-ray diffractogram and thin section

3) the uranium mineralisation was determined from a polished section.

Thin sections were made from most of the samples. A description of these is given in appendix 4 through the kind help of H. Sørensen. Some of the samples were only investigated as plane polished samples. Uranium mineralisation may in most cases be described from these. It is possible to distinguish between homogeneous, partly altered and strongly altered steenstrupine, and pigmentary material may also be detected by this method. The main minerals were determined by X-ray diffractograms.

9.4. Sulphatising Roasting of the Samples

The samples were roasted at 700°C with 5% SO_2 in atmospheric air. The samples were quenched after roasting with a continuous supply of SO_2.

The weight loss through heating to 700°C, the weight increase through roasting, the roasting time, and recovery of uranium are given in table 9.2.

The present roasting experiments were carried out without the addition of waste liquor and pelletising of samples that would be done if the ore was utilized industrially[4]. The waste liquor is a slightly acid solution and

some steenstrupines are easily soluble in it, so some of the uranium would be dissolved by the waste liquor and some by the roasting. Because the roasting process was under investigation in the present experiments, the waste liqour was not added.

Table 9.1

A brief description of the 26 samples investigated

Sample number	Drill core number and dept. (~ meters)	Main minerals	Uranium mineralisation	Remarks
1	mine sample	arf, anal, alb, mic 2)	mainly pigm	
2	mine sample	arf, anal, mic 2)	mainly pigm, a little ste	
3	mine sample	arf, anal, mic 2)	mainly pigm, a little ste	
4	mine sample	arf, anal, alb, mic 1)	not determined	
5	32 33 m	aeg, sod, alb 2)	mainly strongly altered ste	arf is strongly altered to aeg
6	30 13 m	arf, anal, mic 2)	partly altered ste and pigm	
7	15 41 m	arf, anal, mic, nef 2)	partly altered ste and pigm	much neptunite in pigm
8	16 71 m	arf, anal, 2)	partly altered ste	
9	16 73 m	arf, anal, mic, alb 2)	partly altered ste	
10	39 25 m	arf, anal, alb, aeg 1)	pigm	
11	39 64 m	arf, nau, anal, mic 1)	partly altered ste and pigm	
12	39 152 m	arf, alb 1)	partly altered ste and pigm	
13	4 112 m	arf, anal, nat 2)	homogeneous ste	natrolite-rich sample
14	5 120 m	arf, alb, mic, nef 2)	partly altered ste	
15	22 119 m	arf, anal, aeg 2)	partly altered ste, pigm, and mon/tho	arf partly altered to aeg
16	22 111 m	arf, aeg, mic, nat 2)	pigm and mon	arf partly altered to aeg
17	32 11 m	nau, aeg, arf, anal, alb 2)	strongly altered ste	anal poor and nau-rich sample
18	7 113 m	arf, nau, alb 2)	partly altered ste	anal poor sample
19	24 87 m	arf, alb, sod, mic 2)	homogeneous ste	red-brown ste
20	28 90 m	arf, mic, nau 2)	homogeneous ste and mon	colourless ste
21	17 110 m	arf, anal, alb, nat 2)	partly altered ste	
22	40 143 m	arf, mic, aeg, sod, alb, nat 1)	pigm	
23	point 2 on the map	arf, anal, mic 2)	strongly altered ste	large inhomogeneous ste grains
24	point 3 on the map	arf, anal, mic 2)	homogeneous ste, and pigm	
25	point 4 on the map	arf, aeg, anal, nef 2)	pigm	
26	point 5 on the map	arf, anal, aeg 2)	homogeneous ste and pigm	ste of very unusual composition

Table 9.2

Sulphatising roasting of samples to different weight increases

Sample numbers	Drill core numbers	Weight loss by heating (%)	Weight increase by roasting (%)	Roasting time (min)	Recovery of uranium (%)
1	the mine	3.5	6.0	17	47
			12.0	53	50
			19.5	170	54
2	the mine	2.2	6.0	19	60
3	the mine	2.0	6.0	12	44
			12.0	62	62
4	the mine	2.5	6.0	13	32
5	32	1.0	6.0	15	72
			11.5	78	77
6	30	3.75	6.0	15	44
			13.5	40	64
			18.0	62	74
7	15	2.5	6.0	9	27
			14.5	63	33
8	16	2.5	6.0	16	30
			12.0	60	45
			18.0	230	63
9	16	3.25	6.0	16	18
			12.0	48	43
			18.0	93	62
10	39	1.0	6.0	25	65
11	39	1.25	6.0	6	40
12	39	0.5	6.0	6	33
13	4	3.25	6.0	7	20
			12.3	26	30
			17.3	60	42
14	5	1.25	6.0	7	20
			12.0	50	50
			18.8	230	64
15	22	2.0	6.0	12	46
16	22	3.0	6.0	8	35
			15.0	85	38
17	32	3.2	6.0	11	72
			17.8	85	76
18	7	1.25	6.0	6	24
			15.0	38	32
19	24	0.8	6.0	13	28
			12.0	100	42
20	28	1.5	6.0	5	22
21	17	2.0	6.0	7	10
			13.5	48	44
22	40	0.8	6.0	8	39
			12.0	70	84
23		2.5	2.0	8	56
			6.0	40	83
			12.5	140	88
24		3.75	6.0	25	48
			12.0	100	66
25		1.25	6.0	12	70
			13.0	70	80
26		3.0	6.0	25	54
			12.0	123	81

9.4.1. The Rate of Roasting Compared to Ore Composition

There are large differences in the mineralogical composition of the samples, and so the rate of weight increase as a result of sulphatising roasting also varies.

The weight loss through heating of the samples varies from 0.5 to 3.75%. The majority of this water is contained in the minerals analcime and natrolite, so the content of these two minerals varies from a few to almost 40 per cent.

The roasting time for 6% weight increase varies from 5 to 40 min. The slow-reacting samples may, for instance, contain arfvedsonite, analcime, microcline, albite, and aegirine, while the fast-reacting ones may also contain natrolite, sodalite, nepheline, and naujakasite. The last-named minerals were all found to be among the fast-reacting minerals in pure fractions (chapter 4).

The roasting rate measured as a weight increase versus time is probably not the same when the mineral is roasted in a pure fraction or in a lujavrite sample. The different sulphate compositions may affect the rates, and they definitely affect the equilibrium conditions. The stability of $Fe_2(SO_4)_3$ and $Al_2(SO_4)_3$ depends on the composition of the sulphate phase. The reaction rate, however, does not change significantly from the pure samples to the lujavrite ones.

9.4.2. Recovery of Uranium

The recovery of uranium by roasting to 6% weight increase is chosen as a standard of reference.

It is impossible to give the uranium minerals in all samples an identical treatment because of the differences in mineralogical composition and in grain size, and thereby in reaction rate and sulphate composition. This standard of reference is, however, applicable.

The following conclusions may be drawn from these results. Recoveries are high from strongly altered steenstrupine, from pigmentary material and from uranothorite, while they are low from the homogeneous and partly altered steenstrupines. A review of the samples is given below.

The recovery is above 40% in the following samples: 1, 2, 3 (from the mine material), 5, 17 (from drill core 32) 10, 11 (from drill core 39), 15 (from drill core 22) 23, 24, 25, and 26 (from outside Kvanefjeld).

The uranium is contained in strongly altered steenstrupine in the three samples 5, 17, and 23, where it is found in highly concentrated but small areas within the steenstrupine grains. In samples 5 and 17 it is probably bound in an oxide phase, while it is in a silicate phase in sample 23 (section

8.2.4). This fact does not seem to influence the recovery. In section 7.5 it was also demonstrated that a high recovery is obtained from uranothorite.

It must be rather easy for the SO_3 to penetrate through these strongly altered steenstrupine grains and attack the uranium-containing particles. The coherence of the steenstrupine grains may be small because of the phase separation. Some of the silicate phases in the grains are undoubtedly also attacked during roasting.

The strongly altered steenstrupine is only found in these three samples, so it is probably rare in the lujavrites, but in connexion with sulphatising roasting it is very attractive, because of the very high recovery.

Uranium is found almost exclusively in pigmentary material in the two samples 10 and 25, where the recoveries are very high too.

According to H. Sørensen, the same mineralisation is found in samples 22 and 25. It is, however, easier to obtain a high yield from the last sample.

The recovery from samples containing pigmentary material is high, and it may be compared to the recovery from the strongly altered steenstrupine.

Samples numbers 1, 2, 3, 6, and 11 contain an essential part of the uranium in pigmentary material, while another part is contained in steenstrupine of the homogeneous or partly altered type. These two steenstrupine types give a poor recovery as will be shown below. The relatively high recoveries from these samples are therefore due to the pigmentary material.

Sample number 15 contains uranium in partly altered steenstrupine, pigmentary material and uranothorite in connexion to monazite. The relatively high recovery from this sample may be caused by the uranothorite.

The two samples from outside Kvanefjeld, numbers 24 and 26, mainly contain steenstrupine of an unaltered type and some pigmentary material. The recoveries from these samples are higher than could be expected. The steenstrupine in these samples is, however, of a very unsual composition. It has apparently a higher affinity with the sulphatising roasting.

In most of the other samples investigated the main part of the uranium is found in steenstrupine of the homogeneous or partly altered type. There is no remarkable difference in the recoveries from the homogeneous types like those in sample numbers 13, 19, and 20 and the partly altered types like 8, 9, 14, and 21. A higher uranium recovery is obtained from the last-named type, if the roasting is continued to higher weight increases such as 12 or 18%.

The recovery of uranium was only slightly increased in samples 4, 5, 7, 16, 17, 18, 23, and 24 were roasted to higher weight increases than 6%. Sample numbers 5, 17, 23, and 25 gave a very high recovery by roasting

to 6%, and it is apparently difficult to get a recovery higher than 70-85%. Sample numbers 7 and 16 have a rather high content of monazite. The uranium content in this mineral is at most a few parts per thousand, but an essential part of the uranium might be in this mineral in these samples; therefore it is not recovered by the sulphatising roasting. It is not understood why the recovery was only slightly increased in sample numbers 1 and 18. The uranium might be concentrated in a phase that is not roasted. There was no indication of such a phase in the raw material, but it might be formed by the roasting. We know little of the equilibrium conditions in the sulphate phase, and we cannot exclude the possible formation of an insoluble oxide or basic sulphate phase during roasting. This might also explain why the recovery in the other samples cannot exceed 70-85% per cent.

E. Sørensen[72] has shown that a fraction of the sulphates formed from some samples is insoluble in the subsequent leaching. The fraction is increased by continued roasting. Uranium might be connected to these sulphates, although it has not been detected by microprobe investigation of such a sample. The insoluble sulphates are connected to some of the white minerals. The investigations of, for instance, natrolite, (section 7.3), sodalite (section 7.2), analcime (section 7.1), and steenstrupine (chapter 6) showed the existence of a sulphate-silicate layer. The sulphate from this layer is probably very difficult to dissolve, so it might explain the insoluble sulphate.

Fig. 9.3 shows the recovery of uranium versus weight increase for sample numbers 8 and 13. The recovery per added S equivalent is highest

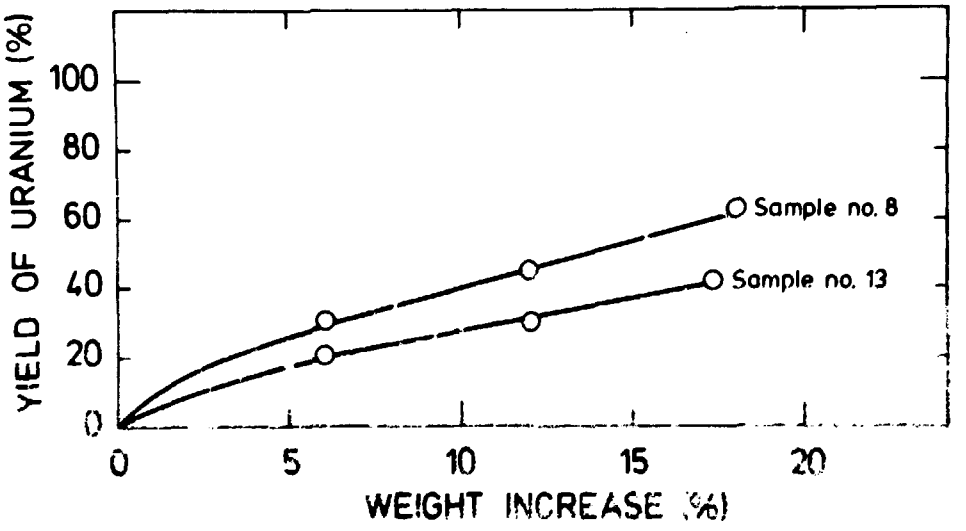

Fig. 9.3. Recovery of uranium versus weight increase for two samples.

for the first few per cent weight increase but for continued roasting it is almost directly proportional to the weight increase. This phenomenon is seen in most of the samples containing steenstrupine of the homogeneous or partly altered type. Presumably the pigmentary material is roasted first and so the high recovery at the beginning of the roasting can be attributed to this material. The uranium recovery from steenstrupine is almost proportional to weight increase as it was previously also shown for the roasting of the pure mineral (section 6.3).

Table 9.3 gives a comparison of the uranium recoveries from the three types of ore from which samples were investigated. There is no indication of one ore type giving better recoveries than the others.

Table 9.3

A comparison of the uranium recoveries from different ore types

	Arfvedsonite lujavrite	Medium- to coarse-grained arfv. luj.	Naukasite lujavrite
Number of samples	16	6	4
Average uranium recovery (6% weight increase)	42.6	36.0	39.5

The best recoveries of uranium were found in samples from near the surface. This is probably because pigmentary material is more widespread in the upper part of the ore. This will be discussed later in section 9.6.

The four samples from outside the area of Kvanefjeld drilled hitherto are probably the most interesting ones in this investigation. The recovery of uranium was high in all of them. The steenstrupine in these samples was strongly altered (sample 23) or had a very unusual composition that makes it more suited for roasting (samples 24 and 26). The samples also contained more pigmentary material than usual, especially sample number 25.

According to H. Sørensen, there should be large reserves of the ore from sample 25 This should be of the same mineralisation as that found at the bottom of drill core 40 (sample number 22). This sample gives a rather high recovery, so there is at least a well-founded conjecture that these samples are more promising than those from the drilled area of Kvanefjeld with respect to sulphatising roasting.

9.5. Sulphatising Roasting of Different Grain Size Fractions

A few experiments were made in order to see how grain size influences the roasting rate of the lujavrites and the recovery of uranium.

Some of the samples investigated in the above section were separated into the three grain size fractions ⟨36, 36-75, and ⟩75 microns. Each fraction makes up at least 20% of the unseparated sample. The following samples were investigated: 1, 6, 7, 13, 14, and 17.

Table 9.4

Sulphatising roasting of different grain size fractions

Sample number	Drill core number	Grain size fraction (microns)	Uranium content (ppm)	Weight increase (%)	Recovery of uranium (%)
		⟨36	865	9.0	57
1	the mine	36-75	651	4.2	45
		⟩75	972	2.2	30
		⟨36	615	10.8	50
6	30	36-75	515	5.0	32
		⟩75	778	3.2	23
		⟨36	423	9.7	42
14	5	36-75	406	5.5	27
		⟩75	786	4.2	14
		⟨36	628	13.3	45
7	17	36-75	654	8.7	25
		⟩75	897	3.3	6
		⟨36	680	16.0	33
13	4	36-75	465	8.5	22
		⟩75	697	5.5	10
		⟨36	546	14.0	70
17	32	36-75	441	6.3	70
		⟩75	448	4.0	72

All the fractions were roasted for 15 minutes at 700°C by a mixture of 5% SO_2 in atmospheric air. The uranium content in the fractions, the weight increase and the recovery of uranium are given in table 9.4.

The fine-grained fractions ⟨36 and especially 36-75 microns were enriched in arfvedsonite, while the coarse-grained one was enriched in white minerals.

Different types of uranium mineralisation were found in these samples; unaltered steenstrupine in number 13, partly altered steenstrupine in numbers 6, 7, and 14, strongly altered steenstrupine in number 17, and pigmentary material in number 1. There was also an essential part of pigmentary material in number 6.

Usually, there is a coherence between the uranium mineralisation and the distribution of uranium in the ground samples. In samples where uranium is mainly found in steenstrupine of the homogeneous or partly altered type, there is usually an enrichment in the coarse-grained fraction. This is because the natural grain size of steenstrupine is normally above 100 microns. In samples where uranium is mainly found in steenstrupine of the strongly altered type or in pigmentary material, there is usually a distinct minimum at 50-75 microns. These two types of mineralisation are alike, because the coherence of the grains must be small on account of the phase separations. The grains are easily ground and they will therefore be found in the fine-grained fraction. Some of the grains will be connected to other grains and therefore be found in the coarser fractions. They may be more connected to white minerals than to arfvedsonite, because there is usually a minimum in the uranium content at 50-75 microns.

A comparison of the present results with the previous ones concerning roasting of unseparated samples shows no remarkable difference in the average roasting rate whether the fractions are roasted separately or whether the unseparated fraction is roasted.

By a very rough calculation, we may suppose the average grain sizes in these fractions to be 25, 56, and 125 microns, respectively. The ratio between the surface areas is then 1:5:25. The ratio for the weight increases for these fractions by roasting for 15 minutes is, on the average, 1:2:3:5 for the investigated samples. The weight increase is therefore approximately directly proportional to the linear grain dimension.

Uranium is recovered very easily from the coarse-grained fraction of the sample containing steenstrupine of the strongly altered type (sample 17), and rather easily from the samples containing much pigmentary material (samples 1 and 6), while the recovery is poor from the samples containing much steenstrupine of the homogeneous and partly altered types.

9.6. Average Samples

E. Sørensen and T. Lundgaard previously made average samples from many drill cores[72]. Numbers 1 and 2 are made from the part of the ore that is covered by gabbro, while 3 and 4 are from the uncovered part. The samples are picked from different horizontal sections in the ore. Each sample consists of two 10-cm-long pieces of the drill core selected at a 10 m interval. Samples 1 and 3 are from levels near the surface, while 2 and 4 are from 50 m lower levels. Appendix 5 gives the drilling core numbers and the depths from which the samples were chosen.

X-ray diffractograms of the 4 samples showed no significant differences in the mineralogical composition. As shown in section 6.3, it is possible to distinguish between analcime and natrolite on the TG curves, and thereby to roughly calculate the contents of these two minerals in the samples. This is done in table 9.5, which also gives the uranium content of the samples. The calculation is based on the theoretical content of water in the two minerals.

Table 9.5

U content in the four average samples and a rough estimate of analcime and natrolite content

Sample number	U content (ppm)	Weight loss by heating to 700°C (%)	% analcime	% natrolite
1	299	2.6	25	5
2	302	2.0	20	3
3	326	3.25	30	9
4	257	2.75	25	7

The uranium contents are in excellent agreement with an average content of approximately 300 ppm for the ore.

The contents of analcime and natrolite are highest in the samples from near the surface.

The samples were roasted to different weight increases at 700°C by a mixture of 5% SO_2 in atmospheric air. Table 9.6 gives the roasting times and the recoveries of uranium. The recoveries of uranium by roasting to 6% weight increase are of the same magnitude as the recoveries from the samples where uranium is mainly found in steenstrupine of the homogeneous or partly altered type. The recovery from sample number 3 is a little higher than from the others. This is undoubtedly because this sample contains more uranium in pigmentary material; it includes pieces from the drilling cores in the same area as the mine material, which was shown to contain much pigmentary material (section 9.4).

The recovery is best from the surface samples. This is probably because of a different pigmentary/steenstrupine ratio and perhaps because of a surface alteration of the uranium minerals.

Some weathering processes have occurred in the ore. Water has penetrated the upper part of the ore. Williaumite is, for instance, dissolved in the upper part. Oxidation has also occurred; on treating samples from the bottom of the drilling cores with diluted sulfuric acid H_2S is released, but this does not occur when a surface sample is treated. Pyro-

Table 9.6

Sulphatising roasting of average samples

Sample	Weight increase, %	Roasting time, min.	Recovery of uranium, %
	6.0	8	24
1	12.0	28	56
	20.0	86	65
	6.0	12	21
2	12.0	36	41
	18.0	113	57
	6.0	12	28
3	12.0	30	51
	19.0	120	80
	6.0	8	19
4	14.0	35	37
	22.5	120	77

thite (FeS) might release H_2S, but it has not been reported in this ore. However, there is no indication that such a weathering process has affected the uranium minerals, except perhaps for samples 24 and 26 (cf. section 8.2.1). Homogeneous steenstrupine is, however, found in the mine material that was taken from only a few metres below the surface.

The recovery of uranium is roughly proportional to weight increase. This was also seen in section 9.4 for samples where the uranium is mostly concentrated in steenstrupine of the homogeneous or partly altered types.

These recoveries of uranium are very small. An addition of waste liquor and a pelletising of the ore would increase the recovery. A few experiments seem to indicate that the recovery is not increased to the same extent for all samples. The best increase in recovery was obtained for sample number 4. This should probably be connected with the observations that there are distinct differences in the rate of solution of steenstrupines in the waste liquor. Some are dissolved in a few minutes (e.g. sample number 13) and others are almost indissoluble, (e.g. sample number 19).

9.7. Discussion

The present experiments have shown that uranium is easily recovered from pigmentary material, strongly altered steenstrupine and from uranothorite, while it is difficult to recover from steenstrupine of the homogeneous and partly altered types. Through roasting to 6% weight increase, the recovery is similar from the two last types. A further roasting gives a better recovery from the partly altered type, but roasting

has to be continued to weight increases above 12% to get a recovery of 50% or more from these samples. These roastings were performed without addition of waste liquor and pelletising of the ore before roasting. Recovery would be increased by such treatment, but it would still be poor.

The roasting of the average samples showed that the main part of the uranium in the Kvanefjeld is contained in steenstrupine of the homogeneous or partly altered type.

Four samples were investigated from outside the areas of Kvanefjeld where the previous drilling programme took place. The recovery from all were better than from the Kvanefjeld samples. The uranium content in this part of the intrusion is probably not much lower than in the area of Kvanefjeld drilled hitherto, and because of the much better recovery these ores are more promising with respect to sulphatising roasting. However, further samples from those areas and especially from drilling cores will have to be investigated before any definite conclusion can be drawn.

10. SUMMARY AND CONCLUSIONS

The present investigations are far from a complete description of the sulphatising roasting of the uranium ore from Kvanefjeld. The subject is much too comprehensive for this.

The investigations concentrated on the reactivity and the mechanism in sulphatising roasting of the different minerals in the ore and a comparison of the uranium mineralisation with the recovery of uranium. Some microprobe investigations were made in this connexion in order to characterise the uranium minerals.

The most widespread minerals in the ore are arfvedsonite, analcime, the feldspars microcline and albite, acmite/aegirine, nepheline, sodalite, and natrolite. The contents decrease through the series.

10.1. Uranium Mineralisation

Uranium is found in the minerals:

Steenstrupine :	Na-Ca-Mn-Fe-rare earth-phospho-silicate.
"Pigmentary material":	Zr-Mn-Ca-silicate.
Monazite :	$CePO_4$.
Thorite:	$(Th, U)SiO_4$
Nb-U compounds	Nb-Ti-U and Nb-Ti-Si-U compounds (including pyrochlore).

Steenstrupine is the main uranium mineral, while pigmentary material is of some importance and the others of minor importance.

Three types of steenstrupine were distinguished in the present investigation:

1. Homogeneous or almost homogeneous steenstrupine.
2. Partly altered steenstrupine.
3. Strongly altered steenstrupine.

The steenstrupine grains are homogeneous or almost homogeneous in the first type. The composition, however, varies from grain to grain, especially in Na, Ca, Fe, and Mn.

Decomposition into a predominantly silicate and a predominantly phosphate phase had occurred in the partly altered steenstrupine. The Ce part of the rare earths was mostly found in the phosphate phase, while the Y part was mostly found in the silicate phase.

A complete decomposition into several silicate and one or two phosphate phases had occurred in the strongly altered steenstrupine. Cerium was

found in the phosphate phase together with small amounts of Th but very little uranium. Yttrium was mostly found in a Ca-Mn-Y silicate phase. Uranium was found in one sample as a Th-U silicate and in another as a U-oxide.

The designation "pigmentary material" is here used to denote altered Zr-silicate minerals containing smaller amounts of uranium. It could be defined as a Zr-Ca-Mn-(Na)-silicate containing small amounts of U and the Y part of the rare earths; Fe, K, Al, Zn, Nb, and Ti are found in some cases, but the Ce part of the rare earths, Th, and P are missing. A phase separation into a Zr silicate and a Ca-Mn-Y-(Na)-silicate phase was observed in many cases. Uranium was usually found in the Zr phase, except in Nb-Ti-containing pigmentary material, where it was always found in a Nb-Ti-U phase. The uranium content was usually below 2%, although it may be higher in Nb-Ti-containing grains.

The original Zr minerals, which are now altered, were not identified, but minerals such as endialyte ($(Na, Ca, Fe)_6$ Zr (OH, Cl)$(Si_3O_9)_2$), lovozerite ($(H, Na, K)_2O$, (Ca, Mn, Mg)O, $(Zr, Ti)O_2$, $6SiO_2$, $3H_2O$) and catapleite ($Na_2Zr\ Si_3O_9$, H_2O) are likely.

Monazite is uranium-deficient and contains at most a few parts per thousand. It is, however, often found in connexion to uranothorite, which may contain up to 20% UO_2.

U-Nb-Ti and U-Nb-Ti-Si compounds are rarer than the other uranium compounds, and probably only a small percentage of the uranium of the Kvanefjeld lujavrites is contained in these compounds.

10.2. Sulphatising Roasting

The ore is treated by SO_2 and air at approximately 700°C in sulphatising roasting. The ore catalyses the formation of SO_3, which attacks some of the minerals whereby a sulphate phase is formed.

Some of the minerals in the ore have been roasted and investigated as pure samples. The minerals natrolite, sodalite, steenstrupine and pyrochlore had fast reaction rates, while arfvedsonite had a medium rate, analcime a slower rate, and albite, microcline, aegirine, and monazite, hardly reacted at all. Nepheline and naujakasite were not investigated in pure samples but the results indicate a fast reaction of these minerals too.

Because of its widespread distribution arfvedsonite is the mineral that contributes most to the sulphates. A very rough calculation gives about 40% of the sulphates from this mineral in an average sample. Another essential part originates from analcime. The six fast-reacting minerals

are not as widespread as arfvedsonite and analcime, but their contribution to the sulphates is essential because of the fast reaction rate.

The roasting rates for the minerals analcime, sodalite, steenstrupine and natrolite increased on addition of water vapour to the roasting gas when roasting at 580°C, but at 700°C a marked effect was only seen for natrolite. A similar effect of water vapour in sulphatising roasting has been reported for some glasses[76, 77, 78]. The reaction with water involved the exchange of sodium ions by hydrogen ions and the reaction was limited by the diffusion of sodium ions through a compacted layer of glass at the surface that arises from a secondary dehydration reaction. Above 700°C the roasting of the glasses was limited by the diffusion of oxygen ions. The mechanisms of the sulphatising roasting of the minerals and of the glasses are undoubtedly in principle identical.

There are some points of resemblance between the roasted minerals. The grains are unchanged in size and shape. We may distinguish between three layers in a roasted mineral grain: a sulphate layer, an altered surface layer and an almost unaltered core. The sulphate layer is unevenly distributed on the surface of the grains. The layers are, however, of different character. In sodalite and steenstrupine the reaction zone is of rather uniform thickness, while it varies in the others, analcime, natrolite and arfvedsonite. The last contains many sulphate-filled cracks around which there are altered layers, characterized by a red colour caused by hematite. The borderline between the altered layer and the sulphates is distinct in the case of arfvedsonite in contrast to the other minerals, where the altered layer might be characterized as a mixed silicate-sulphate layer rich in Si and Al, but poor in Na and S. In the case of sodalite, we may even distinguish between two altered layers, because there is a thin sulphate-silicate layer separating the silicate-sulphate layer rich in Al and Si and the unaltered core. This layer is rich in Na and S, but poor in Si and Al. The borderline between this layer and the unchanged core is well defined. In the case of steenstrupine and arfvedsonite, the borderline between the unaltered core and the altered layer is rather well defined, in contrast to analcime and natrolite.

The altered surface layer is depleted with respect to metal ions, especially Na. The majority of the metal ions in the sulphates originate from this layer and only a minor amount of Na originates from the unchanged core.

The structure of the unaltered core is rather similar to that of the untreated mineral, because X-ray diffractograms show no changes, except

in the case of steenstrupine where a phase transformation, resulting in the formation of a monazite phase and a minor amount of melt, takes place around 700°C.

It is not known whether the mixed silicate-sulphate layer is a real mixed phase or whether the sulphate is found in cracks in the silicate structure. If there are any cracks, they must be very fine, because they were not observed by the microprobe. Mixed silicate-sulphate phases are known in the $CaO-SiO_2-SO_3$ system[68] and might also exist in this predominantly $Al_2O_3-SiO_2-SO_3$ system.

Sulphatising roasting is therefore a combined diffusion-alteration process. Metal ions diffuse especially from the altered part of the grain to the sulphates and, except for arfvedsonite, SO_4^{2-} or SO_3 diffuse into the altered layer. The Na diffusion might be the first step in the roasting. The crystal structure is broken down hereby and the altered layer is formed. The diffusion through this layer is, of course, faster than that through the unaltered structure, and the other metal ions, which have a lower mobility than Na, may therefore also diffuse in this altered layer.

Electroneutrality has to be maintained during roasting so the diffusion of metal ions to the sulphates must be followed by a simultaneous diffusion of an anion to the sulphates, or by a counter diffusion of another cation such as H^+. When roasting at 700°C, the metal ion diffusion must be limited by an oxygen ion diffusion, except for natrolite where a counter diffusion of H^+ might be of some importance, as the reaction rate depends on the content of water vapour in the roasting gas. The oxygen ion diffusion is likely to occur through pores or microcracks because of the low self-diffusion coefficient of this ion. Arfvedsonite contained many sulphate filled cracks and a lot of microcracks must have been formed by the dehydroxylation of analcime and natrolite. Long-range diffusion may therefore occur in these cracks and the diffusion in the lattice structure is therefore short-ranged.

In the case of sodalite, a sulphate-silicate layer rich in Na and S, but poor in Al and Si, is formed between the silicate-sulphate layer and the unchanged core. The ions have to diffuse through this layer to the silicate-sulphate layer and to the sulphates. The sulphate-silicate layer is probably a melt at the reaction temperature and the reaction is controlled by the dissolution of the unchanged core in this melt and the reprecipitation of the silicate-sulphate phase rich in Al and Si.

In the case of steenstrupine, a monazite phase and a minor amount of melt are formed by heating to 700°C. The melt formation and the amorphous

structure must give rather high diffusion coefficients, but it is not known whether the diffusion occur as a bulk diffusion or it occur through pores.

10.3. Recovery of Uranium and Uranium Mineralisation

The connexion between uranium mineralisation and recovery of uranium was investigated. Twenty-six samples taken from different locations in the ore were examined. The uranium mineralisation and the main minerals were determined from thin sections. The samples were roasted to different weight increases, and the recovery of uranium was determined and compared to the mineralisation. The samples were not pelletised before roasting, because some steenstrupines are very easily soluble in the weakly acid solution that is used as pelletising liquid.

The recovery of uranium was low from steenstrupine of the homogeneous and the partly altered types and from monazite. The recoveries from the two steenstrupine types are comparable if they are roasted to 6% weight increase. The partly altered type gives a better recovery if it is roasted to higher weight increases. A high recovery is obtained from the pigmentary material, from steenstrupine of the strongly altered type, and from uranothorite.

Unfortunately, the present results indicate that most of the uranium is contained in steenstrupine of the homogeneous and partly altered types.

Four samples were investigated from areas in which a further drilling programme is to take place. A high recovery was obtained from these samples, so there is a possibility that this part of the ore is better than that drilled hitherto.

A steenstrupine of a very unusual composition was found in one of the last-named samples. The SiO_2/P_2O_5 ratio is ~ 1, where it is ~ 3 in normal steenstrupine, and the Na and Si contents are extremely low. This material might constitute a new mineral.

11. ACKNOWLEDGEMENTS

This work was performed at the Research Establishment Risø and at the Institute of Ceramics, the Technical University of Denmark, under the quidance of N. Hesselbjerg Christensen and E. Sørensen.

The author especially wishes to express his gratitude to E. Sørensen and T. Lundgaard, who suggested this work and gave him much help, and also to N. Hesselbjerg Christensen, to whom he is greatly indebted for kind interest and valuable discussions. Thanks are also due to H. Sørensen for kindly interest and helpful discussions, and to G. Asmund for helpful discussions.

Further, he is indebted to Jette Fosskov and Gerda Krarup for making the uranium analysis and the polished sections, respectively, A. Thorboe and his staff for analyzing an arfvedsonite sample, K. Gram Jeppesen for making a Si analysis, P. Solgaard for making the IR spectra, B. Leth Nielsen for having the thin sections made at the Geological Survey of Greenland, O.V. Pedersen for mineral samples, R. Nordbach Nielsen for assistance with the electron microprobe investigations, J. Rønsbo for making the computer program to calculate the microprobe analysis on steenstrupine, J. Olsen for making the Mössbauer spectra, J. Fenger for help with the Mössbauer investigation and to J. Rose Hansen for an X-ray diffraction investigation of a steenstrupine sample.

Thanks are due to Jennifer Paris for her careful revision of the language.

Finally, he wishes to thank the Danish Atomic Energy Commission for granting him a period of post graduate study and both the Commission and the Institute of Ceramics for placing the experimental facilities at his disposal.

12. REFERENCES

1) G. Asmund, Chemistry and Kinetics of the Sulphating Roasting of Uranium - Bearing Silicates. Risø Report No. 253 (1971) 125 pp.

2) E. Sørensen and T. Lundgaard, Selective Flotation of Steenstrupine and Monazite from Kvanefjeld Lujavrite. Risø Report No. 133 (1966) 17 pp.

3) E. Sørensen and T. Lundgaard, Uranium from Leaching Liquors by Precipitation. Risø Report No. 166 (1967) 13 pp.

4) E. Sørensen, Risø, Denmark, to be published.

5) G. Asmund, T. Lundgaard and E. Sørensen, In: The Recovery of Uranium. Proceedings of a Symposium organized by IAEA and held in Sao Paolo, 17-21 August 1970. (IAEA, Vienna, 1971) (STI/PUB/262) 185-194.

6) H. Sørensen et al., The Uranium Deposit at Kvanefjeld, the Ilimaussaq Intrusion, South Greenland. Grønlands Geologiske Undersøgelser, Rapport No. 60 (1974) 54 pp.

7) H. Sørensen, J. Hansen and E. Bonnesen, Preliminary Account of the Geology of the Kvanefjeld Area of the Ilimaussaq Intrusion, South Greenland. Grønlands Geologiske Undersøgelser, Rapport No. 18 (1969) 40 pp.

8) H. Sørensen, J. Rose Hansen and B. Leth Nielsen, unpublished GGU internal report 1971.

9) O. V. Pedersen. Am. Mineral. 53 (1968) 1780.

10) O. B. Bøggild, The Mineralogy of Greenland. Medd. Grønland 149 No. 3 (1953) 442 pp.

11) H. Sørensen, On the Occurrence of Steenstrupine in the Ilimaussaq Massif, South West Greenland. Medd. Grønland 167 No. 1 (1962) 256 pp.

12) Geochemistry and Mineralogy of Rare Elements and Genetic Types of Their Deposits. Vol. II. Edited by K.A. Vlasow (Israel program for Scientific Translations, Jerusalem, 1966) 322 pp.

13) M. Danø and H. Sørensen, An Examination of Some Rare Minerals from the Nepheline Syenites of South West Greenland. Medd. Grønland 162 No. 5 (1959) 36 pp.

14) V. Buchwald and H. Sørensen, An Autoradiographic Examination on Rocks and Minerals from the Ilimaussaq Batholith, South West Greenland. Medd. Grønland 162 No. 11 (1961) 36 pp.

15) H. Wollenberg, Fission Track Radiography of Uranium and Thorium in Radioactive Minerals. Risø Report No. 228 (1971) 40 pp.

16) J. Hansen, A Study of Radioactive Veins containing Rare-Earth Minerals in the Area Surrounding the Ilimaussaq Alkaline Intrusion in South Greenland. Medd. Grønland 181 No. 8 (1968) 48 pp.

17) M.C. Van Hecke, Sulfation Kinetics of the Bayer Process Residue and Manganese Sea Modules. Thesis: Stanford University. (1973) 99 pp.

18) J.J. Henn, R.A. Clifton and F.A. Peters, Evaluation of the Sulfatization-Reduction Process for Recovering Manganese and Iron Oxide Pellets. BM-RI-7652 (1972) 27 pp.

19) W.E. Lewis et al., Investigation of the Cuyuna Iron- Range Manganese Deposits, Crow Wine County, Minn. Progress Report 1. BM-RI-5400 (1958) 49 pp.

20) C. Prasky, B.L. Marovelli and F.E. Joyce, Evaluating Cuyuna Manganese Resources by Sulfatizing. BM-RI-5887 (1961) 27 pp.

21) C. Prasky, F.E. Joyce, W.S. Swanson, Differential Sulfatizing Process for the Recovery of Ferrograde Manganese. BM-RI-6160 (1963) 30 pp.

22) C. Prasky and G.P. Howard, Sulfatization of Manganiferous Carbonate Slates in a Fluidized Bed Reactor. BM-RI-6258 (1963) 16 pp.

23) F.E. Joyce and C. Prasky, Sulfatization of Manganese Minerals and Selected Gangue Materials. BM-RI-6514 (1964) 11 pp.

24) J.G. Lesokhin, Zh. Prikl. Khim. 35 (1962) 1949-1952.

25) A.W. Fletcher and M. Shelef, Trans. Metall. Soc. AJME 230 (1964) 1721-1724.

26) F.E. Joyce, Extraction of Copper and Nickel from the Duluth Gabbro Complex by Selective High-Temperature Sulfatization. BM-RI-7475 (1971) 15 pp.

27) F.E. Joyce, Sulfatization of Nickelferous Laterites. BM-RI-6644 (1965) 16 pp.

28) A.W. Fletcher and M. Shelef, Unit Processes in Hydrometallurgy. Metall. Soc. Conf. 24 (1963) 946-970.

29) P.G. Thornhill. U.S. Pat. 2, 813, 015 (1957) and 2, 813, 016 (1957).

30) N.V. Hybinette. Brit. Pat. 5806 (1912).

31) F.O. Kichline. U.S. Pat. 1, 590, 525 (1926).

32) W.K. Sproule et al. U.S.Pat. 2, 719, 082 (1955).

33) H. Kurushima and S. Tsunda. J. Met. 7 (1955) 634-638.

34) A.W. Jessup. Eng. Min. J. 155, No. 1 (1954) 72-77.

35) A.W. Sommer and H.H. Kellogg. Trans. Metall. Soc. AJME 215 (1959) 742-744.

36) T. Chao and S.C. Sun. Trans. Soc. Mining Eng. AIME 238 (1967) 420-429.

37) J.M. Krause and N.J. Pittman. U.S. Pat. 3, 148, 022 (1964).

38) C.B. Alcock and M.G. Hocking. Trans. Inst. Mining Metall. Sec. C. 75 No. 712 (1966) 27-36.

39) Dow Chemical Co. Fr. Pat. 1, 321, 476 (1963).

40) J.E.K. Svenke. Swedish Pat. 197, 679 (1964).

41) G. Asmund, The Geological Survey of Greenland, Copenhagen, personal communication, 1976.

42) F. Habashi and R. Dugdale. Metall. Trans. 4 (1973) 1553-1556.

43) D.W. Bainbridge. Metall. Trans. 4 (1973) 1655-1658.

44) M.C. Van Hecke and R.W. Bartlett, Metall. Trans. 4 (1973) 941-947.

45) F. Gales and R. Winand, Metall. Trans. 4 (1973) 883-885.

46) G.K. Wertheim, Mössbauer Effect: Principles and Applications (Academic Press, New York, 1964) 116 pp.

47) E.B. Andersen, En metode til bestemmelse af Fe^{2+}/Fe^{3+} i geologiske prøver ved hjælp af Mössbauereffect, unpublished dissertation, University of Copenhagen 1975.

48) A.J. Stone, H.J. Aagaard and J. Fenger, MOSSPEC, a Programme for Resolving Mössbauer Spectra. Risø-M-1348 (1974) 59 pp.

49) A.G. Maddock, In: Mössbauer Spectroscopy and its Applications. Proceedings of a panel organized by the International Atomic Energy Agency and held in Vienna 24-28 May 1971 (IAEA, Vienna, 1972) 329-347.

50) E.B. Andersen, J. Fenger and J. Rose-Hansen, Determination of Fe^{2+}/Fe^{3+} - ratios in arfvedsonite by Mössbauer spectroscopy. Lithos 8 (1975) 237-246.

51) S. Ghose, A scheme of cation distribution in the amphiboles. Mineral. Mag. 35 (1965) 46-54.

52) W.G. Ernst, Amphiboles. Crystal Chemistry, Phase Relations and Occurrence. (Springer, Berlin, 1968) (Minerals, Rocks and Inorganic Materials. Experimental Mineralogy, vol. 1) 125 pp.

53) W.E. Addison and J.H. Sharp. J. Chem. Soc. (1962) 3693-3698.

54) A.A. Hodgson, A.G. Freeman and H.F.W. Taylor. Mineral. Mag. 35 (1965) 5-30.

55) R.W.T. Wilkins and W. Vedder, In: Reactivity of Solids. Proceedings of the 6th International Symposium, Schenectady, New York, 25-30 August 1968. Edited by J.W. Mitchell et al. (Wiley Interscience, New York 1969) 227-236.

56) J.H. Patterson and D.J. O'Connor. Aust. J. Chem. 19 (1966) 1155-1164.

57) W.G. Ernst and C.M. Wai. Amer. Mineral. 55 (1970) 1226-1258.

58) C.C. Addison et al. J. Chem. Soc. (1962) 1468-1471.

59) W.E. Addison, G.H. Neal and J.H. Sharp. J. Chem. Soc. (1962) 1472-1475.

60) J.H. Patterson. Mineral. Mag. 35 (1965) 31-37.

61) A.A. Hodgson. Mineral. Mag. 35 (1965) 291-305.

62) A.G. Freeman, Mineral. Mag. 35 (1966) 953-957.

63) J.J. Papike, J.R. Clark and J.S. Huebner. Amer. Mineral. 55 (1970) 300-301.

64) K.A. Bol'shakov, P.J. Federov and N.J. Ilina. Russ. J. Inorg. Chem. 8 (1963) 1350-52.

65) K. Wickert. Brennst.-Wärme-Kraft. 16 (1964) 67-76.

66) L.P. Kostin et al. Izv. Vyssh. Uchebn. Zaved, Khim. Khim. Tekhnol. 13 (9) (1970) 1325-27.

67) F. Bergius. German Pat. 299034 (1913).

68) W. Gutt and M.A. Smith. Trans. Br. Ceram. Soc. 66 (1967) 337-345.

69) R.F. Sippel. Geochim. Cosmochim. Acta 27 (1963). 107-120.

70) P.J. Federov and C. Ch'ih-yün. Russ. J. Inorg. Chem. 11 (1966) 362-363.

71) H. Sørensen and V. Buchwald. Medd. Dansk Geol. Foren. 13 (1958) 545-550.

72) E. Sørensen, Risø, Denmark, personal communication 1976.

73) G.A. Sawatsky, F. van der Woude and A.H. Morrish. Phys. Rev. 183 (1969) 383-386.

74) P.J. Federov and K.A. Bolshakov. Russ. J. Inorg. Chem. 4 (1959) 405-407.

75) P. Kirk. Danish Pat. 79,769, aug. 29, 1955.

76) R.W. Douglas and J.O. Isard. J. Soc. Glass. Technol. 33 (1949) 289-335.

77) I. Hilgenfeldt and H. Jebsen-Marwedel. Glastechn. Ber. 31 (1958) 161-170.

78) E. Mochel, M.E. Nordberg, and T.H. Elmer. J. Am. Ceram. Soc. 49 (1966) 585-589.

APPENDIX I

Mössbauer Investigations of Arfvedsonite

I.1. Mössbauer Spectra and Parameters

Some of the Mössbauer spectra are shown in fig. I.1. The preceding treatment of the samples is given in table I.1, which also gives the treatment of some other samples where the parameters are given in table I.2.

The abbreviations I.S, Q.S, and H.W. are used for isomer shift, quadrupole splitting and half-width, respectively. The isomer shifts are given relative to alpha iron.

The spectra of the untreated sample, the sample heated to 300°C, and the two reduced samples may be resolved in three doublets, while the samples heated to temperatures above 300°C and the roasted ones may be resolved in four doublets. This is because Fe^{2+} in the arfvedsonite structure is oxidized by the dehydrogenation that takes place at 300-500°C. The spectra of the samples heated to 300, 400, and 500°C show that Fe^{2+} in M_1 absorption is diminished from 52.2% to 18.4%. Thus the oxidation must have taken place at this lattice position. The new absorption must therefore be Fe^{3+} in M_1. The Fe^{2+} content in Fe^{2+} in M_3 seems to increase at the same time. This could be explained by an original Fe^{3+} content in this position, which is now reduced, or by a reduction of some original Fe^{3+} in the M_2 position, which now overlaps the original Fe^{2+} in M_3 absorption. The Fe^{3+} in M_2 absorption seems to be rather unchanged, but the standard deviation on this absorption area is large because of the overlap with the new Fe^{3+} in M_1 absorption.

These complicated spectra are difficult to resolve. There is usually more than one statistically acceptable resolution. The spectra of the heat-treated and roasted samples have to be resolved in four doublets, but the positions of these are uncertain, especially for the two Fe^{3+} doublets. The present resolution, where the new doublet is thought to have a higher quadrupol splitting than the original one, must be correct because the spectrum is seen to be changed by an increased absorption at the position of the new doublet, and because the parameters of the original absorptions are not much changed. The structure of the oxyamphibole is very simular to that of the amphibole, and so the two Mössbauer spectra must be alike.

The spectra of the long-time heated samples 10 and 11 are even more complicated because acmite is found in these smaples. Hematite was also

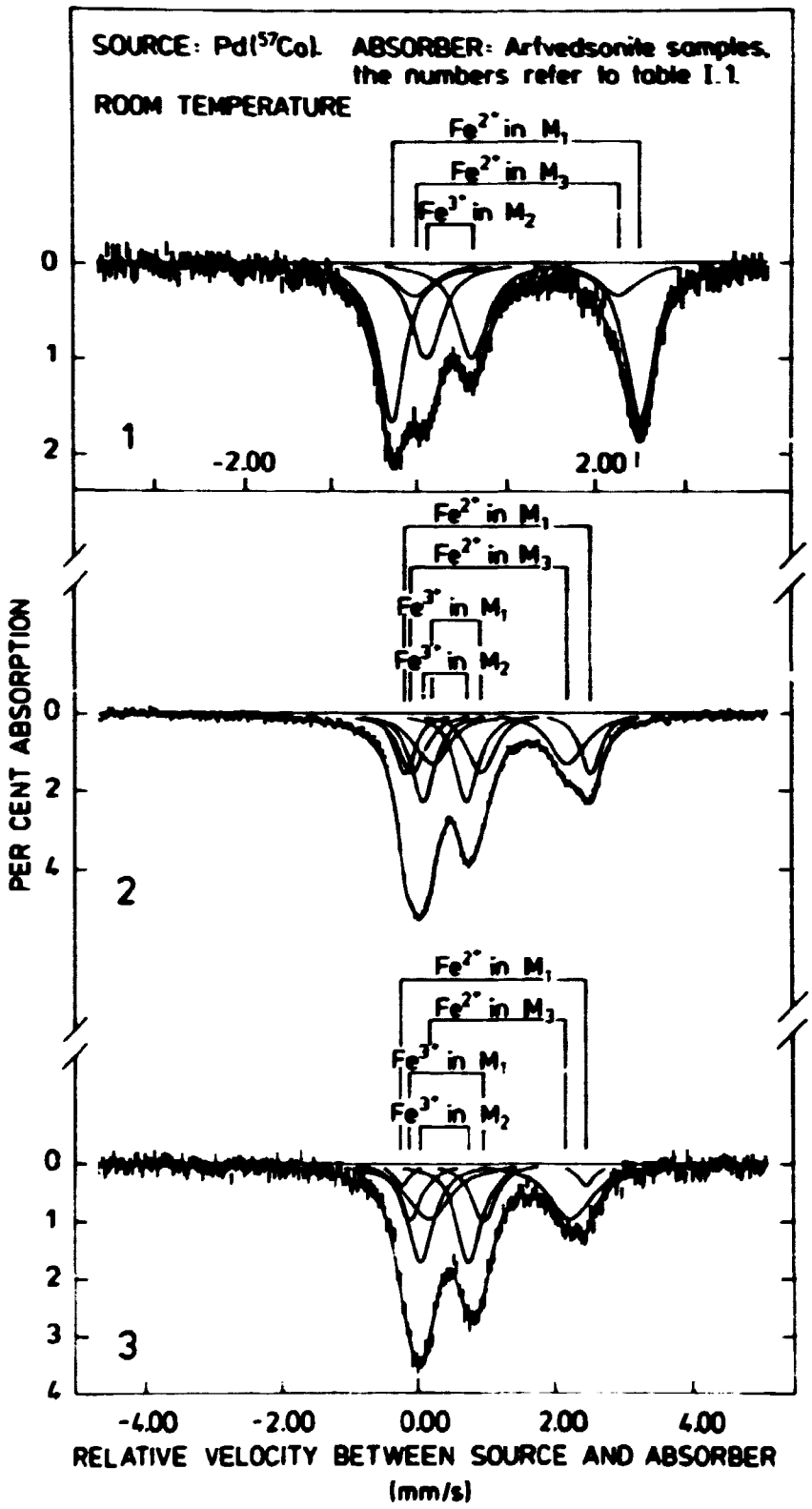

Fig. I.1. Mössbauer spectra.

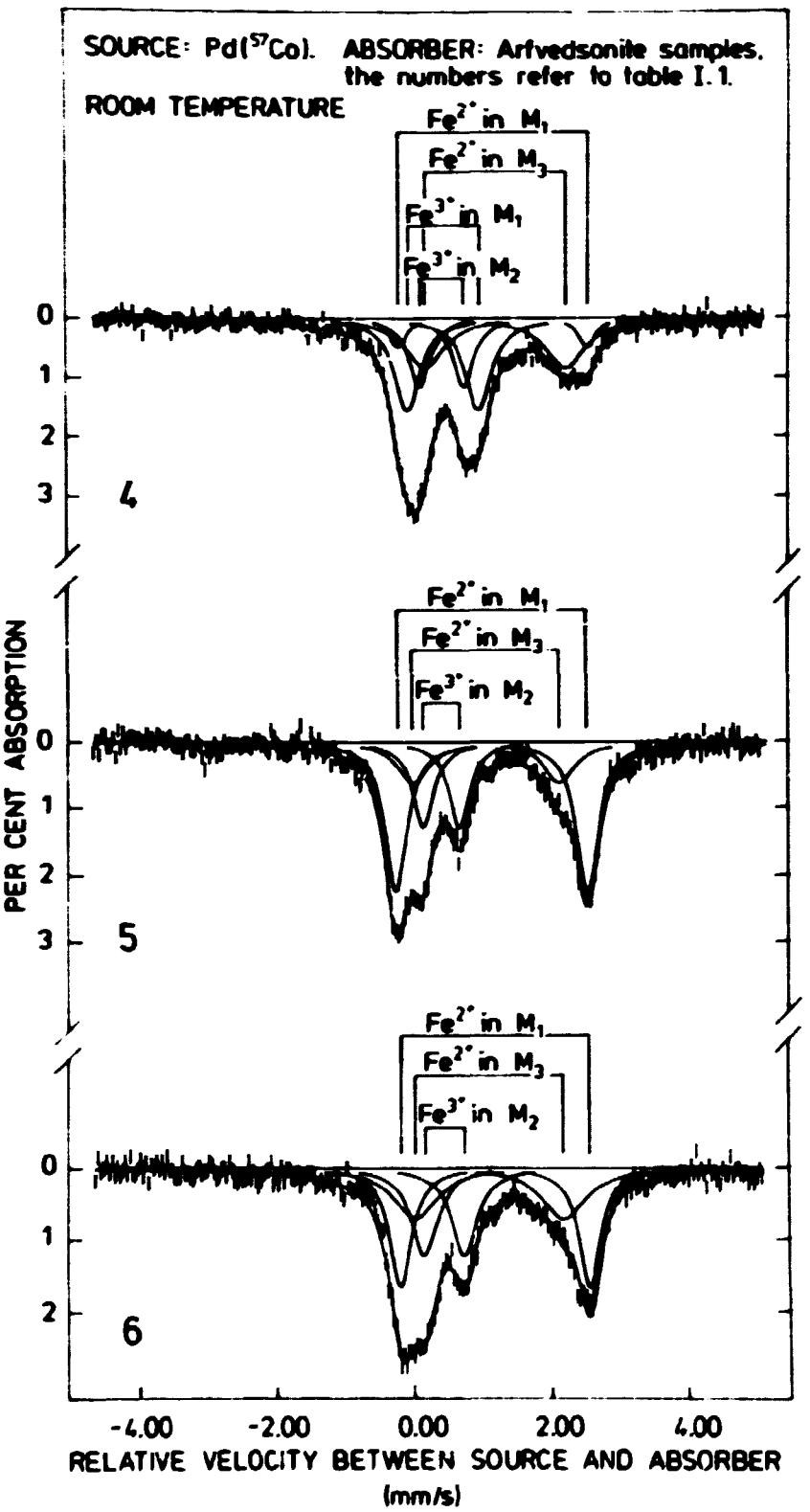
SOURCE: Pd(^{57}Co). ABSORBER: Arfvedsonite samples, the numbers refer to table I.1.
ROOM TEMPERATURE
Fe^{2+} in M$_1$
Fe^{2+} in M$_3$
Fe^{3+} in M$_1$
Fe^{3+} in M$_2$
4
5
6
PER CENT ABSORPTION
0
1
2
3
-4.00
-2.00
0.00
2.00
4.00
RELATIVE VELOCITY BETWEEN SOURCE AND ABSORBER
(mm/s)

Table I. 1

Preceding treatment of arfvedsonite samples

Sample number	Grain size fraction (microns)	Treatment
1		untreated
2	< 20	heated to 500°C and immediately cooled
3	56-400	heated to 695°C for 2 hours
4	56-400	roasted to 6.0% weight increase at 695°C
5		sample number 3 reduced by H_2 at 600°C for 4 hours
6		sample number 4 reduced by H_2 at 600°C for 4 hours
7	< 20	heated to 300°C and immediately cooled
8	< 20	heated to 400°C and immediately cooled
9	< 20	heated to 690°C for 30 minutes and immediately cooled
10	< 20	heated to 660°C for 5 hours
11	< 20	heated to 690°C for 66 hours

The calculated parameters of these samples are given in table I. 2.

formed in the case of number 11, but it was dissolved in concentrated HCl. The original Fe^{2+} in M_1 absorption was almost lost and it was not possible to resolve the spectrum in two Fe^{2+} absorptions in sample number 11.

Ernst and Wai investigated the heat-treatment of ribeckite. The Mössbauer spectra of this amphibole and samples heat-treated to 700°C are, in principle, identical to the arfvedsonite spectra, so the same processes must have occurred. However, these authors interpret the spectra differently. Table I. 3 shows the difference in interpretation of the four absorptions.

If the interpretation of Ernst and Wai is correct, then the two Fe^{2+} absorptions must change positions during the heat-treatment, and this was not seen in the present case. Ernst and Wai only heat-treated ribeckite to 700°C and not to any intermediate temperatures. If the present interpretation is applied to the data of Ernst and Wai, the Fe^{2+} - Fe^{3+} contents of the lattice positions would be as shown in table I. 4.

This could indicate that nothing occurred but an oxidation at M_1. However, the standard deviations are not given, so we cannot say anything about the reliability of the absorption area determination. The standard

deviations are thought to be rather large because of an overlapping similar to that seen in arfvedsonite.

Samples 3 and 4 may be compared since they were given the same treatment, except for the roasting of sample 4. The spectra of the two samples are identical. The parameters are not completely identical, because of the great overlap between the absorptions. The computer program has difficulties in resolving the spectra as several solutions are statistically acceptable, and the program chooses the statistically best one, which is not necessarily the correct solution.

Table 1.2

Mössbauer parameters

Sample number	Absorption	I.S (mm/s)	Q.S. (mm/s)	H.W. (mm/s)	Absorption area (%)	Standard deviation (%)
1	Fe^{2+}_{2+} in M_1	1.13	2.80	0.37	50.8	9.0
	Fe^{3+}_{2+} in M_3	1.13	2.29	0.54	15.2	11.5
	Fe^{3+} in M_2^3	0.39	0.52	0.42	34.0	1.3
2	Fe^{2+}_{2+} in M_1	1.16	2.72	0.35	18.4	1.9
	Fe^{3+}_{2+} in M_3	1.18	1.99	0.62	27.4	2.9
	Fe^{3+} in M_3^2	0.39	0.65	0.40	30.6	5.9
	Fe^{3+} in M_1	0.42	1.03	0.47	23.8	6.3
3	Fe^{2+}_{2+} in M_1	1.09	2.68	0.27	5.6	3.0
	Fe^{3+}_{2+} in M_3	1.18	2.06	0.74	36.8	4.9
	Fe^{3+} in M_3^2	0.38	0.71	0.42	37.4	15.0
	Fe^{3+} in M_1	0.41	1.00	0.40	20.2	15.4
4	Fe^{2+}_{2+} in M_1	1.12	2.76	0.29	7.6	4.3
	Fe^{3+}_{2+} in M_3	1.15	2.09	0.71	31.6	8.0
	Fe^{3+} in M_3^2	0.38	0.61	0.38	23.0	11.0
	Fe^{3+} in M_1	0.40	1.05	0.45	37.8	12.4
5	Fe^{2+}_{2+} in M_1	1.15	2.80	0.38	51.8	3.7
	Fe^{3+}_{2+} in M_3	1.06	2.14	0.55	20.0	5.2
	Fe^{3+} in M_2^3	0.41	0.53	0.37	28.0	1.2
6	Fe^{2+}_{2+} in M_1	1.15	2.76	0.37	37.6	2.8
	Fe^{3+}_{2+} in M_3	1.08	2.10	0.57	26.2	3.8
	Fe^{3+} in M_2^3	0.41	0.59	0.47	36.4	1.1
7	Fe^{2+}_{2+} in M_1	1.15	2.78	0.37	52.2	4.2
	Fe^{3+}_{2+} in M_3	1.14	2.22	0.53	16.0	5.0
	Fe^{3+} in M_2^3	0.43	0.54	0.39	31.8	0.8
8	Fe^{2+}_{2+} in M_1	1.14	2.81	0.31	24.6	6.0
	Fe^{3+}_{2+} in M_3	1.08	2.40	0.52	29.6	8.2
	Fe^{3+} in M_3^2	0.41	0.51	0.39	32.0	12.2
	Fe^{3+} in M_1	0.48	0.93	0.46	14.0	14.0
9	Fe^{2+}_{2+} in M_1	1.22	2.58	0.39	10.2	6.1
	Fe^{2+}_{2+} in M_3	1.18	2.01	0.82	24.8	7.3
	Fe^{3+} in M_2^3	0.39	0.80	0.33	20.0	6.6
	Fe^{3+} in M_1^2	0.38	1.03	0.49	44.8	9.7
10	Fe^{2+}_{2+} in M_1	1.21	2.54	0.33	8.2	2.7
	Fe^{2+}_{2+} in M_3	1.19	1.99	0.60	22.4	13.4
	Fe^{3+} in M_2^3	0.40	0.55	0.28	12.4	3.5
	Fe^{3+} in M_1^2	0.37	0.97	0.54	57.0	30.9
11	Fe^{2+}_{2+} in M_3	1.07	2.46	0.68	22.2	2.0
	Fe^{3+} in M_2^3	0.40	0.53	0.29	11.4	9.3
	Fe^{3+} in M_1	0.42	0.91	0.54	66.2	10.9

Table I. 3

The different interpretations of heat-treated ribeckite and arfvedsonite spectra

Ernst and Wai		The present investigation
Fe^{2+} in M_1	=	Fe^{2+} in M_3
Fe^{2+} in M_3	=	Fe^{2+} in M_1
Fe^{3+} in M_2	=	Fe^{3+} in M_2
Fe^{3+} in $M_1 + M_3$	=	Fe^{3+} in M_1

Table I. 4

The contents of Fe^{2+} and Fe^{3+} on different lattice positions in ribeckite

	Fe^{2+} absorptions		Fe^{3+} absorptions	
	Fe^{2+} in M_1	Fe^{2+} in M_3	Fe^{3+} in M_2	Fe^{3+} in M_1
Untreated ribeckite	36.4	19.0	44.6	
Heated to 700°C for 1 hour	11.5	21.3	42.6	24.6

I. 2 f-factor Correction

Iron atoms may be bonded differently in different lattice positions in arfvedsonite. Thus their f-factor (cf. section 5.11) may differ, and they may not be detected with the same efficiency.

There is a possibility of determining the ratio between the f-factors for different lattice sites by recording Mössbauer spectra at different temperatures (cf. G.A. Sawatzky, F. van der Woude and A.H. Morrish[73], and E.B. Andersen, J. Fenger, and J. Rose Hansen[50]). The temperature dependence of the f-factor is given by[50]

$$f(T) = \exp\left(-\frac{6E_R}{k_B \Theta_D^2}\right) \quad \text{for } T \gtrsim \frac{\Theta_D}{2}, \tag{1}$$

where E_R is the recoil energy of the γ-quantum ($1.95 \cdot 10^{-3}$ eV in the case of ^{57}Fe), k_B is the Boltzmann constant (0.862 eV K^{-1}) and T is the absolute temperature. Θ_D is the so-called Debye temperature. Thus Θ_D may be determined by

$$\Theta_D = \left(-\frac{6E_R}{k_B} \cdot \frac{dT}{d(\ln f)}\right)^{\frac{1}{2}} . \qquad (2)$$

If there are two different Fe positions in a lattice, then the ratio between the contents of these is given by

$$\frac{n_I}{n_{II}} = \frac{A_I}{A_{II}} \cdot \frac{f_{II}}{f_I} , \qquad (3)$$

where A is the measured absorption area. If equation 1 is used in 3, we have

$$\frac{n_I}{n_{II}} = \frac{A_I}{A_{II}} \exp\left(\frac{6E_R T}{k_B}\left(\frac{1}{\Theta_{DI}^2} - \frac{1}{\Theta_{DII}^2}\right)\right) . \qquad (4)$$

The Debye temperatures for the two positions may be determined by a delineation of lnA = lnT versus T (cf. equation 2) and thus the correction ratio may be determined from equation 4.

In the case of arfvedsonite, we have three different Fe-containing lattice positions. In the calculations of E. B. Andersen, J. Fenger, and J. Rose Hansen[50], the two Fe^{2+} positions were treated together. The situation is more complicated in the case of the heat-treated arfvedsonite,

Table I.5

Mössbauer parameters of a heat-treated sample at two different temperatures

Temperature (°C)	Absorption	I.S. (mm/s)	Q.S. (mm/s)	Fe^{2+} absorption area (%)
22	Fe^{2+} in M_1	1.15±0.01	2.72±0.01	45.3±1.0
	Fe^{2+} in M_3	1.19±0.01	1.96±0.02	
	Fe^{3+} in M_2	0.38±0.01	1.66±0.02	
	Fe^{3+} in M_1	0.40±0.01	1.02±0.01	
-196	Fe^{2+} in M_1	1.24±0.02	2.96±0.02	48.0±1.8
	Fe^{2+} in M_3	1.33±0.01	2.11±0.03	
	Fe^{3+} in M_2	0.47±0.02	0.89±0.03	
	Fe^{3+} in M_1	0.51±0.02	1.16±0.08	

because here we have both two Fe^{2+} and two Fe^{3+} positions. We have to consider them as 1 of each in the calculation.

The measurements were made on an arfvedsonite sample heated to

500°C (sample number 3, section I.1). The measurements were made at room temperature (22°C) and at -196°C. The parameters are given in table I.5. Two measurements were made at 22°C and three at -196°C.

Both isomer shift and quadrupole splitting increase for decreasing temperature.

These measurements did not have the same geometry in the Mössbauer arrangement, and because the total intensity of the spectrum depends on both geometry and temperature, we cannot use the above equation for determining θ_I and θ_{II}. However, we may approximate equation 4 by

$$\frac{n_I}{n_{II}} = \frac{A_I}{A_{II}} \left(1 - \frac{6E_R}{k_B} \left(\frac{1}{\theta^2_{DI}} - \frac{1}{\theta^2_{DII}}\right) T\right)$$

$$\frac{A_{II}}{A_I} = \frac{n_{II}}{n_I} \left(1 - \frac{6E_R}{k_B} \left(\frac{1}{\theta^2_{DI}} - \frac{1}{\theta^2_{DII}}\right) T\right). \qquad (5)$$

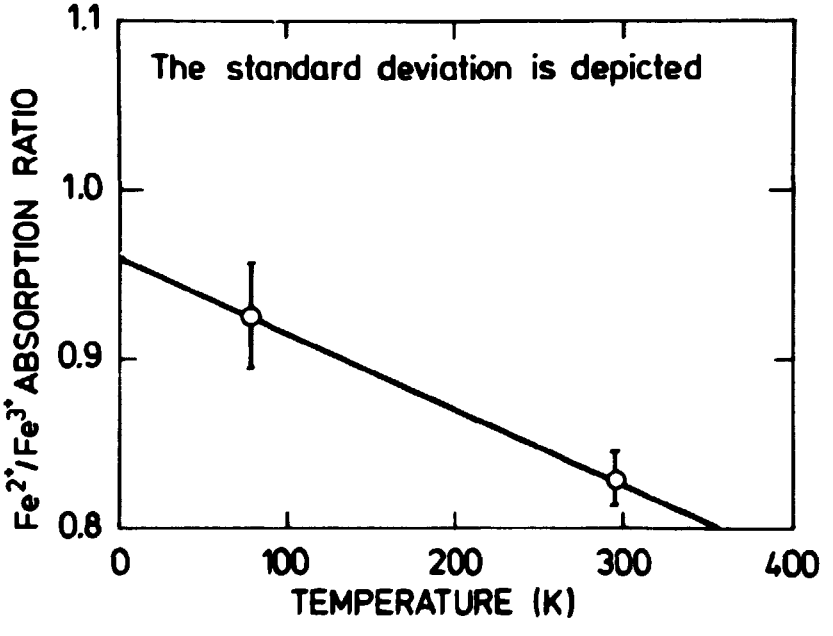

Fig. I.2. Fe^{2+}/Fe^{3+} absorption area versus temperature.

The area ratio is depicted versus temperature in fig. I.2. $(\frac{1}{\theta^2_{DI}} - \frac{1}{\theta^2_{DII}})$ is hereby calculated to $0.340 \times 10^{-6} K^{-2}$, and $\exp\left(\frac{6E_R T}{k_B}\left(\frac{1}{\theta^2_{DI}} - \frac{1}{\theta^2_{DII}}\right)\right) = 1.15 \pm 0.06$ at room temperature. The Fe^{2+}/Fe^{3+} ratio determined has therefore to be multiplied by this factor in order to determine the real value.

The present determination may only be regarded as a rough estimate because of the approaches made, and also because the low temperature measurements are made below $\theta_D/2$. The Debye temperatures were in[50] determined to 350 ± 12 K for Fe^{2+} and 490 ± 37 K for Fe^{3+} for arfvedsonite. The correction factor of 1.17 ± 0.02 determined in[50] may therefore also be used for the heat-treated and roasted samples.

APPENDIX II

X-ray Diffractions of Arfvedsonite

Table II.1 gives the diffraction lines of the untreated pegmatite arfvedsonite, of the samples heated to 400°C and 700°C, respectively, of the samples roasted to 12.5% weight increase at 700°C, of the average diffractogram of the roasted or heat-treated and then reduced samples, and of the ASTM standard card file for arfvedsonite, acmite, hematite, $Na_3Fe(SO_4)_3$ and $NaFe(SO_4)_2$.

The following abbreviations are used:

d: Internal spacing in Ångstrøm
Int: Intensity
vs: very strong
s: strong
m: medium
w: weak
vw: very weak
-D: diffuse line
A: Arfvedsonite
Ac: Acmite
H: Hematite
NF: $NaFe(SO_4)_2$
N3F: $Na_3Fe(SO_4)_3$
var: variation in internal spacing (Å)

Table II. 1

X-ray Diffractions of Arfvedsonite

Untreated		Heated to 400°C		Heated to 700°C		
d. (Å)	Int	d. (Å)	Int	d. (Å)	Int	phase
8.6	vs	8.5	vs	8.7	s	
4.5	m	4.5	m-D	6.5	w	Ac
4.00	w	4.0	w	4.5	m	
3.70	vw	3.69	vw	4.02	w	
3.41	m	3.39	m	3.69	w	
3.29	w	3.28	w	3.41	m	
3.17	m	3.14	m	3.29	w	
2.98	vw	2.96	vw	3.15	m	
2.85	vw	2.81	vw	3.02	m-D	Ac
2.71	s	2.73	vw	2.93	w	Ac
2.59	m	2.70	s	2.81	vw	
2.52	m	2.59	m	2.72	m	
2.34	w	2.53	m	2.60	w	
2.28	w	2.34	w	2.54	m-D	Ac
2.17	w	2.27	w	2.50	vw	Ac
2.05	vw	2.18	w	2.34	vw	
2.02	vw	2.16	vw	2.27	w	
+ weaker lines		2.04	vw	2.22	vw	Ac
⟨ 2.00 Å		2.02	vw	2.16	w	
		+ weaker lines ⟨ 2.00 Å		2.06	vw	
				2.02	vw	
				+ weaker lines ⟨ 2.00 Å		

Roasted to 12.5% weight increase			Reduced samples (average)			Arfvedsonite ASTM card file 14-633	
d. (Å)	Int	phase	d. (Å)	Var	Int	d. (Å)	Int (relative)
8.4	m	A	8.5	0.04	s	9.05	2
7.3	w	NF	4.5	0.03	m	8.51	70
6.8	w	N3F	3.40	0.01	m	4.82	8
6.0	vw		3.28	0.01	w	4.53	14
4.45	w	A	3.12	0.01	m	4.26	2
4.20	w	NF	2.94	0.01	w	3.883	18
4.00	w	A+N3F	2.71	0.01	s	3.423	45
3.75	w	NF	2.59	0.01	m	3.296	20
3.69	s	H+A	2.53	0.01	m	3.181	100
3.43	w	NF	2.32	0.01	vw	3.028	4
3.39	w	A	2.27	0.01	w	2.991	15
3.15	m	A+N3F	2.17	0.01	vw	2.834	12
3.05	m	N3F	2.13	0.01	vw	2.732	80
2.95	w	A	2.06	0.01	w	2.604	35
2.80	w	NF				2.550	25
2.69	s-D	H+A				2.406	10
2.50	s-D	H+A				2.345	24
2.36	w	A				2.339	2
2.31	vw					2.283	20
2.25	vw	A				2.158	35
2.20	vw	H				2.082	10
2.15	vw					2.043	20
2.04	vw	N3F				+ weaker lines ⟨ 2.00 Å	
2.00	vw	NF					
1.82	m	H					
1.68	m	H					
1.59	vw						
1.58	vw						
1.51	vw	NF					
1.48	m	H					
1.45	m	H					

Hematite ASTM card file 13-534		Acmite ASTM card file 3-0621		$NaFe(SO_4)_2$ ASTM card line 3-0311	
d. (Å)	Int (relative)	d (Å)	Int (relative)	d. (Å)	Int (relative)
3.69	25	6.50	40	7.20	75
2.69	100	4.43	40	4.02	20
2.51	50	3.64	7	3.74	100
2.20	30	2.99	100	3.44	75
1.84	40	2.91	40	2.78	75
1.69	60	2.54	60	2.72	30
1.48	35	2.48	27	2.58	40
1.45	35	2.20	20	2.36	50
1.31	20	2.12	20	2.09	34
(only strong lines)		2.03	20	2.01	25
		1.73	13	1.65	25
		1.51	13	(only strong lines)	
		1.40	13		

$Na_3Fe(SO_4)_3$ ASTM card file 3-509	
d. (Å)	Int (relative)
6.80	75
3.98	40
3.18	100
3.04	75
2.64	20
2.39	20
2.03	20
1.86	30
1.58	20
1.54	20
(only strong lines)	

APPENDIX III

X-ray Diffractions of Steenstrupine

X-ray diffraction lines are given for the steenstrupine fraction from drill core 1, and of samples heated to 700, 800 and 960°C, respectively, in table III. 1. Also given are the ASTM card files for monazite, $(U, Th)O_2$ and steenstrupine. The same abbreviations are used as in appendix II together with the following new ones:

M: Monazite

U: $(U, Th)O_2$

Table III. 1

X-ray Diffractions of Steenstrupine

Raw material d. (Å)	Int	phase
6.7	vw	
6.3	vw	Ac
4.40	vw	Ac
2.97	w	Ac
2.89	vw	
2.51	vw	Ac
2.46	vw	Ac
2.27	vw	
2.23	vw	
2.21	vw	
2.19	vw	

Heated to 960°C d. (Å)	Int	phase
6.7	vw	
4.68	vw	M
4.29	vw	
4.18	w	M
4.18	vw	
3.53	w-D	M
3.30	m	M
3.13	s	U
3.10	m	M
2.99	vw	M
2.96	vw	
2.86	m	M
2.71	m	U
2.60	w	M
2.39	vw	
2.19	vw	M
2.15	vw	M
2.145	vw	
2.14	vw	M
1.97	w	M
1.92	m	U
1.89	vw	M
1.80	vw	M
1.77	vw	M
1.74	vw	M
1.69	vw	M
1.635	m	U
1.57	vw	U
1.54	vw	M

Heated to 700°C d. (Å)	Int	phase
3.05-		
3.15	w-D	M(+U)
2.97	w	Ac
2.87	vw-D	M
2.52	vw	Ac
2.46	vw	Ac
2.24	vw	
2.10	vw	
2.09	vw	

Monazite ASTM card file 11-356 d. (Å)	Int
5.22	13
4.66	16
4.17	25
3.51	25
3.30	50
3.09	100
2.90	18
2.87	70
2.61	18
2.44	18
2.19	18
2.15	25
2.13	25
1.961	25
1.895	13
1.870	18
1.859	18
1.762	18
1.737	25
1.687	13
1.535	13
(only strong lines)	

Heated to 800°C d. (Å)	Int	phase
4.50	w	
4.40	w	Ac
3.50	vw-D	M
3.35	s	
3.30	w	M
3.15	m-D	U
3.10	m	M
2.99	vw	Ac
2.87	m	M
2.76	w	
2.72	w-D	U
2.65	vw	
2.52	vw	Ac
2.45	vw	Ac
2.28	vw	
2.19	vw-D	
2.14	vw-D	

$(U, Th)O_2$ ASTM card file 5-549 d. (Å)	Int (relative)
3.16	100
2.73	50
1.94	80
1.65	80
1.58	20
1.25	30
(only strong lines)	

APPENDIX IV

Description of the 26 Lujavrite Samples Investigated

A description is given of all the lujavrite samples mentioned in chapters 8 and 9. Most of the samples were investigated in thin sections; a few were investigated in polished sections. The essential minerals were determined from the thin sections and from X-ray diffractograms. Uranium mineralisation was determined from the thin sections and, in cases where these did not exist, from polished sections. It is possible to distinguish between the three steenstrupine types and the pigmentary material by reflection microscopical investigations.

The thin sections were kindly examined by H. Sørensen and the description was much improved by his comments.

Sample number 1.

Arfvedsonite lujavrite from the mine material.
Uranium content: 934 ppm.
Mineralisation (thin section of a grain size fraction $>$ 75 microns + diffractogram). The essential minerals are arfvedsonite, analcime, microcline, and albite. Uranium is mainly contained in pigmentary material. Steenstrupine of the partly altered type might also be found in smaller amounts, but it has not been definitely identified.

Sample number 2.

Medium-to coarse-grained arfvedsonite lujavrite from the mine material.
Uranium content: 412 ppm.
Mineralisation (thin section + diffractogram). The essential minerals are arfvedsonite, analcime, and microcline. Albite, neptunite, brown sphalerite, steenstrupine, and monazite are found in minor amounts. Arfvedsonite often found in aggregates of small crystals. Pigmentary material is the most important uranium mineral, but steenstrupine of a rather homogeneous type and monazite/uranothorite are also found. The pigmentary grains are often found in connexion with neptunite. The steenstrupine grains are isotropic and yellow, although the colour varies inside the grains. They frequently appear crackled and are partly altered in some areas.

Sample number 3.

Medium-to-coarse-grained arfvedsonite lujavrite from the mine material.
Uranium content: 532 ppm.
Mineralisation (thin section + diffractogram).
This sample is almost identical to number 2. The steenstrupine content is lower and it looks more altered than that of sample 2. However, isotropic and rather homogeneous areas are still found in the grains. The sphalerite content is rather high in this sample.

Sample number 4.

Medium-to-coarse-grained arfvedsonite lujavrite from the mine material.
Uranium content: 359 ppm.
Mineralisation (diffractogram). The essential minerals are arfvedsonite, analcime, microcline, and albite. Uranium mineralisation was not determined.

Sample number 5.

Arfvedsonite lujavrite from drill core 32 (32.90 - 33.35 m depth).
Uranium content: 404 ppm.
Mineralisation (thin section + diffractogram). The essential minerals are aegirine, albite, and sodalite. There are minor amounts of analcime, arfvedsonite, nepheline, and microcline. Arfvedsonite is much altered to aegirine in this sample. Uranium is contained in strongly altered steenstrupine and pigmentary material.

Sample number 6.

Arfvedsonite lujavrite from drill core 30 (12.06 - 14.36 m depth).
Uranium content: 586 ppm.
Mineralisation (thin section + diffractogram). The essential minerals are arfvedsonite, analcime, and microcline. There are minor amounts of nepheline, aegirine, and steenstrupine. The analcime ground mass contains corroded grains of microcline and nepheline. Uranium is contained in partly altered steenstrupine and in pigmentary material, in which the sample is rather rich. The sample might be inhomogeneous because a thin section from 14.37 m depth shows a sheared volcanic rock.

Sample number 7.

Medium-to coarse-grained arfvedsonite lujavrite from drill core 15 (41.08 - 41.35 m depth).
Uranium content: 263 ppm.
Mineralisation (thin section + diffractogram). The essential minerals are arfvedsonite, analcime, microcline and nepheline. There are minor amounts of aegirine, sphalerite, endialyte, neptunite, and steenstrupine. Arfvedsonite is mostly found in aggregates of small crystals. A minor part of it is altered into aegirine. Uranium is found in partly altered steenstrupine and in pigmentary material, which in this case is altered endialyte. Fresh grains of this mineral are also found.

Sample number 8.

Arfvedsonite lujavrite from drill core 16 (70.50 - 71.45 m depth).
Uranium content: 751 ppm.
Mineralisation (thin section + diffractogram). The essential minerals are arfvedsonite and analcime. There are minor amounts of albite, steenstrupine, nepheline, aegirine, and neptunite. There are also a few grains of a faintly yellow sphalerite. There are corroded grains of albite and nepheline in the analcime ground mass. The sample is rich in partly altered steenstrupine but poor in pigmentary material. Some of the steenstrupine grains seem to have a zonar structure.

Sample number 9.

Medium-to coarse-grained arfvedsonite lujavrite from drill core 16 (72.65 - 73.45 m depth).
Uranium content: 396 ppm.
Mineralisation (diffractogram + polished section). The essential minerals are arfvedsonite, analcime, albite, microcline, and a little aegirine. Uranium is contained in partly altered steenstrupine.

Sample number 10.

Arfvedsonite lujavrite from drill core 39 (25.25 - 25.40 m depth).
Uranium content 257 ppm.
Mineralisation (diffractogram + polished section). Arfvedsonite, analcime, albite, and aegirine. Uranium is mainly contained in pigmentary material (this was confirmed by a microprobe examination). The sample is not

characteristic of the drill core, because the Th content is extremely low just around the chosen sample[8].

Sample number 11.

Naujakasite lujavrite from drill core 39 (64.00 - 64.20 m depth).
Uranium content: 226 ppm.
Mineralisation (diffractogram + polished section). The essential minerals are arfvedsonite, naujakasite, analcime, and microcline. The sample is rich in pigmentary material but partly altered steenstrupine is also found.

Sample number 12.

Arfvedsonite lujavrite from drill core 39 (151.20 - 153.20 m depth).
Uranium content: 388 ppm.
Mineralisation (diffractogram + polished section). The essential minerals are arfvedsonite and albite. There is a minor amount of nepheline. Uranium is found in both partly altered steenstrupine and in pigmentary material.

Sample number 13.

Arfvedsonite lujavrite from drill core 4 (112.05 - 112.50 m depth).
Uranium content: 492 ppm.
Mineralisation (thin section + diffractogram). Arfvedsonite, analcime, and natrolite. There are minor amounts of the two felspars, nepheline and steenstrupine. Corroded grains of the felspars and the nepheline are found in the analcime ground-mass of the thin section. A TG curve shows that the amounts of natrolite and analcime are approximately equal. Uranium is found in a homogeneous steenstrupine. The grains are isotropic and faintly yellow. They usually have well developed crystal faces.

Sample number 14.

Arfvedsonite lujavrite from drill core 5 (119.05 - 120.85 m depth).
Uranium content: 486 ppm.
Mineralisation (thin section + diffractogram). The essential minerals are arfvedsonite, albite, nepheline, and natrolite. There are minor amounts of aegirine, steenstrupine, and yellow sphalerite. Uranium is mainly found in partly altered steenstrupine, but also in a little pigmentary material.

Sample number 15.

Arfvedsonite lujavrite from drill core 22 (118.40 - 119.00 m depth).
Uranium content: 328 ppm.
Mineralisation (thin section + diffractogram). The essential minerals are arfvedsonite, analcime and aegirine. There are smaller amounts of sodalite, microcline, nepheline, and steenstrupine. Arfvedsonite is in some areas completely altered to aegirine. Uranium is found in steenstrupine of the partly altered type, in pigmentary material and in uranothorite associated to monazite.

Sample number 16.

Medium-to coarse-grained arfvedsonite lujavrite from drill core number 22 (110.82 - 111.08 m depth).
Uranium content: 161 ppm.
Mineralisation (thin section + diffractogram). Arfvedsonite, aegirine, microcline, and natrolite. There are minor amounts of analcime, sodalite, monazite, and neptunite. Arfvedsonite is partly altered to aegirine. Uranium is found in pigmentary material and in monazite. The sample is rich in monazite, so an essential part of the uranium can be found in this mineral although the content is at most a few parts per thousand. Uranothorite was not found in this sample. The pigmentary material is associated to much neptunite.

Sample number 17.

Naujakasite lujavrite from drill core 32 (10.70 - 11.10 m depth).
Uranium content: 516 ppm.
Mineralisation (thin section + diffractogram). The essential minerals are naujakasite, aegirine, analcime, albite, and arfvedsonite. There are minor amounts of strongly altered steenstrupine and of a red-brown sphalerite. Arfvedsonite is much altered to aegirine. Naujakasite is also altered, because it has a brown colour. Uranium is mainly found in strongly altered steenstrupine, but there is also a minor amount of pigmentary material.

Sample number 18.

Naujakasite lujavrite from drill core 7 (113.10 - 113.40 m depth).
Uranium content: 607 ppm.

Mineralisation (thin section + diffractogram). The essential minerals are naujakasite, arfvedsonite, and albite. There are minor amounts of natrolite, steenstrupine and microcline. The sample is very poor in analcime. Uranium is contained in partly altered steenstrupine and in a little pigmentary material. Many of the steenstrupine grains have a zonal structure.

Sample number 19.

Arfvedsonite lujavrite from drill core 24 (86.50 - 86.75 m depth).
Uranium content: 912 ppm.
Mineralisation (thin section + diffractogram). The essential minerals are arfvedsonite, albite, microcline, and sodalite. There are small amounts of aegirine and steenstrupine. The steenstrupine has a red-brown colour that varies inside the grains. They are partly isotropic and anisotropic. The grains are not completely homogeneous. This steenstrupine might be defined as being intermediate between the homogeneous and the partly altered type. (cf. section 8.2).

Sample number 20.

Naujakasite lujavrite from drill core 28 (90.25 - 90.60 m depth).
Uranium content: 395 ppm.
Mineralisation (thin section + diffractogram). The essential minerals are naujakasite, arfvedsonite, and microcline. There are minor amounts of aegirine, monazite, and steenstrupine. Arfvedsonite is partly altered to aegirine. Uranium is found in steenstrupine, pigmentary material and monazite. The steenstrupine is sparse; it is homogeneous, isotropic and colourless. There is much monazite, but uranothorite was not detected by microprobe examination.

Sample number 21.

Arfvedsonite lujavrite from drill core 17 (110.10 - 110.60 m depth).
Uranium content: 742 ppm.
Mineralisation (thin section + diffractogram). The essential minerals are arfvedsonite, albite, analcime, and natrolite. There are minor amounts of nepheline, ussingite, aegirine, steenstrupine, and a little villiaumite. Albite and nepheline are found as corroded grains in the analcime-natrolite ground mass. Arfvedsonite is in some areas partly altered to aegirine. Uranium is mainly found in partly altered steenstrupine, but pigmentary material is also found.

Sample number 22.

Arfvedsonite lujavrite from drill core 40 (152.44 - 152.85 m depth).
Uranium content: 310 ppm.
Mineralisation (diffractogram + polished section). The essential minerals are arfvedsonite, microcline, albite, sodalite, aegirine, and natrolite. Uranium is mainly found in pigmentary material. Many of these grains are $\rangle$ 100 microns.

Sample number 23.

Arfvedsonite lujavrite from the foot of Steenstrup Mountain.
Uranium content: 506 ppm.
Mineralisation (thin section + diffractogram). The essential minerals are arfvedsonite, analcime, and microcline. There is a minor amount of aegirine. Uranium is mainly found in strongly altered steenstrupine. The grains are large, very irregular and very inhomogeneous.

Sample number 24.

Arfvedsonite lujavrite from the Tasseq slope (outcrops of lujavrite).
Uranium content: 506 ppm.
Mineralisation (thin section + diffractogram). The essential minerals are arfvedsonite, analcime, and microcline. There are minor amounts of nepheline and steenstrupine. Corroded microcline and nepheline grains are found in the analcime ground mass. The sample is rather rich in pigmentary material, but most uranium is found in a rather homogeneous steenstrupine. It is difficult to determine whether this steenstrupine is homogeneous, because many grains have both altered and unaltered areas. In most grains there are homogeneous and isotropic areas, so the alteration seems to differ from that seen in the partly altered steenstrupine type. It might be the result of some weathering process, because the sample is from the surface. There seems to be a chemical difference between the homogeneous and unaltered grains and the homogeneous areas in the altered grain of steenstrupine, because the SiO_2/P_2O_5 ratio is approximately 3 in the first and 2 in the second case.

Sample 25.

Arfvedsonite lujavrite from the northern area of Kvanefjeld (Fixpoint 114).
Uranium content: 285 ppm.

Mineralisation (thin section + diffractogram). The essential minerals are aegirine, analcime, arfvedsonite, and nepheline. There are minor amounts of the felspars. Nepheline and the felspars are much altered to analcime, as also arfvedsonite to aegirine. Uranium is found in pigmentary material.

Sample number 26.

Arfvedsonite lujavrite from the northern area of Kvanefjeld (Fixpoint 108). Uranium content: 415 ppm.
Mineralisation (thin section + diffractogram). The essential minerals are arfvedsonite, analcime and aegirine. There are minor amounts of nepheline, microcline, sodalite, and steenstrupine. The steenstrupine in this sample has a very unusual composition (cf. table 8.2). It is weakly anisotropic. The SiO_2/P_2O_5 ratio is approximately 1. Some of the grains are altered in the same way as the steenstrupine in sample number 24.

APPENDIX V

Average samples

Table V.I. gives the drill core numbers and the depths from which the average samples were chosen. Two pieces approximately 10 cm in length were chosen at 10 m intervals from each drill core.

Sample numbers	Drill core number	Depth (m)	Sample numbers	Drill core number	Depth (m)
1	1	37 47	3	6	26 26
	2	47 57		15	21 31
	3	62 72		18	21 31
	5	67 77		20	16 26
	8	32 42		22	11 21
	9	27 37		23	11 21
	16	47 57		25	1 11
	17	52 62		26	16 26
	21	47 57		27	1 11
				29	6 16
2	3	110 120		30	11 21
	4	120 130		31	26 36
	5	112 122		33	16 26
	7	92 102			
	9	72 82	4	6	74 84
	10	82 92		15	74 84
	11	132 142		18	70 80
	12	102 112		20	67 77
	14	116 126		22	64 74
	16	92 102		23	64 74
	17	97 107		25	54 64
	21	92 102		26	69 79
				27	54 64
				31	69 79
				33	67 77

B-S-E 360 x 360 MICRONS

PLATE 1.

B-S-E 180 x 180 MICRONS

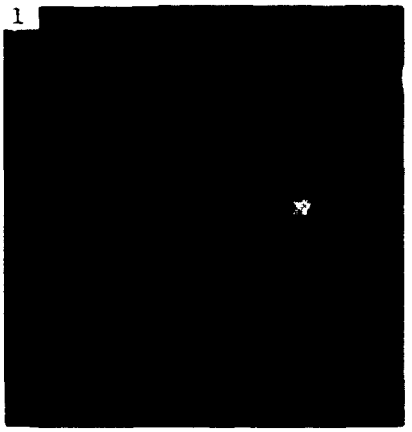

Si 3

P 4

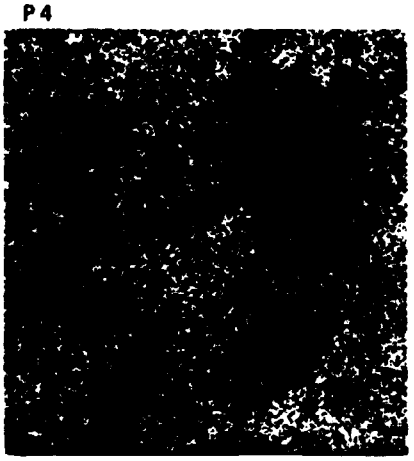

U 5

Th 6

Ce 7

Y 8

PLATE 2

Fe 9

Mn 10

Ca 11

Na 12

Al 13

Zn 14

Zr 15

PLATE 3

Si 1

P 2

U 3

Th 4

Zn 5

B-S-E 360 x 360 MICRONS

Si 2

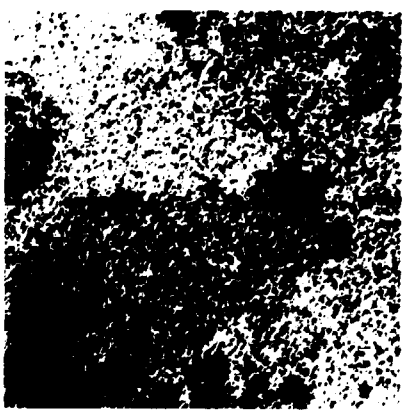

PLATE 4

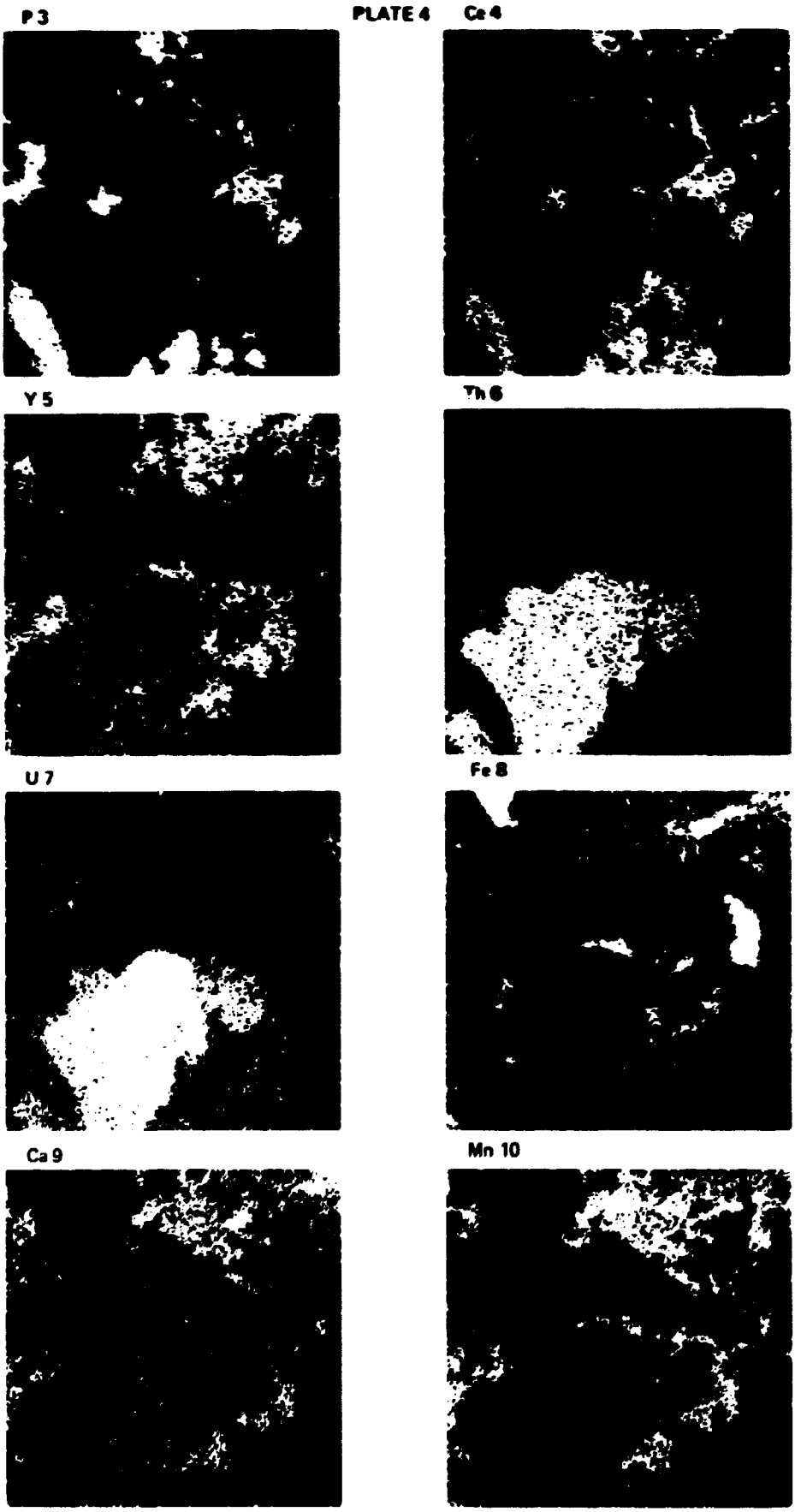

PLATE 5

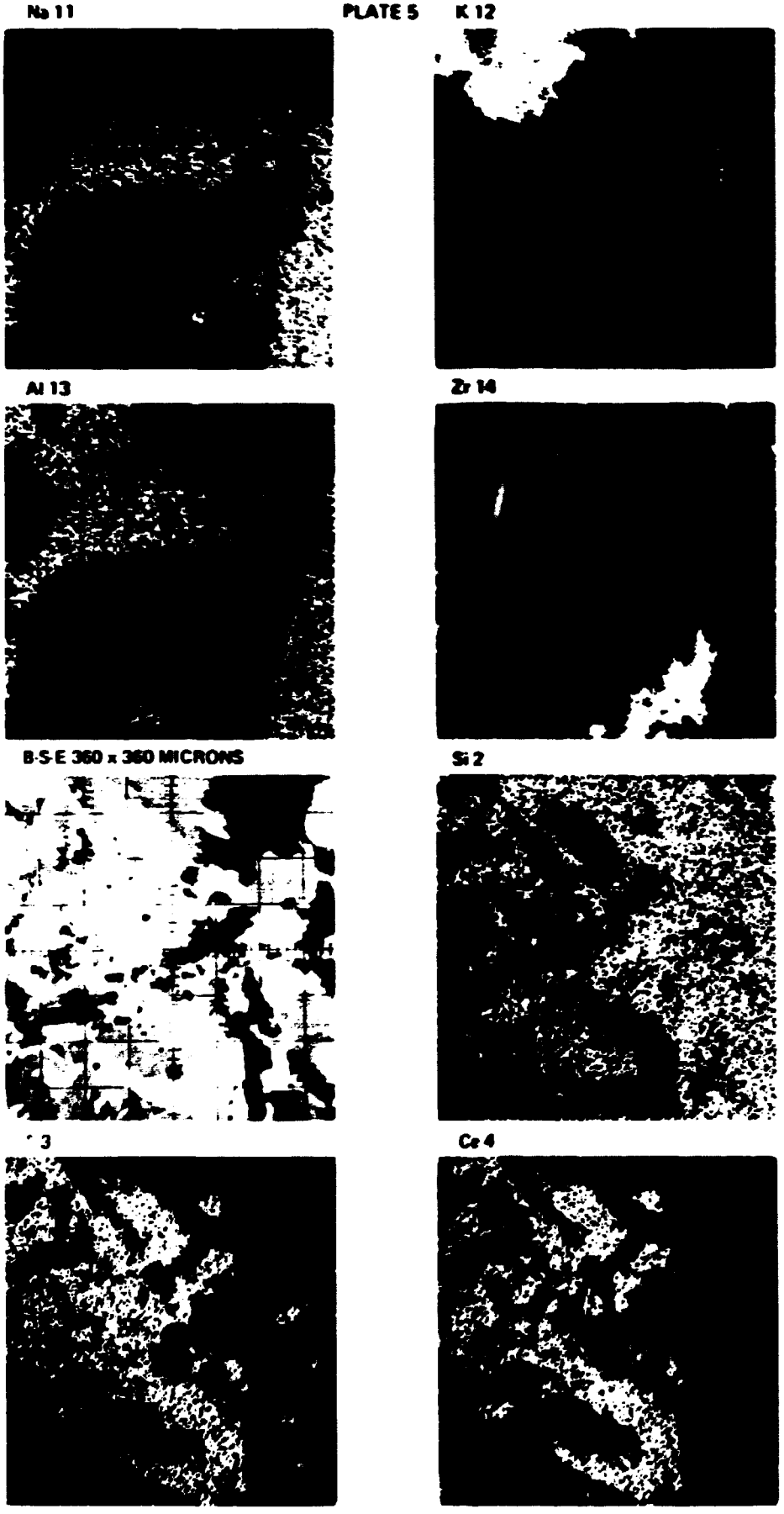

PLATE 6

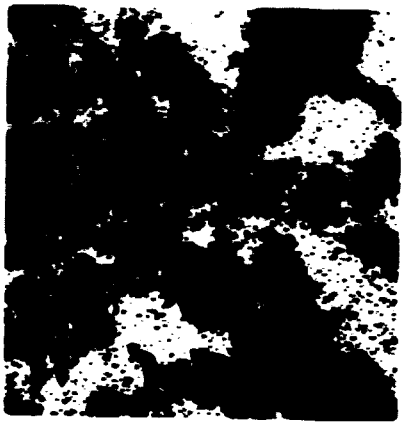

PLATE 7

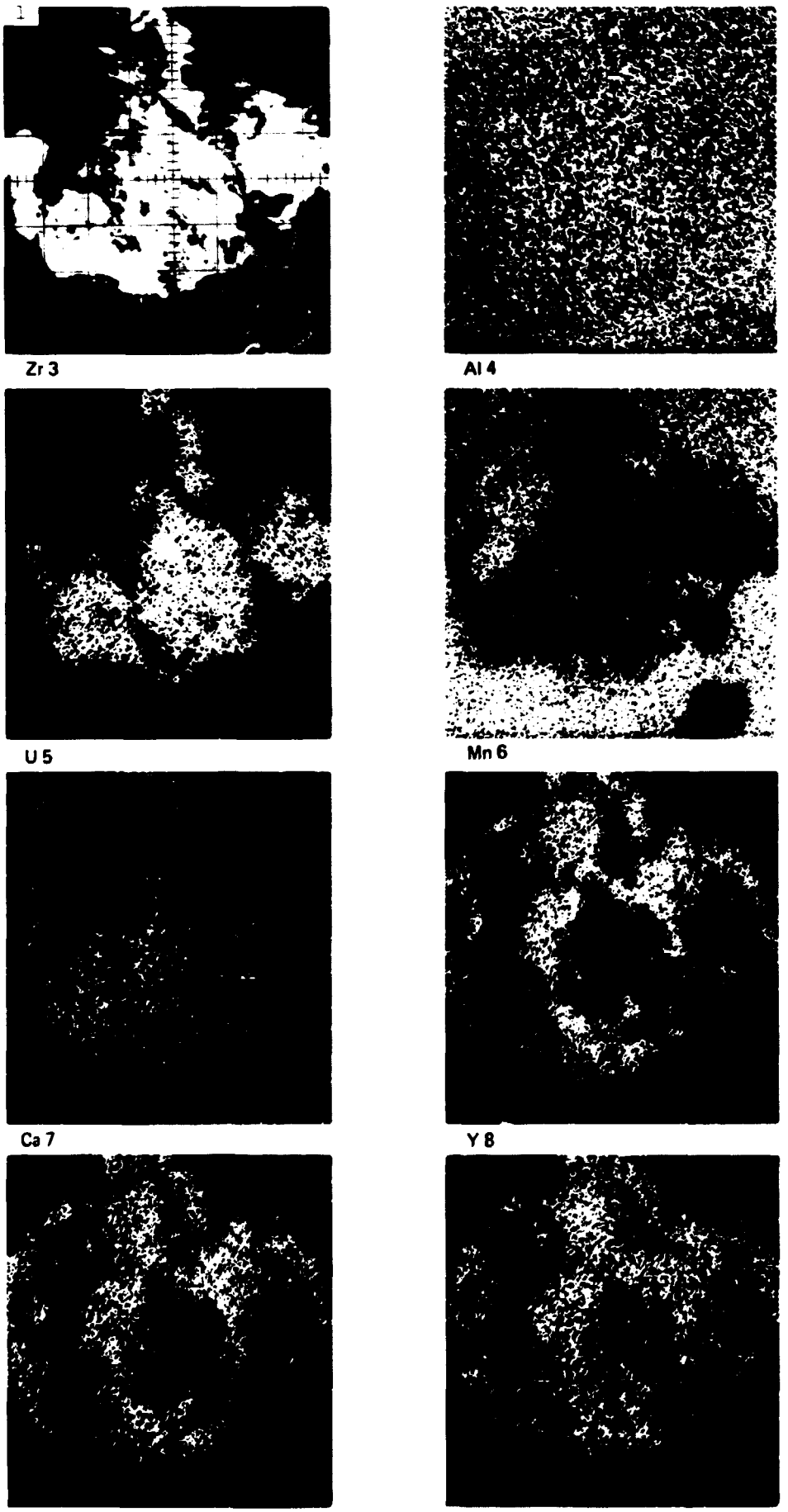

PLATE 8

Fe 9

Ti 10

B-S-E 180 x 180 MICRONS

Si 2

U 3

Ti 4

Nb 5

Zn 6

PLATE 9

Zr 7

Y 8

Mn 9

Ca 10

Fe 11

K 12

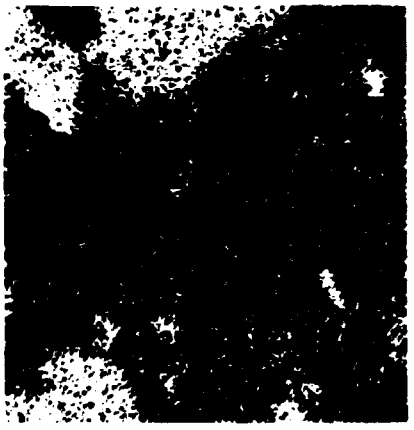

Na 13

Al 14

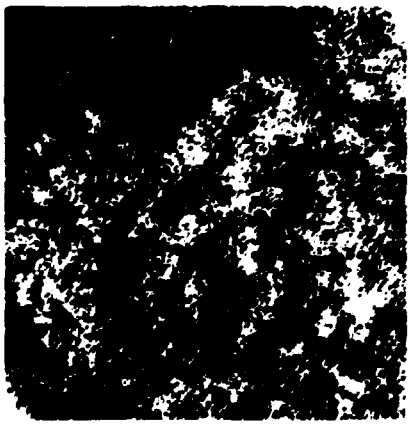

B-S-E 90 x 90 MICRONS PLATE 10

Si 2

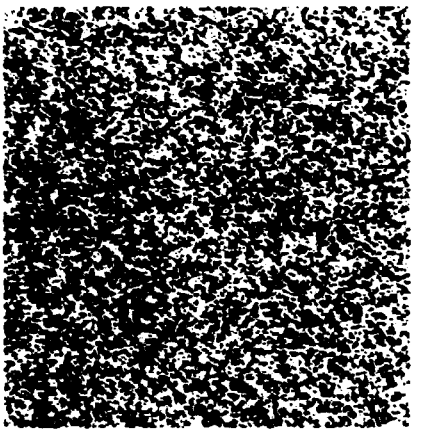

Zr 3

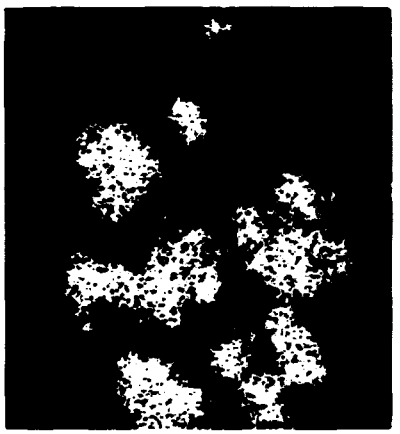

U 4

Mn 5

Ca 6

Y 7

Fe 8

PLATE 11

Zn 9

Na 10

K 11

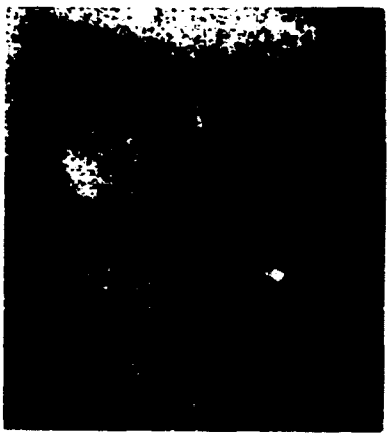

Al 12

B-S-E 90 x 90 MICRONS

1

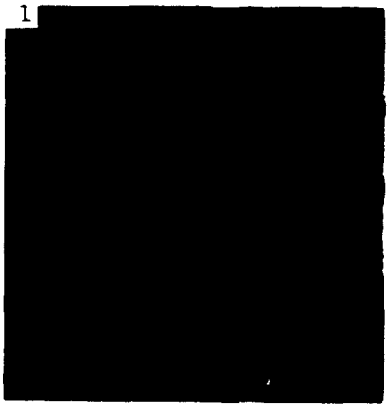

Si 2

Zr 3

U 4

PLATE 12

Ti 5

Nb 6

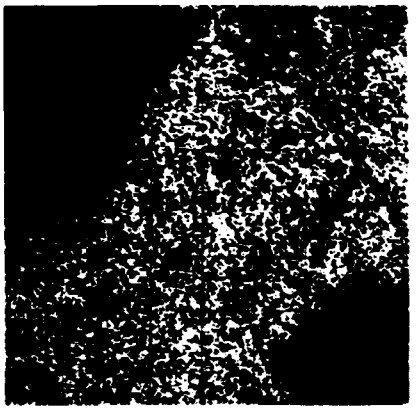

Y 7

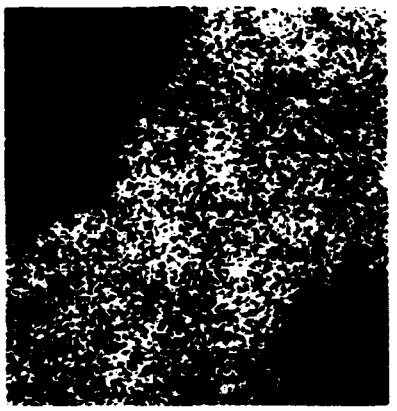

Ce 8

Mn 9

Ca 10

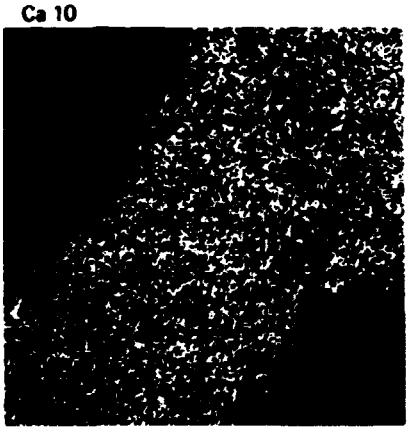

Na 11

Fe 12

PLATE 13

B-S-E 360 x 360 MICRONS

Si 2

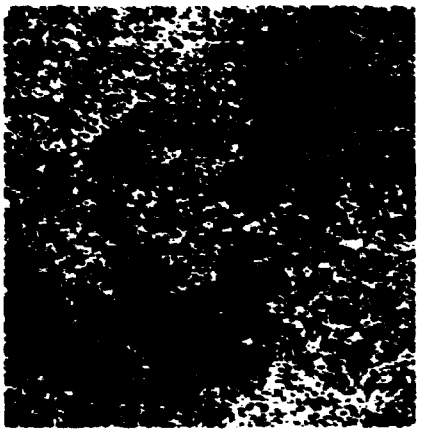

P 3

U 4

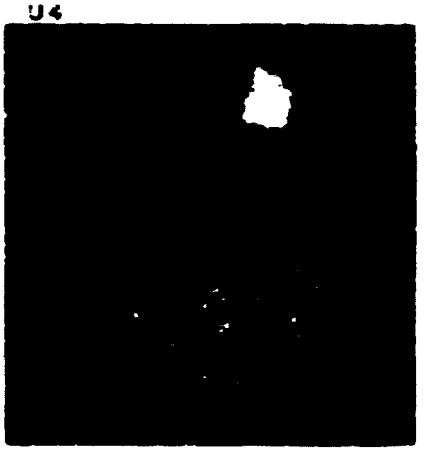

Th 5

B-S-E 360 x 360 MICRONS

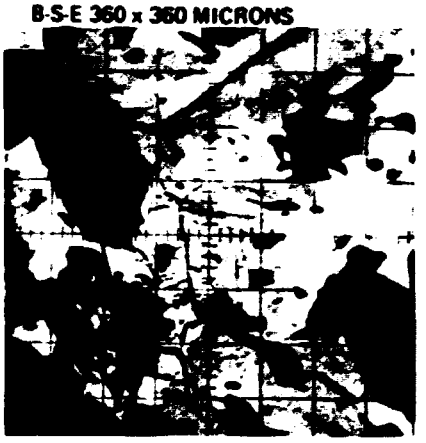

Si 2

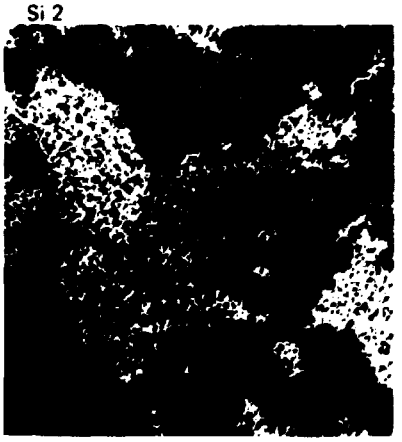

P 3

PLATE 14

U 4

Th 5

ISBN 87-550-0483-0